ISSN 1916-6117 (online)
ISBN 978-1-4868-7218-3 (PDF)

ISSN 0826-9580 (print)
ISBN 978-1-4868-7218-3 (print)

THESE TERMS GOVERN YOUR USE OF THIS DOCUMENT

Your use of this Ontario Geological Survey document (the "Content") is governed by the terms set out on this page ("Terms of Use"). By downloading this Content, you (the "User") have accepted, and have agreed to be bound by, the Terms of Use.

Content: This Content is offered by the Province of Ontario's *Ministry of Mines* (MINES, or the Ministry) as a public service, on an "as-is" basis. Recommendations and statements of opinion expressed in the Content are those of the author or authors and are not to be construed as statement of government policy. You are solely responsible for your use of the Content. You should not rely on the Content for legal advice nor as authoritative in your particular circumstances. Users should verify the accuracy and applicability of any Content before acting on it. The Ministry does not guarantee, or make any warranty express or implied, that the Content is current, accurate, complete or reliable. The Ministry is not responsible for any damage however caused, which results, directly or indirectly, from your use of the Content. The Ministry assumes no legal liability or responsibility for the Content whatsoever.

Links to Other Web Sites: This Content may contain links, to Web sites that are not operated by MINES. Linked Web sites may not be available in French. The Ministry neither endorses nor assumes any responsibility for the safety, accuracy or availability of linked Web sites or the information contained on them. The linked Web sites, their operation and content are the responsibility of the person or entity for which they were created or maintained (the "Owner"). Both your use of a linked Web site, and your right to use or reproduce information or materials from a linked Web site, are subject to the terms of use governing that particular Web site. Any comments or inquiries regarding a linked Web site must be directed to its Owner.

Copyright: Canadian and international intellectual property laws protect the Content. Unless otherwise indicated, copyright is held by the King's Printer for Ontario.

It is recommended that reference to the Content be made in the following form:

Hamilton, M., Montreuil, J.-F., Adlakha, E., Corriveau, L. and Bain, W. 2023. Base, critical, and precious metals mineralization in the metasomatic iron and alkali-calcic systems of the Southern Province in the Sudbury area: A geological guidebook; Geological Association of Canada–Mineralogical Association of Canada–Society for Geology Applied to Mineral Deposits, Joint Annual Meeting, Sudbury, Ontario, May 25–27, 2023, Field Trip FT01 Guidebook, Ontario Geological Survey, Open File Report 6391, 66p.

Use and Reproduction of Content: The Content may be used and reproduced only in accordance with applicable intellectual property laws. *Non-commercial* use of unsubstantial excerpts of the Content is permitted provided that appropriate credit is given and Crown copyright is acknowledged. Any substantial reproduction of the Content or any *commercial* use of all or part of the Content is prohibited without the prior written permission of MINES. Substantial reproduction includes the reproduction of any illustration or figure, such as, but not limited to graphs, charts and maps. Commercial use includes commercial distribution of the Content, the reproduction of multiple copies of the Content for any purpose whether or not commercial, use of the Content in commercial publications, and the creation of value-added products using the Content.

Contact:

FOR FURTHER INFORMATION ON	PLEASE CONTACT:	BY TELEPHONE:	BY E-MAIL:
The Reproduction of the EIP or Content	MINES Publication Services	Local: (705) 670-5691 Toll-Free: 1-888-415-9845, ext. 5691 (inside Canada, United States)	Pubsales.ndm@ontario.ca
The Purchase of MINES Publications	MINES Publication Sales	Local: (705) 670-5691 Toll-Free: 1-888-415-9845, ext. 5691 (inside Canada, United States)	Pubsales.ndm@ontario.ca
Crown Copyright	King's Printer	Local: (416) 326-2678 Toll-Free: 1-800-668-9938 (inside Canada, United States)	Copyright@ontario.ca

Ontario

Ontario Geological Survey
Open File Report 6391

Base, Critical, and Precious Metals Mineralization in the Metasomatic Iron and Alkali-Calcic Systems of the Southern Province in the Sudbury Area: A Geological Guidebook

2023

Ontario

ONTARIO GEOLOGICAL SURVEY

Open File Report 6391

Metasomatic Iron and Alkali-Calcic Systems of the Southern Province in the Sudbury Area: A Geological Guidebook

by

M. Hamilton, J.-F. Montreuil, E. Adlakha, L. Corriveau and W. Bain

2023

Parts of this publication may be quoted if credit is given. It is recommended that reference to this publication be made in the following form:

Hamilton, M., Montreuil, J.-F., Adlakha, E., Corriveau, L. and Bain, W. 2023. Base, critical, and precious metals mineralization in the metasomatic iron and alkali-calcic systems of the Southern Province in the Sudbury area: A geological guidebook; Geological Association of Canada–Mineralogical Association of Canada–Society for Geology Applied to Mineral Deposits, Joint Annual Meeting, Sudbury, Ontario, May 25–27, 2023, Field Trip FT01 Guidebook, Ontario Geological Survey, Open File Report 6391, 66p.

Users of OGS products should be aware that Indigenous communities may have Aboriginal or treaty rights or other interests that overlap with areas of mineral potential and exploration.

© King's Printer for Ontario, 2023

© King's Printer for Ontario, 2023

ISBN 978-1-4868-7217-6 (print)
ISBN 978-1-4868-7218-3 (PDF)

Open File Reports of the Ontario Geological Survey are available for viewing at the John B. Gammon Geoscience Library in Sudbury and at the regional Mines and Minerals office whose district includes the area covered by the report (see below).

Copies can be purchased at Publication Sales and the office whose district includes the area covered by the report. Although a particular report may not be in stock at locations other than the Publication Sales office in Sudbury, they can generally be obtained within 3 working days. All telephone, fax, mail and e-mail orders should be directed to the Publication Sales office in Sudbury. Purchases may be made using cash, debit card, VISA, MasterCard, cheque or money order. Cheques or money orders should be made payable to the *Minister of Finance*.

John B. Gammon Geoscience Library 933 Ramsey Lake Road, Level B2 Sudbury, Ontario P3E 6B5	Tel:	(705) 670-5614
Publication Sales 933 Ramsey Lake Rd., Level B2 Sudbury, Ontario P3E 6B5	Tel: Toll-free: Fax: E-mail:	(705) 670-5691 (local) 1-888-415-9845 ext. 5691 (705) 670-5770 pubsales.ndm@ontario.ca

Regional Mines and Minerals Offices:

Kenora – Suite 104, 810 Robertson St., Kenora P9N 4J2

Kirkland Lake – 1451 Hwy. 66, P.O. Box 40, Swastika P0K 1T0

Red Lake – 227 Howey Street, P.O. Box 324, Red Lake P0V 2M0

Sault Ste. Marie – 740 Great Northern Rd., Sault Ste. Marie P6A 5M1

Southern Ontario – 126 Old Troy Rd., Tweed K0K 3J0

Sudbury – 933 Ramsey Lake Rd., Level B2, Sudbury P3E 6B5

Thunder Bay – Suite B002, 435 James St. S., Thunder Bay P7E 6S7

Timmins – Ontario Government Complex, P.O. Bag 3060, 5520 Hwy. 101 East, South Porcupine P0N 1H0

Every possible effort has been made to ensure the accuracy of the information contained in this report; however, the Ontario Ministry of Mines does not assume liability for errors that may occur. Source references are included in the report and users are urged to verify critical information.

If you wish to reproduce any of the text, tables or illustrations in this report, please write for permission to the Manager, Publication Services, Ministry of Mines, 933 Ramsey Lake Road, Level A3, Sudbury, Ontario P3E 6B5.

Cette publication est disponible en anglais seulement.

Parts of this report may be quoted if credit is given. It is recommended that reference be made in the following form:

Hamilton, M., Montreuil, J.-F., Adlakha, E., Corriveau, L. and Bain, W. 2023. Base, critical, and precious metals mineralization in the metasomatic iron and alkali-calcic systems of the Southern Province in the Sudbury area: A geological guidebook; Geological Association of Canada–Mineralogical Association of Canada–Society for Geology Applied to Mineral Deposits, Joint Annual Meeting, Sudbury, Ontario, May 25–27, 2023, Field Trip FT01 Guidebook, Ontario Geological Survey, Open File Report 6391, 66p.

Contents

FIGURES

PHOTOS

TABLES

Preface

This geological field trip guidebook was prepared initially for use with a field trip (trip number FT01) for the joint annual meeting of the Geological Association of Canada, the Mineralogical Association of Canada and the Society for Geology Applied to Mineral Deposits (GAC–MAC–SGA) in Sudbury, Ontario, May 25–27, 2023.

Sudbury is one of the world's premier nickel-copper mining districts, a significant platinum group element (PGE) producer, and one of the oldest, largest, and best-exposed meteorite impact sites on Earth. As the world's largest integrated mining technology cluster, Sudbury has a vibrant mineral exploration and mining community that includes several major producers, numerous junior exploration companies, dozens of mining supply and service companies, 3 post-secondary educational institutions and associated exploration and mining centres, and several Ontario government mining and mineral ministry offices, making Sudbury one of the best places in the world to host a multidisciplinary meeting of this type. The City of Greater Sudbury, the largest city by landmass in Ontario, lies amidst glacially shaped ridges, green boreal forests, and contains 330 lakes over 10 hectares in size and 112 lakes over 100 hectares in size. The success of more than 40 continuous years of environmental reclamation efforts has led to numerous national and international awards, including a Government of Canada *Environmental Achievement Award*, a United States *Chevron Conservation Award*, and a United Nations *Local Government Honours Award*. And, as part of Sudbury's continuing regreening efforts, the milestone 10 millionth tree was planted in July 2022.

The theme of the GAC–MAC–SGA meeting—"Discovering Ancient to Modern Earth"—reflects the location of the meeting at the intersection of the Archean Superior Province and Proterozoic Southern and Grenville provinces, and Paleozoic–Quaternary cover sequences. The hybrid conference included a technical program of oral and poster presentations in Symposia, Special Sessions and Regular Sessions covering the complete spectrum of geoscience disciplines, which were complemented by 10 field trips, 6 workshops and 1 short course.

The meeting was hosted by the Harquail School of Earth Sciences and the Mineral Exploration Research Centre (MERC) at Laurentian University.

Abstract

Metasomatic iron and alkali-calcic (MIAC) mineral systems are regional hydrothermal systems extending over tens of kilometres and defining metallogenic belts of up to 1500 km long. These systems are significant but challenging targets for mineral exploration as they produce a wide range of deposit types with highly distinct metal associations. Their iron oxide-copper-gold (IOCG) deposits and their large variety of critical and precious metal deposits can have Ag, Au, Bi, Co, Cu, Fe, Mo, Ni, P, Pb, REE, U, W and Zn as primary commodities or by-products. Under the leadership of the Targeted Geoscience Initiative of the Geological Survey of Canada and supported by academia, industry and other governmental collaborators, a new framework has been established to define the relation between mineralization and alteration in MIAC systems. Using an alteration facies approach to mapping and describing drill core, a predictive exploration model based on alteration mapping and the identification of major corridors of fluid circulation can be developed to guide mineral exploration in MIAC systems.

In the Sudbury area (Ontario, Canada), the Long Lake gold, the Norstar copper-gold and the Scadding gold mines are the largest concentrations of mineralization associated with a MIAC system so far discovered in the Southern Geological Province. These past-producing mines are part of what is known as the Sudbury Gold Camp. This field trip will present the alteration facies and mineralization types that are indicative of a MIAC system in the Wanapitei region of the Southern Province. The diversity of observed mineral deposits relates to the involvement of multiple fluid sources that collected into large-scale plumes of fluids. The fluid plume then induced extensive leaching of compositionally diverse geological units and subsequent spatial overlaps of multiple alteration facies in restricted areas of the upper crust along preferential fluid circulation corridors.

MIAC systems show a wide range of diversity in terms of their degree of iron enrichment and the character of iron-bearing mineral assemblages within mineralized zones. In most currently mined MIAC systems, iron oxides (magnetite and hematite) are the primary mineralizing component and are associated with iron-rich polymetallic iron-oxide–dominated deposit types (e.g., IOCG and iron oxide-apatite deposits). MIAC systems can also generate zones of iron-rich mineralization in which iron silicates, iron sulfides and iron carbonates are the primary repositories of iron and iron oxides are sparse or absent. Moreover, MIAC systems also incorporate iron-poor mineralization styles in which iron oxides occur in low abundance, or are absent, and mineralized zones are associated with alkali-calcic alteration facies with varied quartz and carbonate content.

This field trip will illustrate a fraction of the diversity of iron-oxide–deficient to iron-poor alteration facies and mineralization types that are possible in those systems and how they relate with iron oxide-bearing alteration facies. To enhance the understanding of the mineralogy and the relation between alteration facies and mineralization, high-resolution X-ray fluorescence (XRF) maps of a suite of samples are presented in this guidebook. The field trip stops will also illustrate how the local attributes of the geological units of the area are influencing the geometry of the zones of alteration and mineralization. In the field trip area, in addition to the re-assessment of the new mineral potential of the past-producing gold mines, diamond-drilling results across prospects within the broad regional MIAC system suggest potential mineralization of significance at the Alwyn copper-gold, the Bristol Breccia gold-cobalt, the Glade gold, the Limestone nickel-platinum group element, the McLeod gold-copper and the Palkovics gold-cobalt prospects.

Worldwide, albitite corridors provide interconnections among deposits at the scale of mineral systems and their metallogenic belts, especially in areas that are sufficiently exposed to provide a broader regional field geology perspective. In this respect, the demonstration that albitite occurs, and that albitite corridors extend throughout the Huronian Supergroup from Cobalt to Sault Ste. Marie, is a key first element in re-assessing the mineral potential of the region.

Base, Critical, and Precious Metals Mineralization in the Metasomatic Iron and Alkali-Calcic Systems of the Southern Province in the Sudbury Area: A Geological Guidebook

Mallory Hamilton[1], Jean-François Montreuil[1], Erin Adlakha[2], Louise Corriveau[3] and Wyatt Bain[4]

Ontario Geological Survey
Open File Report 6391
2023

---

[1]Project Geologist, MacDonald Mines Exploration, 145 Wellington St. West, Suite 1001, Toronto, Ontario, M5J 1H8 mhamilton@macdonaldmines.com

[1]Chief Geologist, MacDonald Mines Exploration, 145 Wellington St. West, Suite 1001, Toronto, Ontario, M5J 1H8 jfmontreuil@macdonaldmines.com

[2]Department Chair, Associate Professor, Department of Geology, Saint Mary's University, Halifax, Nova Scotia erin.adlakha@smu.ca

[3]Research scientist, Geological Survey of Canada, Natural Resources Canada, 490 de la Couronne, Québec, Québec, G1K 9A9 louise.corriveau@NRCan-RNCan.gc.ca

[4]Postdoctoral Fellow, Lakehead University, Thunder Bay, Ontario wmbain@lakeheadu.ca

Introduction

The Sudbury region is well-known for the world-class nickel-copper-platinum group element (Ni-Cu-PGE) deposits associated with the Sudbury Igneous Complex (SIC). The Southern Province around Sudbury is also known for its enigmatic gold and polymetallic gold deposits that include the former Long Lake, Scadding and Norstar mines, all of which were exploited at some point during the 20th century. Previous scientific (Schandl and Gorton 2007; Potter 2009), government (Gates 1991; Corriveau 2007; Farrow 2016) and industry work (Yarie and Wray 2019) have proposed that Scadding Township and the Wanapitei area had potential for iron oxide-copper-gold (IOCG) deposits. Recent progress in the understanding of the geological, geophysical and geochemical footprints of metasomatic iron and alkali-calcic (MIAC) mineral systems in Canada and globally (Corriveau et al. 2010a, 2016, 2022a-e; Hayward et al. 2013; Montreuil et al. 2013, 2015, 2016a, 2016b; McCafferty et al. 2019; Adlakha et al. 2022; Blein et al. 2022; Chen and Zhao 2022) and extensive alteration mapping across the Scadding and other regional prospects of the Wanapitei Lake area illustrate that the former Scadding gold and polymetallic prospects in the area belong to a MIAC system, the demonstration of which is provided in this guidebook. This demonstration provides additional support that regional scale MIAC mineral systems extend across the Sudbury district and host some of its former gold mines beyond Scadding Township. If correct, this would considerably expand the exploration potential of the Southern Province in northeastern Ontario, considering that diagnostic indicators of MIAC systems are also observed in the Cobalt–Temagami and the Sault Ste. Marie areas (e.g., hematite breccia in albitite *in* Potter 2009).

Within the MIAC systems terminology, *metasomatic* is reflective of the extreme changes in composition and mineral assemblages undergone by host rocks through fluid-rock reactions at local to regional scale (Blein et al. 2022; Corriveau et al. 2022a). *Iron and alkali-calcic* describes the systematic associations in the varied proportions of alkalis (Na, K), alkaline-earths (Ca, Mg, Ba) and iron (Fe) in a series of diagnostic minerals within the alteration facies that they form (Corriveau et al. 2022b). These alteration facies result from the suite of metasomatic fluid-rock reactions that occurs during the spatial and temporal evolution of these mineral systems (Corriveau et al. 2016, 2022a, 2022b). Each alteration facies can be associated with specific mineralization types that are variably endowed in base, critical and/or precious minerals (Corriveau et al. 2022a, 2022c).

Seminal papers (Hitzman et al. 1992; Williams et al. 2005; Porter 2010a, 2010b; Ehrig et al. 2012), extensive compilations (Dhnaram et al. 2021), and books and special issues (Porter 2000, 2002, 2010a; Skirrow and Davidson 2007; Corriveau and Mumin 2010; Slack et al. 2016; Corriveau et al. 2022e) provide extensive descriptions of the diversity of deposit types associated with MIAC systems. A key distinguishing aspect of MIAC systems is their significant metallogenic potential considering their association with iron oxide-copper-gold (IOCG) and iron oxide-apatite (IOA) deposits, and with a growing inventory of iron-rich to iron-poor base, critical and precious mineral deposits that cannot be classified as IOCG deposits *sensu stricto* (Corriveau et al. 2016, 2022a; Hofstra et al. 2021). Compilation of known deposits within MIAC systems (Corriveau et al. 2018) indicates that their resources and reserves contain as primary commodities or by-products Ag, *Al*, Au, Bi, Co, Cu, F, Fe, *In*, Mo, Ni, P, Pb, PGE, Re, REE, *Sb*, *Te*, W, U, *V* and Zn (16 critical mineral commodities identified by the Government of Canada are highlighted in red, known resources are in standard font and potential by-products are in italics; Natural Resources Canada 2021). The wide range of conventional and critical mineral commodities formed in MIAC systems emphasizes both their importance to the global economy and their high value as an exploration target with a high degree of resiliency to economic cycles.

These deposit types are part of the solution for diversifying Canada's critical mineral production (Gadd et al. 2022). Considering the large spectrum of deposits that occur in MIAC systems, the distinctive range in degree of iron enrichment in mineralized zones and alteration facies, and the fact that mineralization in these systems can be dominantly iron-oxides, iron-sulfides, iron-silicates or iron-

carbonates, ***M**etasomatic **I**ron and **A**lkali-**C**alcic (MIAC) system* is a key designation which accounts for the diversity of mineralization styles and deposit types that can occur within a mining district.

Building on the recent progress in the understanding of MIAC systems, this field trip in the Wanapitei Lake area in the Southern Province will present the alteration facies and mineralization types that are indicative of the presence of a MIAC system in the region. The field trip will illustrate only a fraction of the diversity of iron oxide-bearing to iron oxide-deficient to iron-poor alteration facies and mineralization types that are possible in those systems and how they relate with iron and alkali-calcic alteration facies that are described in detail in Corriveau et al. (2022d). This guidebook also provides details on how the local geology of specific areas (e.g., the mineralogy, geochemistry, and distribution of geological units) influences the geometry of the zones of alteration and mineralization, as shown during various stops on this field trip.

To document and image the mineralogy and the spatial and/or textural relationships between alteration facies and mineralization, this guidebook includes high-resolution Micro X-Ray Fluorescence (μXRF) false colour elemental distribution maps for representative samples of the alteration and mineralization styles discussed throughout this trip. The μXRF maps enable characterization of the complex mineralogy and timing relationship between alteration facies and mineralization that are systematics of different systems at the scale of drill core. Analyses were performed using a Bruker M4 TornadoPLUS μXRF spectrometer at the Mineral Imaging and Analysis Lab at Saint Mary's University, Halifax. For MIAC systems, this instrument enables high-resolution imaging (using a beam width of 20 μm) of the key chemical and mineralogical distributions and textures at the scale of drill core. At this scale, the timing relationships among alteration facies are best studied because the scale of thin sections is too small to properly record the prograde evolution of systems as discussed in detail in Corriveau et al. (2022b). Until now, field observations have been coupled with hydrofluoric acid (HF) etching and cobaltinitrite staining to characterize the metasomatic processes at this scale (Corriveau et al. 2010a, 2022b). The benchtop XRF removes the health and safety issues of HF use in laboratories while providing additional exceptional information on metasomatic processes, such as the distribution of critical minerals.

This field trip complements a special session at the Sudbury 2023 GAC–MAC–SGA meeting where the processes forming MIAC systems will be compared with those forming other iron-rich mineral deposits such as magmatic nelsonites and their titanium and phosphate deposits, iron-carbonatites, magnetite-cumulates and their vanadium deposits, etc. Iron-rich deposits have become an increasingly important exploration target as many can be richly endowed in critical metals and other commodities that are key for a greener future (Gadd et al. 2022). These deposits all share atypical origins that force novel research avenues and models (Tornos et al. 2017; Bain et al. 2020). The shared iron-rich nature might suggest a common process driving the availability and mobility of iron and critical melts, as well as the stability of the host mineral phases. However, consensus is lacking, and the answers may not be unique. Genetic models for these systems invoke a wide range of contrasting magmatic and metasomatic processes, and key questions regarding the dominance of and/or feedback between processes on the system and deposit scales pervade. Moreover, recent research suggests the potential involvement of a range of fluid types in iron- and critical metal-rich systems that are distinct from the silicate melts and aqueous chloride solutions typically involved in the formation of conventional base- and precious-metal resources. Taken together, these factors underpin a vigorous and wide-ranging contemporary debate focused on the formation of a spectrum of iron oxide-dominated and iron-rich deposit types that represent a frontier of ore deposit research.

SAFETY

All field trip stops are located off main gravel roads or are along private mine roads, bush roads and/or trails. Although two-wheel drive vehicles are capable of accessing most stops, vehicles with higher clearance and all-wheel or four-wheel drive are preferred. Additionally, bush roads and/or trails may be accessed by others using all-terrain vehicles (ATVs) and other off-road vehicles; therefore, care should always be exercised when parking to allow for other motorists to get past while vehicles are parked. Use of safety vests and/or bright clothing is also recommended to improve your visibility to other motorists. Sturdy boots are needed to access and walk across the outcrops and along the trails. In May, the ground might be still wet in places from the snow melt. A hat is also recommended to protect from the sun.

Hazards on the Scadding mine site include three large pits. The pits are filled with water, and the East-West pit has additional fencing around it because of steep rock faces and falling hazards. Outcrops on top of the East-West pit will be examined during Stop 4. Extreme caution is to be used while visiting this stop because of the steep rock cliff close to the edge of the pit; therefore, participants will be divided into two groups based on numbers to ensure everyone has space to safely observe the stop. Access to this stop will be via a short path starting at the bottom of the pit; therefore, participants should also be conscious of "slips, trips and falls" hazards.

Cell phone service coverage varies by service provider, and may not always be present, especially around the Alwyn Mine stop (Stop 8). A SpotX satellite communications device will be carried by trip leaders to all stops. This device is capable of sending out help messages, being tracked from home base, and contacting emergency services.

Regional Geology and Geological Setting

This excursion covers a selection of alteration and mineralization zones located approximately 25 km east of the city of Greater Sudbury in the Paleoproterozoic (2.45–2.16 Ga) Southern Province, Ontario, Canada (Card et al. 1972; Bennett et al. 1991; Krogh et al. 1984). The Southern Province is a fold and thrust belt principally composed of supracrustal and intrusive units that stretch from Minnesota (United States) to the Cobalt area (Ontario) and locally into western Quebec. In Ontario, the Southern Province is exposed continuously from the city of Sault Ste. Marie east toward the Quebec–Ontario border. The Huronian Supergroup is the most important geological unit in the Ontarian section of the Southern Province, which also includes the Sudbury impact structure, which occurred at 1.85 Ga (Krogh et al. 1984). The Sudbury impact structure had an initial diameter estimated to exceed 200 km, which transformed into its now smaller, elliptical shape during the late stages of the Penokean Orogeny, from 1.9 to 1.83 Ga (Deutsh et al. 1995; Rousell et al. 1997; Riller 2005; Tschirhart and Morris 2012; Bleeker and Kamo 2022). The Sudbury impact structure includes the Sudbury Igneous Complex (SIC) and the richly endowed nickel-copper-platinum group element (Ni-Cu-PGE) deposits for which the city of Greater Sudbury is famous (cf. Naldrett 1984; Spray et al. 2004). In the Sudbury area where the field trip takes place, the Southern Province is bounded to the north by Archean rocks of the Superior Province and to the east and southeast by the high-grade metamorphic rocks of the Grenville Province (Figure 1). To the southwest, along the north shore of Lake Huron the Southern Province is overlain by Paleozoic sedimentary rocks.

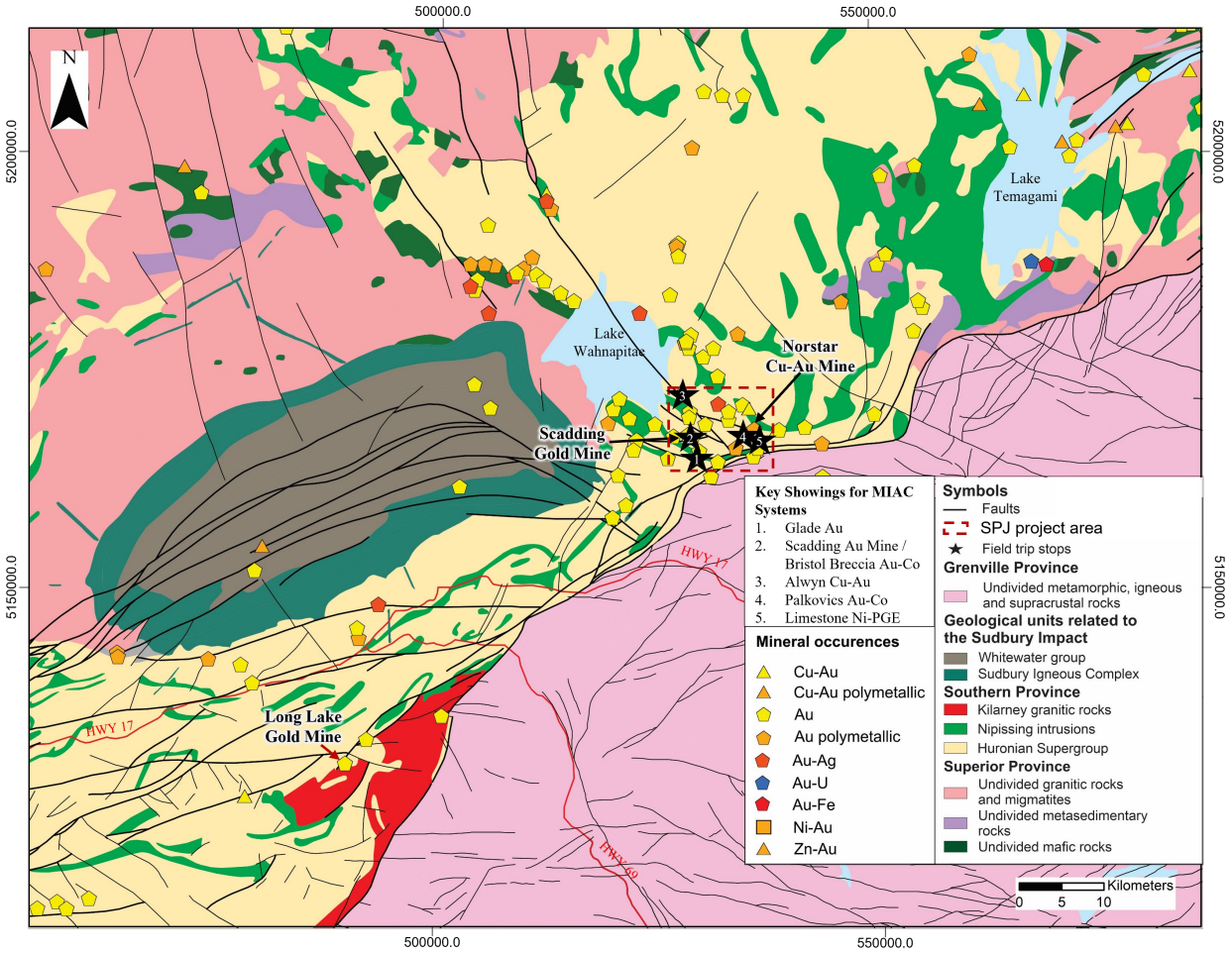

Figure 1. Regional geology of the Sudbury area. Geology *modified from* Ontario Geological Survey (2011) with selected polymetallic mineral occurrences in the Southern Province *from* Ontario Geological Survey (2023). Universal Transverse Mercator (UTM) co-ordinates using North American Datum 83 (NAD83) Zone 17N.

HURONIAN SUPERGROUP

The Huronian Supergroup is a 5 to 10 km thick stratigraphic succession divided into four groups, with a fifth suggested by some authors (Figure 2; Robertson et al. 1969; Wood 1973; Bennett et al. 1991; Al-Hashim 2016). The Elliot Group forms the basal unit of the Huronian Supergroup and unconformably overlies the rocks of the Superior Province (Al-Hashim 2016). It is composed of a mixture of sedimentary and volcanic units, and its development is interpreted to have occurred during the initial rifting of the Superior Province, as indicated by a U-Pb age on zircons at 2452.5±6.2 Ma in a volcanic unit in the Thessalon area of the Southern Province (Ketchum et al. 2013). The Hough Lake, Quirke Lake and Cobalt groups overlie the Elliot Lake Group and represent three distinct episodes of sedimentation associated with glaciogenic and/or tectonic uplift and/or subsidence cycles and the accompanying sea level transgressions and regressions (cf. Bennett et al. 1991). Each group includes a basal conglomerate unit, which is overlain by a pelite and greywacke unit, and then by a quartz-feldspar sandstone unit (cf. Robertson et al. 1969; Bennett et al. 1991). The Quirke Lake Group is unique in the stratigraphic sequence, as it is the only group that contains a carbonate-dominated unit, the Espanola Formation, which occurs at the level of the pelite-greywacke unit in the other groups, and which overlies the Bruce Formation conglomerate (cf. Robertson et al. 1969; Bennett et al. 1991; Bekker et al. 2005; Al-Hashim

2016). The Hough Lake Group conformably to disconformably overlies the Elliot Lake Group (Al-Hashim 2016). In the Bruce Mines and Espanola areas, the Cobalt Group is observed to unconformably overlie both the Hough Lake and Quirke Lake groups, whereas in the Cobalt area, it unconformably overlies the Superior Province. The Hough Lake and Quirke Lake groups are interpreted to have been deposited into a rift basin, whereas the overlying Cobalt Group is interpreted as being deposited along a passive margin at the southern margin of the rifted Superior Province.

INTRUSIVE EVENTS IN THE SOUTHERN PROVINCE

Many generations of intrusions are present in the units of the Huronian Supergroup in the Ontario section of the Southern Province, and some also occur in the Archean rocks of the Superior Province (*see* Figure 2). Syn-rift felsic intrusions, such as the Creighton pluton, were emplaced between *circa* 2.48 Ga and 2.46 Ga (Bleeker et al. 2015) and typically intruded the volcanic units of the Elliot Lake Group. The East Bull Lake intrusive complex, the Shakespeare-Dunlop, and River Valley mafic intrusions were emplaced from 2.49 Ga to 2.47 Ga close to the base of the Huronian Supergroup supracrustal rocks, resulting from early-stage rifting in the Superior Province during that time (Krogh et al. 1984; James et al. 2002). The period between 2.219 Ga and 2.210 Ga corresponded to the emplacement of the Nipissing gabbroic sills throughout the Southern Province (Lightfoot and Naldrett 1996; Davey et al. 2019; Corfu and Andrews 1986). This mafic magmatism was followed by two periods of felsic and mafic magmatism (and

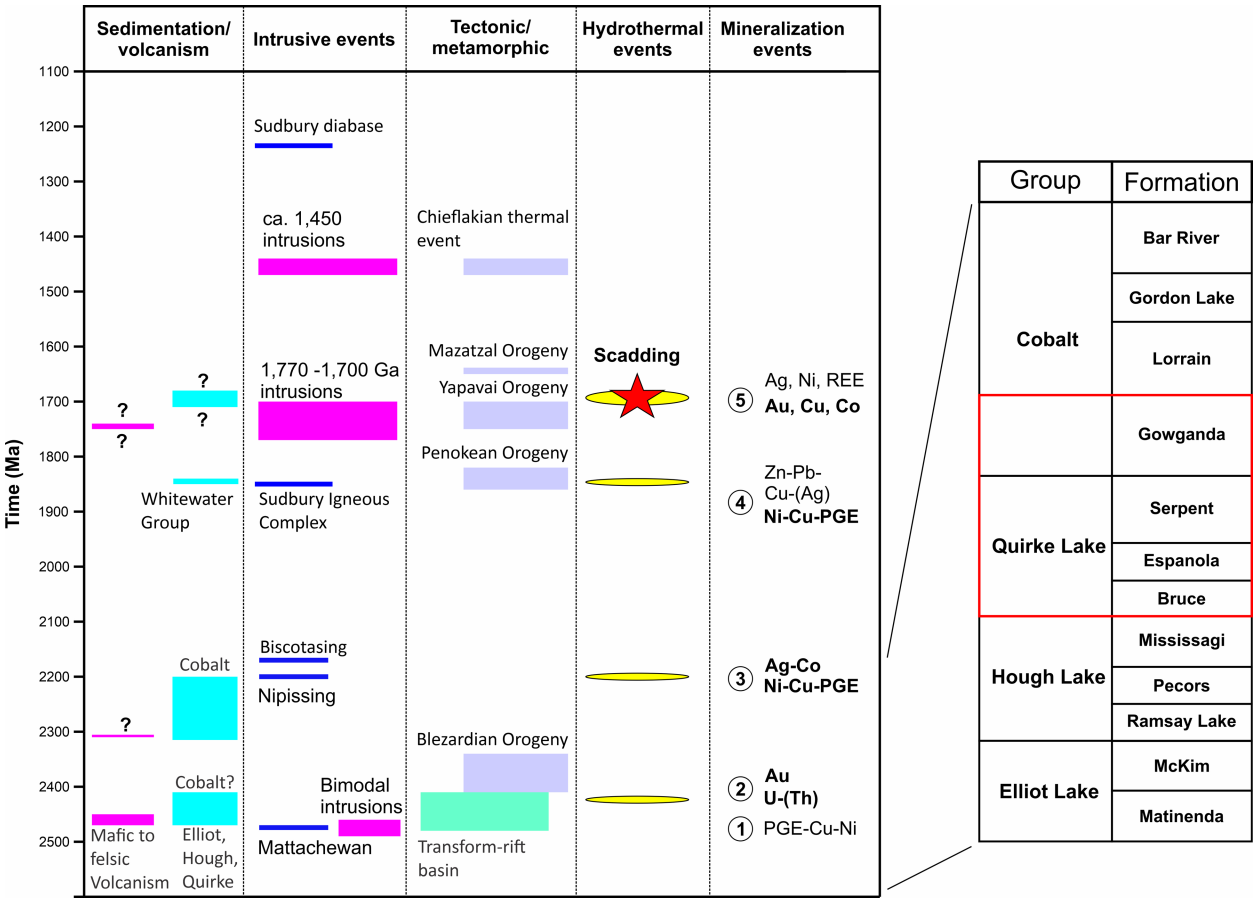

Figure 2. Geological history of the Southern Province (left) with the current Huronian Group stratigraphic nomenclature scheme on the right (stratigraphy *from* Robertson et al. 1969; figure inspired *from* Ames et al. 2008). Red lines indicate the stratigraphic units of most relevance to the field trip stops.

volcanism) that occurred between 1.77 Ga and 1.69 Ga and at *circa* 1.45 Ga, both within the Southern Province and immediately to the south in the Killarney Magmatic Belt (Davidson et al. 1992; Krogh 1994). The older period of felsic and mafic magmatism includes the intrusions of the Killarney granitic suite (which also occur within the Grenville Province, not shown in Figure 1), which in the Southern Province includes the Eden Lake Pluton, the Killarney Pluton and the Cutler Batholith. The younger period of felsic magmatism at *circa* 1.45 includes the Chief Lake granite and granitic pegmatite intrusion (Krogh 1994; Davidson et al. 1992).

A variety of mafic dikes occur within the Superior and the Southern provinces. The oldest of these, the Matachewan dike swarm, was emplaced at *circa* 2.46 Ga (Bleeker et al. 2015), similar in timing to the emplacement of the East Bull Lake and related intrusions, but pre-Huronian Supergroup deposition. Dikes of the Biscotasing (2.167 Ga), Marathon (2.124–2.102 Ga) and "Trap" (*circa* 1.75 Ga) dike swarms are also known to cut rocks of the Huronian Supergroup (Bleeker et al. 2015; Easton et al. 2020). The northwest-trending Sudbury (olivine) dike swarm was emplaced at 1.238 Ga (Krogh et al. 1987), and along with the east-trending Grenville dike swarm (0.59 Ga), represents the youngest generation of dike swarm emplacement in the Sudbury area.

OROGENY AND DEFORMATION IN THE SOUTHERN PROVINCE

Multiple deformation events affected the units of the Southern Province (*see* Figure 2). The apocryphal Blezardian Orogeny, supposedly bracketed to a period from 2415 to 2343 Ma (Raharimahefa et al. 2014), is considered by some workers to have affected the lower groups of the Huronian Supergroup, although clear evidence for this orogenic event has remained elusive (Jackson 2001; Raharimahefa et al. 2014). Evidence of Nipissing sills intruded across the axial planes of regional folds that formed before their emplacement could be related to the Blezardian Orogeny, but it could be evidence also for a syn-Nipissing gabbro deformation event (Jackson 2001). The Penokean Orogeny, from 1.86 Ga to 1.82 Ga, is well constrained in the Lake Superior region, where it affects correlative units of the Southern Province in the United States (Schulz and Cannon 2007). The Penokean Orogeny was originally interpreted to represent a significant deformation and metamorphic event in the Ontario section of the Southern Province; however, research work west of Sudbury and in the surrounding areas is suggesting that the effects of Penokean orogenic compression are marginal in the Sudbury area (Jackson 2001; Piercey et al. 2007; Mukwakwami et al. 2014; Raharimahefa et al. 2014; Bleeker et al. 2015). A key regional deformation marker across the region are the "Sudbury Breccias", related to the Sudbury impact event at 1.85 Ga, with their diagnostic fluidization flow texture, that extend from the impact structure outward for at least 100 km (cf. Dressler 1984; Roussel et al. 2003).

Important tectonic deformation associated with some metamorphism in the Southern Province occurred during the Yavapai Orogeny in a time period bracketed in the Sudbury area between 1.744 Ga and 1.704 Ga (Davidson et al. 1992; Jackson 2001; Piercey et al. 2007; Raharimahefa et al. 2014). The Mazatzal Orogeny (*circa* 1.65 Ga) caused shear zone reactivation in the South Range of the Sudbury impact structure and is recorded by overprinting tectonic fabrics (Bailey et al. 2004; Papapavlou et al. 2018). Lastly, the Grenville Front, last active at *circa* 0.99 Ga (Krogh 1994), separates rocks of the Southern Province from the high-grade (amphibolite to granulite facies) metamorphic rocks of the Grenville Province. In the Sudbury area east of the SIC, rocks of the Southern Province located within 1 km of the Grenville Front in the footwall are variably rotated and transposed by Grenville Province tectonic fabric. Fault and shear zone reactivation in the Southern Province near the Grenville Province also are associated with deformation taking place during the Grenville Orogeny (*sensu lato*).

The Murray Fault System is a network of typically north-verging and moderately south-dipping, east-trending faults and deformation zones in the Southern Province. West and south of the SIC, the

Murray Fault is the largest structure of the Murray Fault System and marks the boundary between two metamorphic domains (Jackson 2001). The Murray Fault is interpreted as an original rift-related fault that was active during sedimentation of the Huronian Supergroup and was reactivated during each subsequent orogeny that affected the Southern Province (cf. Fueten and Redmond 1992; Jackson 2001). A network of faults tentatively associated with the Murray Fault System forms the South Range Shear Zone that crosscuts and deforms the SIC (Shanks and Schwerdtner 1991). West of the Sudbury area, peak-Yavapai orogenic deformation formed open to sub-isoclinal and upright to inclined folds and well-developed foliations trending parallel to the Murray Fault (Murphy 1999). East of the SIC, the Murray Fault merges with the Grenville Front and is interpreted to become the location of the basal thrust of the Grenville Orogen (cf. Davidson and Ketchum 1993). This extension of the Murray Fault in the Wanapitei Lake area, immediately north of the Grenville Front, is named the Ess Creek deformation zone (Easton and Murphy 2002).

Networks of northwest-trending faults are also important structures in the Southern Province (Easton 2006). In the field trip area, the most important structure of that set is the north-northwest-trending McLaren Lake Fault. With its parallel and satellite deformation zones, it is referred to herein as the McLaren Lake Fault Zone ("MLFZ"), extending approximately 12 km southeast of Lake Wahnapitae on the SPJ Project site until it gets deflected into the Grenville Front. In the field trip area, the MLFZ is associated with copper-gold mineralization in quartz-carbonate veins at the historical Alwyn-Porcupine and Ashigami mines. Along with the Murray Fault System, northwest-trending structures are typically associated with alteration and mineralization associated with the development of the MIAC system (*see* Figures 1 and 2; Gates 1991; Potter 2009).

ATTRIBUTES OF METASOMATIC IRON AND ALKALI-CALCIC SYSTEMS

Metasomatic iron and alkali-calcic systems are continental-scale mineral systems typically located along deep lithosphere roots that provide a mantle to upper crust connection during continental orogeneses. A single MIAC system can extend over 50 km and can be interconnected with others along hundreds of kilometres. A MIAC system can also form as trains of metallogenic belts over a thousand kilometres long (Chen and Zhao 2022). Their formation is generally contemporaneous with a magmatic flare-up that forms early volcanic centres and subvolcanic intrusions prior to (e.g., Great Bear magmatic zone, Olympic Cu-Au Province), or coeval with (e.g., Andes), episodes of voluminous magmatism that form batholiths or other large intrusive complexes (Montreuil et al. 2016a; Ootes et al. 2017; Wade et al. 2019; Del Real et al. 2021). The temporal and spatial evolution of the large fluid plumes that mobilize Fe, alkalis, and other elements, and drive systematic suites of metasomatic reactions, is the primary factor controlling the evolution of MIAC systems (Corriveau et al. 2022a-d). The nature and genesis of mineralizing fluids (i.e., liquids, vapors, melts, combinations thereof, etc.) within these plumes is controversial, and definitively not unique, but based on the common occurrence of coeval magmatism within MIAC systems, some components of the fluids within the plume possibly arise either as a direct product of melt-fluid evolution and/or as a by-product of melt-host rock interactions at depth, and as metasomatism proceeds regionally, inducing extensive recharge and discharge of elements within the plume (e.g., Hofstra et al. 2016; Tornos et al. 2017; Ovalle et al. 2018; Hou et al. 2018; Bain et al. 2020; Corriveau et al. 2022c).

In all cases, fluid egress away from its source is focused along local and regional discontinuities (e.g., fault and shear zones, some grounded into trans-lithospheric structures, and at the more local scale, contacts between rock units, contacts between different beds or laminations, hinge zones of folds, etc.) where fluid-rock reactions give rise to metasomatism on various scales within a geological province (Williams et al. 2005; Austin and Blenkinsop 2008; Kontak et al. 2008; Oliver et al. 2017; Corriveau et al. 2016; Hayward et al. 2016; Montreuil et al. 2016b). In the same way, mineral deposits are formed

where favorable geological traps are present along these discontinuities and where the metasomatic system has evolved to alteration facies compatible with mineralization (Figure 3; Corriveau et al. 2016, 2022c; Hayward et al. 2016; Montreuil et al. 2016b; Blein et al. 2022).

Metasomatic iron and alkali-calcic systems evolve temporally and spatially following a relatively systematic suite of metasomatic reactions that involve iron (Fe), alkaline (Na, K), alkaline-earth elements (Ca, Mg, Ba), Si and CO_2. Sodic (Na) metasomatism resulting in the formation of corridors of albitite occurs in the early stages of the evolution of a MIAC system and marks the initial ingress of fluids and heat carried by the fluid plume in the geological province (Oliver et al. 2004). Sodic-metasomatism is the most spatially extensive manifestation of metasomatism in MIAC systems and occurs along geological discontinuities at all scales. The distribution of albitite corridors can provide valuable information on areas of enhanced crustal permeability in the geological province, as was used by Farrow (2016) in the Ontario Geological Survey Recommendation for Exploration. In areas where carbonate units are present, the formation of skarn can be contemporaneous with sodic alteration (Corriveau et al. 2022b) and the association of skarn to systems developing IOCG deposits is common at regional to deposit scale (Ismail 2015; Montreuil et al. 2016b; Fabris et al. 2018; Keyser et al. 2022).

Sodic metasomatism is then followed by the formation of diagnostic iron-rich to iron-poor alteration facies. For iron-rich alteration facies, Fe is typically combined with alkaline (Na, K), alkaline-earth elements (Ca, Mg, Ba), silica (Si) or carbonate (CO_2). Iron-rich alteration facies and their relative timing relationships are described in detail in Corriveau et al. (2022b, 2022d) for systems in Canada and giant mining districts in Australia and are not reviewed herein any further. Each iron-rich alteration facies can be associated with specific mineralization types and metal assemblages that can be prognosticated based on the suite

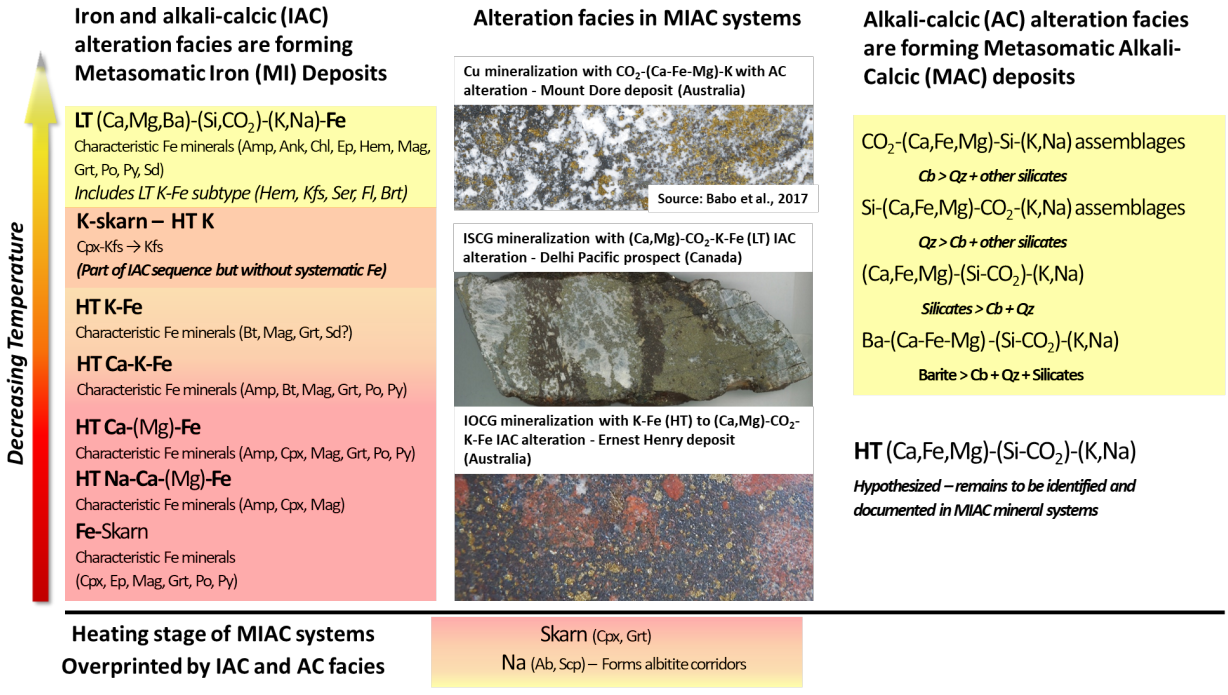

Figure 3. MIAC alteration facies as a function of temperature. Abbreviations: AC, alkali-calcic; HT, high temperature; IAC, iron and alkali-calcic; LT, low temperature.

of major elements associated with iron (Corriveau et al. 2022a, 2022c). For iron-poor alteration facies, CO_2, Si, alkaline and alkaline-earth elements are variably combined, but the association between specific facies and mineralization types remains to be established. Figure 3 illustrates the alteration facies relative to the temperature of formation that are possible in MIAC systems.

The mineral deposits formed in MIAC systems can be grouped in two classes that are based on the association between peak mineralization and iron-rich or iron-poor alteration facies. For deposits in which peak mineralization is associated with iron-rich alteration facies, eight classes of mineral deposits can be defined (Corriveau et al. 2022c; Montreuil et al. 2022).

- A class of **Fe** deposits that include skarn iron, iron oxide and iron oxide apatite (IOA) deposits.
- A class of iron-rich **W** deposits in which tungsten (W) mineralization is typically associated with skarn (Fe) assemblages to form skarn-tungsten deposits.
- A class of iron-rich **REE** deposits in which the rare earth elements (REE) are typically sourced, remobilized and concentrated from a pre-existing IOA deposit. The zones of REE mineralization at potentially economic grades can spatially overlap with IOA mineralization to form IOA-REE deposits or can be decoupled from the IOA deposit to form breccia-hosted-REE or iron silicate-REE deposits.
- A class of polymetallic and iron-rich **Ni** deposits that can include cobalt (Co), Cu and PGE. In certain iron-rich Ni deposits, the zones of Ni mineralization contain abundant iron oxide and apatite to form IOA-Ni deposits. In other deposits or prospects, the zones of Ni mineralization contain abundant iron sulfides without significant iron oxides or apatite to form iron sulfide or iron sulfide-apatite Ni mineralization.
- A class of polymetallic and iron-rich **Co** deposits that are typically rich in arsenic (As) and in which significant gold (Au), bismuth (Bi) and Cu can be present. The zones of Co mineralization in polymetallic Co deposits are typically associated with abundant iron oxides or iron silicates to form polymetallic iron oxide-Co or polymetallic iron silicate-Co deposits.
- A class of polymetallic **Cu** deposits in which the zones of Cu mineralization can contain abundant iron oxide, iron silicate or iron sulfides, and in which significant Ag, Au, Co and uranium (U) can be present. This class of deposits encompasses iron sulphide copper-gold (ISCG), magnetite and hematite-group iron oxide copper-gold (IOCG) deposits, iron silicate-copper-gold deposits and skarn (Cu-Au) deposits. Skarn (Cu-Au) deposits are related to Cu-Au mineralization formed at the potassic skarn alteration facies.
- A class of iron-rich **Au** deposits that can be Au-only or polymetallic deposits with significant Ag, Bi and Cu. Gold mineralization is typically associated with abundant iron silicates or iron oxides to form iron oxide-gold or iron silicate-gold deposits.
- A class of iron-rich **U** deposits in which U mineralization is typically associated with iron oxide or iron silicates. Typically, the zones of U mineralization are albitite-hosted. This class includes albitite-hosted U and iron oxide-U deposits.

Although not as well-constrained as their iron-rich counterparts, at least three classes of mineral deposits can be defined for deposits in which peak mineralization is associated with iron-poor alteration facies (Babo et al. 2017; Le 2021; Corriveau et al. 2022c; Montreuil et al. 2022). Additional classes of deposits containing REE and U are likely present in MIAC systems, but more work remains to be done to define them.

- A class of iron-poor **Au** deposits that can include Co and that can be albitite-hosted. In this class of deposits, Au mineralization is typically the associated alteration facies forming carbonate-quartz to quartz-carbonate mineral assemblages.

- A class of iron-poor **Cu** deposits that can also include significant Ag, Au and zinc (Zn) and that can be albitite hosted. In this class of deposits, Cu mineralization is associated with alteration facies forming carbonate-quartz to quartz-carbonate mineral assemblages.
- A class of iron-poor **Mo-Re** (molybdenum-rhenium) deposits in which Mo mineralization is associated with intense potassic alteration that can overprint pre-existing albitites.

ALTERATION AND MINERALIZATION IN THE SOUTHERN PROVINCE ASSOCIATED WITH MIAC HYDROTHERMAL ACTIVITY

In terms of alteration and mineralization, five periods of significant mineralization can be identified in the Southern Province (*see* Figure 2). In chronological order they are:

1. Ni-Cu-PGE mineralization associated with the emplacement of syn-rifting intrusions prior to and during the early stages of sedimentation and deposition of the Huronian Supergroup.
2. Syn-sedimentation, placer uranium and placer gold mineralization in the Elliot Lake and Hough Lake groups of the Huronian Supergroup, with uranium primarily found in the Elliot Lake Group.
3. Magmatic Ni-Cu-PGE and hydrothermal silver-cobalt mineralization associated with the emplacement of the Nipissing intrusive suite (referred to as the Nipissing event).
4. Ni-Cu-PGE mineralization associated with the Sudbury impact structure.
5. Polymetallic and iron-rich to iron-poor mineralization, commonly albitite-hosted, that is associated with the regional development of a MIAC system in the Southern Province (referred to herein as the Scadding event).

The field trip is centred on mineralization and hydrothermal alteration associated with the Scadding event that corresponds to the regional development of this MIAC system. The minimum extent of interconnected MIAC systems in the region is indicated by corridors of sodic alteration and albitite in the Southern Province that extend for at least 340 km, from Bruce Mines east toward Temagami (Figure 4; Gates 1991; Wray and Yarie 2018). U-Pb geochronology on zircon indicates ages between 1.74 Ga and 1.70 Ga for sodic alteration and albitite formation, providing timing constraints on the Scadding event (Schandl and Gorton 1994; Schandl and Gorton 2007). This time period is contemporaneous with granitic magmatism that formed the Killarney intrusive suite bodies emplaced into the sedimentary rocks of the Southern Province during the Yapavai Orogeny (*see* Figure 2). Where observed, the albitite and some of the superimposed alteration facies are folded, brecciated and deformed. This indicates that Yapavai deformation was occurring as albitization and MIAC alteration proceeded. In the Sudbury area, the main structures associated with sodic alteration and zones of polymetallic mineralization superimposed on albitite and sodic alteration include the Murray Fault System west of Sudbury, the network of north-northwest-trending structures like the McLaren Lake Fault Zone combined with east-trending structures east of the Sudbury, and at the local scale, the Sudbury impact breccia zones in the SPJ property (*see* Figures 1 and 4).

In the Sudbury area, the Long Lake gold, Norstar copper-gold and Scadding gold mines are the largest concentrations of mineralization associated with the Wanapitei Lake area MIAC system discovered so far (*see* Figure 1). These mines are part of what is known as the Sudbury Gold Camp. In the field trip area, prospects that can be related to the MIAC system, and with diamond-drilling results suggesting potential mineralization of significance, include the Alwyn copper-gold, the Scadding Mine Bristol Breccia gold-cobalt, the Glade gold, the Limestone nickel-platinum group element, the McLeod gold-copper and the Palkovics gold-cobalt prospects (*see* Figure 1).

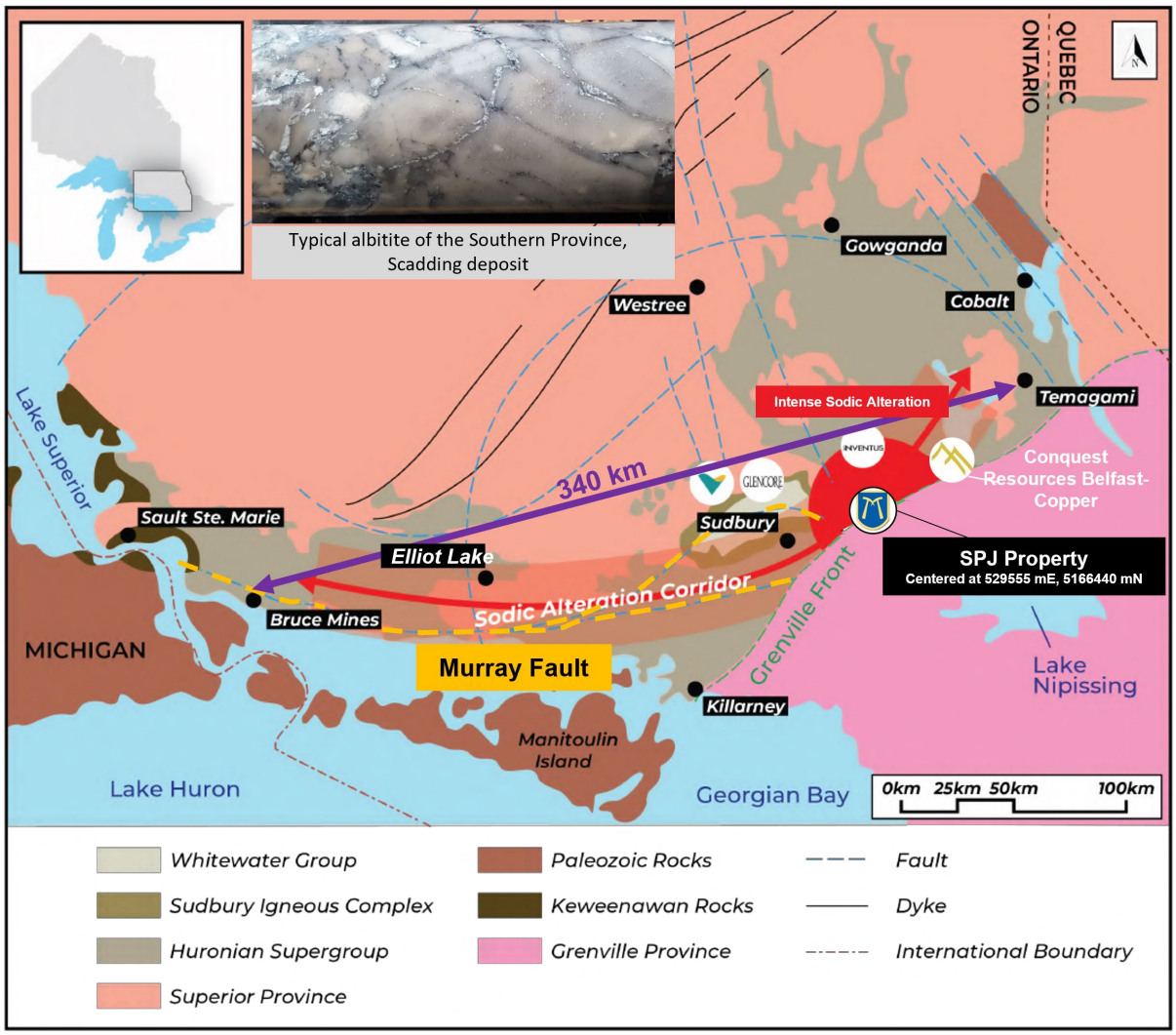

Figure 4. Regional extent of sodic alteration in the Southern Province (*after* Gates 1991; Farrow 2016). UTM co-ordinates (NAD83 Zone 17N) shown for the location of Scadding Mine.

Geological Summary of the Field Trip Area East of the Sudbury Igneous Complex

The field trip examines rocks of the Quirke Lake Group (Serpent Formation quartzite, Espanola Formation limestone, Bruce Formation conglomerate) and Cobalt Group (Gowganda Formation conglomerates and siltstones) of the Huronian Supergroup, mafic intrusive rocks of the Nipissing intrusive suite, undivided felsic intrusions that are overprinted by the MIAC system, zones of Sudbury Breccia formed after Nipissing gabbro emplacement and Sudbury swarm diabase dikes (*see* Figures 1 and 2). The high-grade metamorphic rocks of the Grenville Province are located immediately south of the field trip area (Easton and Murphy 2002), whereas the Sudbury Igneous Complex (SIC) is located west of the field trip area (Figures 1 and 5).

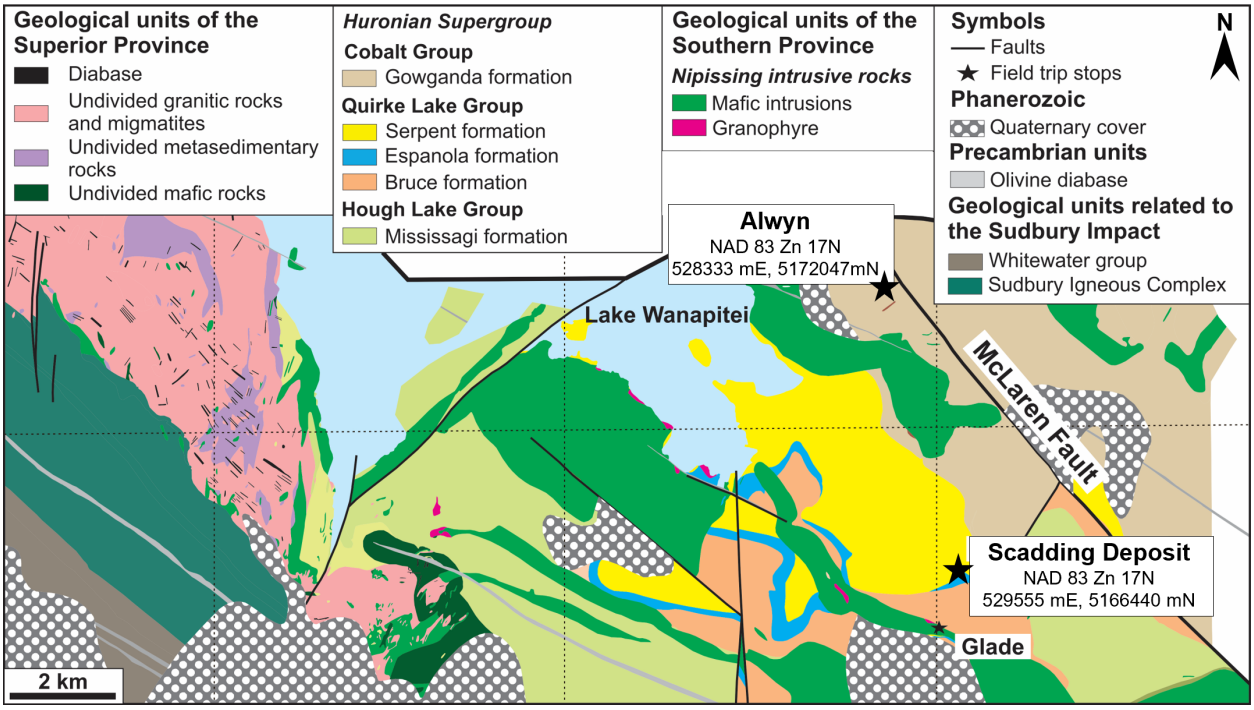

Figure 5. Detailed geology map contextualizing the geological context of the field stops of the field trip. Geology digitized and modified *from* Dressler (1980). UTM co-ordinates (NAD83 Zone 17) shown for the Scadding deposit.

SEDIMENTARY ROCKS OF THE HURONIAN SUPERGROUP

Quirke Lake Group – Bruce Formation

The Bruce Formation is a clast-poor, polymictic pebble conglomerate. The rock is matrix supported and typically has 5 to 15% clasts that range in size from less than 1 cm to 20 cm. The Bruce Formation conglomerate is dark grey to green and typically has 0.1 to 1% disseminated pyrrhotite and pyrite when intersected in diamond-drill core on the Scadding mine site. Deformation is expressed commonly as shearing in this unit with folding and brecciation being subordinate. In the Scadding and Glade area, no significant mineralization zones have been observed so far in the Bruce Formation. At the Palkovics gold and cobalt prospects, it is possible that alteration and mineralization overprints Bruce Formation conglomerate, although the stratigraphy in this area, impacted and transposed by Grenvillian (*sensu lato*) deformation and truncated by many networks of fault zones, is not as well constrained as in the Scadding and Glade area.

Quirke Lake Group – Espanola Formation

The Espanola Formation is composed of limestone, limey siltstone, and siltstone layers. Ductile deformation is common in this formation, as seen by penetrative micro- to large-scale folding in the bedding. Deformation in the Espanola Formation is likely polyphase and resulted in a pinching and swelling geometry for the Espanola Formation along its stratigraphic contacts with the Serpent and Bruce formations, or along mafic intrusions of the Nipissing suite. The colour of the Espanola Formation is variable, depending on the primary composition of individual layers and the presence or absence of alteration overprint, and ranges between black, grey, white, red and green.

In the field trip area, the Espanola Formation represents a very important unit for the genesis of mineralization and alteration. The Serpent–Espanola Formation contact at the Scadding Mine and a Nipissing–Espanola Formation contact at the Glade prospect are both preferential areas of mineralization, deformation and alteration. At Scadding, brecciation and gold mineralization are preferentially partitioned in the rocks of the Serpent Formation that overlies the Espanola Formation. At Glade, gold mineralization that occurs in the Nipissing intrusion also penetrates pervasively into the Espanola Formation. At both locations, hydrothermal alteration is also quite pervasive and intense in the Espanola Formation. In the Limestone trench area, incipient nickel-copper mineralization associated with strong amphibole and amphibole-apatite replacement is centred around a carbonate unit that is possibly part of the Espanola Formation. Here, the carbonate-rich unit (now totally metasomatized) acted as a reactive unit around which alteration and nickel-copper mineralization could occur.

Quirke Lake Group – Serpent Formation

The Serpent Formation is dominated by a quartz-rich sandstone with subordinate silty layers toward its lower contact with the Espanola Formation. It ranges in colour from grey to pink. In the area of the Scadding deposit, the sandstone of the Serpent Formation is moderately to strongly albitized. Primary sedimentary features in the massive sandstone beds are not abundant. Typically, east-trending bedding and laminations can be observed locally in sandstone beds but are better defined in the lower silty layers close to the contact with the Espanola Formation. In strongly albitized zones, all the primary textures of the sedimentary rocks of the Serpent Formation are destroyed and the unit is completely albitized and referred to as an albitite.

All major gold zones forming the Scadding deposit are hosted within breccias and strong replacement zones in the Serpent Formation, which are developed in the axial zones of folds and at contacts with the Espanola Formation. West of the Scadding deposit, the Serpent Formation is also host to a carbonate- and quartz-cemented breccia referred to as the Bristol Breccia. This breccia frequently carries anomalous gold and cobalt values where it becomes rich in fine-grained pyrite that overprints clasts and matrix.

Cobalt Group – Gowganda Formation

The Gowganda Formation sedimentary rocks in proximity to the Alwyn Mine area consist primarily of very fine- to fine-grained, grey-green siltstone and mudstone with minor beds containing rounded granitic clasts less than 2 to 3 cm in size. Alteration consists of weak to moderate pervasive chlorite, weak to moderate patchy to pervasive carbonate and trace to weak hematite-filling fractures (particularly associated with veins). Additional localized weak to moderate albitization and/or silicification occurs in halos around mineralized veins and in weak halos along shear zones. Quartz-carbonate veins (calcite and Mn-dolomite) ± chalcopyrite and pyrite occur sporadically throughout the Gowganda Formation sedimentary rocks, with a higher concentration of veining and mineralization located around the historical Alwyn Mine.

INTRUSIVE ROCKS

Nipissing Intrusive Suite

The intrusions of the Nipissing suite are abundant in the field trip area. They are predominantly gabbro sills (historically referred to as diabase, although they are typically too coarse-grained for diabase) that are fine- to medium-grained, dark grey to slightly green and massive. Geochemical profiles in the Glade area

indicate that the mafic domains of the Nipissing units are composite units formed by compositionally different intrusive phases, as previously described by Lightfoot and Naldrett (1996). In certain intrusions with more primitive compositions, observations in the Glade area indicate the presence of magmatic platinum group element-copper-nickel (PGE-Cu-Ni) mineralization forming disseminations of chalcopyrite and pyrrhotite. Subsidiary narrow tonalite dikes are also occurring sporadically throughout Nipissing intrusions on the SPJ Project. These dikelets are pinky-beige, fine- to medium-grained and massive.

In the Glade area, the intrusions of the Nipissing suite are affected by extensive deformation and alteration associated with gold mineralization. The deformation zones are typically centred on pre-existing corridors of Sudbury Breccia, indicating that peak-deformation and associated alteration and mineralization post-dated the formation of the breccias. In the Glade area, the locally strong intensity of deformation and alteration formed mappable domains at surface that are respectively defined as sheared and hydrothermal diabase units. The sheared diabase unit is distinguished from the regular diabase based on grain size reduction and intensity of shearing centred on pre-existing corridors of Sudbury Breccia. Shearing is generally not penetrative in the diabase away from pre-existing zones of rheological weaknesses, and these zones of deformation can become preferential sites for the emplacement quartz and quartz-chlorite veins, or pervasive chlorite replacement fronts that are gold mineralized. The hydrothermal diabase is characterized by the presence of moderate to strongly abundant, rounded blue quartz eyes and is typically proximal to areas of gold mineralized quartz and quartz-chlorite veins.

Undivided Felsic Intrusions

A series of undivided felsic intrusive units occur in the McLeod, Jovan and Brady Pit areas on the property and were only observed within a few hundred metres north of the Grenville Front. The origin and timing of emplacement of those felsic intrusive units is uncertain but is known to predate the formation of the MIAC systems, as the felsic intrusions are affected by alteration, deformation and mineralization related to the MIAC system. At the Jovan and McLeod showings, field relations suggest that the felsic intrusions are possible felsic end members of the Nipissing intrusive suite comparable to those observed in the Glade area, whereas others could represent strongly albitized diabase of the Nipissing suite. Weak blue quartz eyes were observed in felsic intrusions exposed in some trenches at McLeod, where this unit can be host to significant copper-gold mineralization with concentrations of up to 5% pyrite-arseniferous pyrite ± chalcopyrite in fractures or joints.

In the Limestone trench area where they were intersected in drill core, a series of felsic intrusions do not show any spatial relations with intrusions of the Nipissing suite. These felsic intrusions have a tonalitic and leucocratic composition. Individual intrusions are fine- to medium-grained, light to medium grey and are massive to foliated. Hydrothermal alteration consists of weak (grey) to strong (tan-pink) albitization and/or silicification, weak disseminated biotite, and weak patchy chlorite. Mineralization in those units consists of disseminated arseniferous pyrite overprinting areas of sodic alteration that is associated with low-grade gold mineralization. Traces of molybdenite were also observed in drill core in areas of strong alteration formed in the felsic intrusions.

Olivine Diabase

The Scadding mine site is cut by three near-vertical, northwest-trending olivine diabase dikes that range in width from 2 to 20 m. The dikes are dark grey, magnetic, and have chilled margins. The dikes have been emplaced post-mineralization and are likely associated with the Sudbury diabase dike swarm.

SUDBURY BRECCIA

In the geological units surrounding the SIC, the Sudbury impact event formed extensive zones and corridors of pseudotachylitic breccias named Sudbury Breccia (cf. Dressler 1984; Rousell et al. 2003; Lafrance and Kamber 2010; O'Callaghan et al. 2016). Sudbury Breccia is typically made of a glassy to microcrystalline matrix that hosts rock clasts of varied sizes, typically derived from the local country rock. Sudbury Breccia is interpreted to have formed during the *in-situ* melting of local rock types and subsequent rapid crystallization of the melts as the compression shockwave of the impact traversed the surrounding rock units. Compositionally the matrix of the Sudbury Breccia is in general indistinguishable from the clasts. The breccias display a flow foliation that is highly diagnostic in the field (Parmenter et al. 2002).

Sudbury Breccia bodies have been observed at surface at Glade and in diamond-drill core from Scadding Mine and Glade. In the Glade area at surface, Sudbury Breccia bodies occur as networks of centimetre- to metre-wide corridors of brecciation formed in Nipissing intrusions that become preferentially re-activated as shear zones. The matrix of the Sudbury Breccia bodies is very fine-grained, with rounded clasts of the host rock units and flow-like foliation, which is characteristic of Sudbury Breccia as they formed during intense cataclasis and friction melting of the host rocks. In the Nipissing intrusion exposed in the Glade area, the contacts between the different geological units acted as preferential areas for the formation of Sudbury Breccia. Examples include areas of felsic injections in the mafic units of the Nipissing intrusions. The felsic and tonalite dikes and injections are also brecciated by Sudbury Breccia formation, indicating that their emplacement predated the formation of the breccias at 1.85 Ga.

In the Glade area, in diamond-drill core and at surface, the deformed corridors of Sudbury Breccia are zones of preferential alteration, veining and mineralization. The breccias are variably albitized and then overprinted by gold-mineralized chlorite replacement, or cut by quartz and quartz-chlorite veins in the apical parts of the systems. These Sudbury Breccia bodies are a primary control on deformation and fluid-infiltration in the Nipissing intrusions away from the Nipissing–Espanola Formation contact.

ALTERATION FACIES, DEFORMATION AND MINERALIZATION IN THE FIELD TRIP AREA ASSOCIATED WITH THE MIAC MINERAL SYSTEM

In the field trip area, the MIAC system formed a suite of iron-rich to iron-poor alteration facies associated with different types of mineralization that can be grouped using the MIAC alteration facies framework (Table 1). Detailed photos and XRF maps of each alteration facies are presented in this section and in the section detailing individual field trip stops. The presence of folded and albitized or magnetite-altered beds, combined with sodic alteration and magnetite veins cutting across the main folds of the area, suggest that hydrothermal alteration and mineralization correspond with regional deformation associated with the Yapavai Orogeny. All the alteration facies associated with the MIAC system overprint sodic alteration and albitite, and they are variably deformed by and transposed into Yapavai tectonic fabrics.

Table 1. Summary of iron-rich and iron-poor MIAC alteration facies documented in the Southern Province.

Alteration Facies		Associated Minerals	Mineralization Minerals	Mineralization	Example
Fe-rich MIAC Alteration	Na	Ab			340 km long interconnected corridors from Bruce Mines to Temagami (including SPJ)
	Skarn (Fe)	Cpx, Cpx-Py, Cpx-Mag, Cpx-Mag-Grt, Mag-Grt and Mag	Sch, Po, Py	W	South of Scadding
	HT Ca-Fe	Amp, Amp-Po, Amp-Ap-Po, Amp-Mag	Po, Pen, Ccp	Ni-(Co-Cu)-PGE incipient	Limestone Trenches (Core 9)
	HT K-Fe	Bt and Bt-Kfs	Ccp, Py	Cu-Au	Temagami area
	LT K-Fe	Kfs-Hem	Ccp, Py	Cu-Au	Alwyn Mine (transitioning at depth – Core 8)
	LT Mg-Si-(Na,K)-Fe	Chl, Chl-Mag, Chl-Po, Chl-Py, Mag, Chl-Qtz	Native Au, Apy, Py, Po	Au	Scadding Mine (Stops 1 to 5, Core 5 and 6)
Fe-poor MIAC Alteration	LT CO_2-(Ca,Fe,Mg)-Si	Fe-Dol-Qtz to Qtz-Fe-Dol	Co-Py, Co-Apy, Py, Ccp-Py	Au, Au-Co, Cu-Au	Palkovics, Bristol Breccia, Alwyn Mine (Cores 3, 1 and 4, 2 and 8, respectively)
	LT Si-(Ca,Fe,Mg)-CO_2	Qtz- Fe-Dol	Apy, Ccp	Cu-Au	McLeod
	Si-(Fe)-K	Qtz-Hem-Kfs	Ccp, Py	Cu-Au	Alwyn Mine (Stop 8, Core 8)
	Si-(Fe,Mg)	Qtz, Qtz-Chl	Native Au, Apy, Py, Po	Au	Glade (Stop 7, Core 7)

Abbreviations:

Minerals: Ab, albite; Amp, amphibole; Ap, apatite; Apy, arsenopyrite; Bt, biotite; Chl, chlorite; Co-Py, cobalt-bearing pyrite; Ccp, chalcopyrite; Fe-Dol, iron dolomite; Grt, garnet; Hem, hematite; Kfs, potassium feldspar; Mag, magnetite; Pen, pentlandite; Po, pyrrhotite; Py, pyrite; Qtz, quartz; Sch, schellite.

Mineralization: Au, gold; Co, cobalt, Cu, copper; Ni, nickel; PGE, platinum group elements; W, tungsten.

Other: LT, low-temperature; HT, high-temperature.

Sodic Alteration

Sodic alteration is spatially extensive in the field trip area. It is preferentially distributed along discontinuities that can be lithological contacts, faults, fractures and shear zones and affects, at varied intensity, all the major geological units except for the olivine diabase dikes. In the Nipissing intrusions of the Glade area, certain corridors of deformed Sudbury Breccia have also become preferential zones for sodic alteration. Where it is incipient to strong, sodic alteration can be visually difficult to recognize and does not necessarily lead to major textural or colour changes in the precursor unit. This is exemplified in the Gowganda Formation conglomerate in the Alwyn area, where sodic alteration occurs as a diffuse replacement of the rock matrix without marked colour or textural changes (*see* Day 2 section "Examining Diamond-Drill Core at the Scadding Mine Core Shack", Core 2). In the Sudbury Breccia bodies at Glade, where sodic alteration is also moderate to strong, only weak colour changes suggest the presence of sodic alteration (*see* Day 2 section "Examining diamond-drill core at the Scadding Mine Core Shack", Core 7). In areas where it becomes intense, sodic alteration typically forms albitite after any types of precursor units and usually results in the destruction of all the primary textures of the hosts. Visually, albitite can look like chert, zones of strong silicification, felsic intrusions, quartzite, etc. Mineralogically, the albitite is primarily composed of albite and quartz and no mineralization is associated with sodic alteration and albitite formation.

Sodic alteration and the resulting albitite are overprinted by all the MIAC alteration facies that are observable in the field trip area (see the photos of all the core in the section "Examining Diamond-Drill Core at the Scadding Mine Core Shack"). Major zones of breccias like the Bristol Breccia, located west of the Scadding deposit, are typically formed after albitite. In the breccias, albitite fragments are variably preserved (*see* section "Examining Diamond-Drill Core at the Scadding Mine Core Shack", Core 4). Worldwide, albitite corridors form preferential zones of brecciation, as they are zones of high porosity where the albitite, associated with extensive leaching of host rocks, has not been replaced or recrystallized (Engvik et al. 2008; Putnis 2015). In addition, many albitite corridors form along fault zones such as mapped in the Cloncurry district in Australia (*see* Porter 2010b, his Figure 5). Faulting induces extensive fracture network and interconnected damage zones along which fluid-rock reactions induced extensive replacement of host rocks by albite to form albitite (Poulet et al. 2012; Corriveau et al. 2022b, 2022d). Reactivation of fault zones induces brecciation of the porous albitite commonly along pre-existing fractures, with albite haloes forming large albitite breccia which can then be replaced and mineralized (Montreuil et al. 2015; Corriveau et al. 2022d). Clasts bordered by earlier fracture with albite haloes may preserve original haloes and host fracture haloes internally, as is observed in a large clast in Photo 1. Early damage zones replaced irregularly by albite can also be preserved, as also observed in the same large clast in Photo 1. A lack of a regular halo along an entire fragment suggests that haloes may have formed earlier than brecciation as earlier fracture haloes but are not conclusive thereof, as clast commonly get re-brecciated during brecciation of albitite and may have acquired a halo during a brecciation event coeval with renewed albitization.

Photo 1. Intense brecciation of albitized sedimentary host associated with the LT (Si,CO_2)-(Ca,Fe,Mg)-Si alteration facies at the Long trench showing. The variably albitized clasts are cemented in a quartz-iron-dolomite matrix with varied pyrite content and associated with gold-cobalt mineralization.

HT Ca-(Mg)-Fe Alteration Associated with Incipient Ni-PGE Mineralization

At the current level of exposure, HT Ca-(Mg)-Fe alteration was only observed in the Limestone trench area where it corresponds to a magnetic high and a few hundred metres-long low resistivity zone at depth (*see* section "Examining Diamond-Drill Core at the Scadding Mine Core Shack", Core 9). In diamond-drill core where it was intersected, HT Ca-(Mg)-Fe alteration forms zones of strong replacement, typically selective and stratabound, of sedimentary units and overprints earlier sodic alteration (*see* section "Examining Diamond-Drill Core at the Scadding Mine Core Shack", Core 9). The zone of strong HT Ca-(Mg)-Fe replacement is centred on the relicts of limestone that could be associated with the Espanola Formation surrounded by bedded siliciclastic sedimentary rocks. The presence of carbonate hosts can favour the development of extensive HT Ca-Fe alteration as observed in the NICO deposit of the Great Bear magmatic zone and its host system (Montreuil et al. 2016a, 2016b).

The mineralogical expression of iron metasomatism associated with this alteration facies is variable. Actinolite is the main iron mineral formed by HT Ca-(Mg)-Fe alteration, and magnetite or pyrrhotite are the complementary iron minerals. Pyrrhotite is abundant in areas of anomalous nickel-copper-PGE mineralization, whereas magnetite is more abundant in the shoulders of those zones of incipient mineralization. Apatite is abundant with actinolite and pyrrhotite in certain areas of alteration (*see* section "Examining Diamond-Drill Core at the Scadding Mine Core Shack", Core 9).

LT (Si,CO_2)-(Ca,Fe,Mg) Alteration Facies Associated with Au, Au-Co and Co or Ag-Au-Cu Mineralization

After sodic alteration, the LT (Si,CO_2)-(Ca,Fe,Mg) alteration facies is the most spatially extensive MIAC alteration type in the field trip area (*see* section "Examining Diamond-Drill Core at the Scadding Mine Core Shack", Cores 1, 2, 3, 4 and 8). Alteration typically consists of Fe-dolomite and quartz in variable proportions that overprint sodic alteration. Pyrite, arseniferous pyrite, cobalt-bearing arseniferous pyrite and chalcopyrite are typical mineralization minerals associated with this alteration facies (*see* section "Examining Diamond-Drill Core at the Scadding Mine Core Shack", Cores 1, 2, 3, 4 and 8). Minerals in this alteration facies occur as replacement fronts and veins which cement many breccia zones. LT (Si,CO_2)-(Ca,Fe,Mg) alteration is proximal or directly hosting zones of mineralization around which its spatial extension can exceed by tens to hundreds of metres the footprint of mineralization (*see* Photos 1 and 2). Macroscopic observations and the tabletop XRF maps indicate that, mineralogically (*see* section "Examining Diamond-Drill Core at the Scadding Mine Core Shack", Cores 1, 2, 3, 4 and 8), this alteration facies evolves from mineral assemblages in which Fe-dolomite dominates over quartz (i.e., forming a LT CO_2-(Ca,Fe,Mg)-Si alteration facies), to assemblages where quartz predominates over Fe-dolomite (i.e., forming a LT Si-(Ca,Fe,Mg)-CO_2 alteration facies), to sulfide mineralization that overprints them all. In the Bristol Breccia near the Scadding deposit, ferroan-dolomite, quartz and pyrite associated with the LT (Si,CO_2)-(Ca,Fe,Mg) alteration facies are overprinted by chlorite and magnetite associated with the LT Mg-Si-(K,Na)-Fe alteration facies.

Around the Scadding deposit and in the Palkovics trend, ferroan dolomite can have a spectacular and characteristic visual expression in the rocks it alters. For example, it forms coarse, rhombohedral crystals of ferroan dolomite with minor quartz that grew through constant volume replacement of the precursor rock, typically an albitite and its variably albitized clastic sedimentary host (*see* Photo 2 and section "Examining Diamond-Drill Core at the Scadding Mine Core Shack", Cores 1 and 3). In such rocks, albitization is present both as stratabound replacement and as fronts cutting across the laminations. The latter is observed to replace the host without disrupting the very thin sedimentary laminations defined by

darker, very fine-grained minerals shown to be rich in titanium through micro-XRF imaging (*see* section "Examining Diamond-Drill Core at the Scadding Mine Core Shack", Core 1). Stratabound and crosscutting fronts of albitization have in many cases preserved the sedimentary laminations (*see* Photo 3). The fine sedimentary laminations and the albitite replacement are commonly locally faulted (Photos 3B and 3F). Along a single fracture, albitized rocks are sharply cut by the fracture, albitized haloes have developed along part of the fractures, or material similar to the very-fine dark mineral of the lamination occurs along the fracture. All these features are then overgrown by the ferroan dolomite crystals without any disruption visible (macroscopically and in the tabletop XRF maps: *see* section "Examining Diamond-Drill Core at the Scadding Mine Core Shack", Core 1), which indicates the constant volume replacement. A relative alignment of ferroan-dolomite crystals in those zones of replacement is observed and can be associated with pre-existing discontinuities in the unit like sedimentary layers or networks of small faults and fractures that enable fluid infiltration. The rhombohedrons grow along both sides of these minor faults, and only locally along the fractures. The rhombohedral crystals range locally from being fairly transparent to host layering (*see* Photo 3), to replacing layering completely and becoming more intensely white in colour (locally in Photos 3B, 3D, 3F). Crystals may have a dark margin (Photos 3D and 3E). Isovolumetric metasomatism and preservation

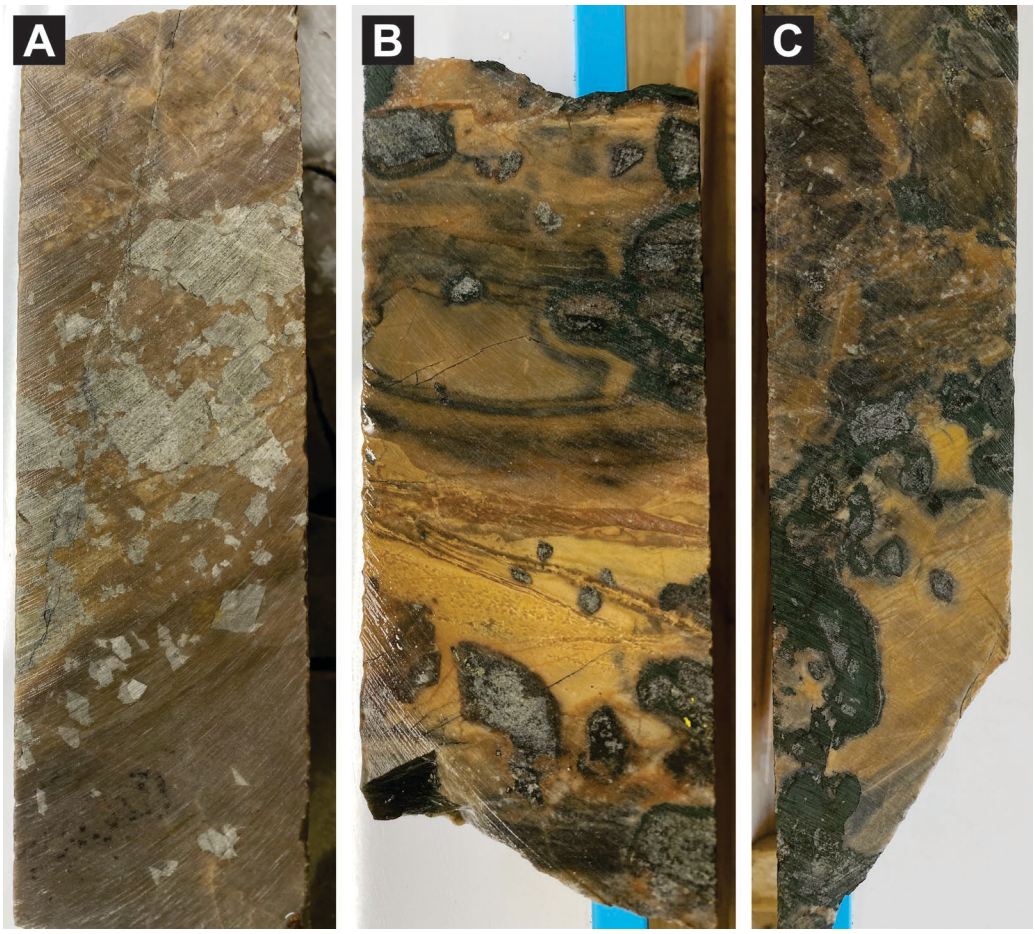

Photo 2. Coarse ferroan dolomite crystals progressively overprinted by chlorite-magnetite alteration associated with gold mineralization in the western extension of the Scadding deposit. **A.** Ferroan-dolomite crystal overprinting sodic alteration located 10 m above the zone of intensifying chlorite-magnetite alteration. **B.** Progressive replacement of the ferroan-dolomite crystals by chlorite and magnetite. **C.** Ferroan-dolomite crystals are almost completely replaced by chlorite-magnetite. All the drill core pictures are from HQ core size with a diameter of 63.5 mm (HQ stands for the size of the core).

of host textures is common in MIAC systems as they are in many other metasomatic rocks (Putnis 2009). Abundant evidence for such isovolumetric replacement has been documented in plagioclase phyric volcanic rocks of the Great Bear magmatic zone (Corriveau et al. 2010a, 2010b, 2016, 2022b, 2022d) but the ferroan-dolomite replacement at Scadding is the most spectacular one to date we have observed in sedimentary rocks.

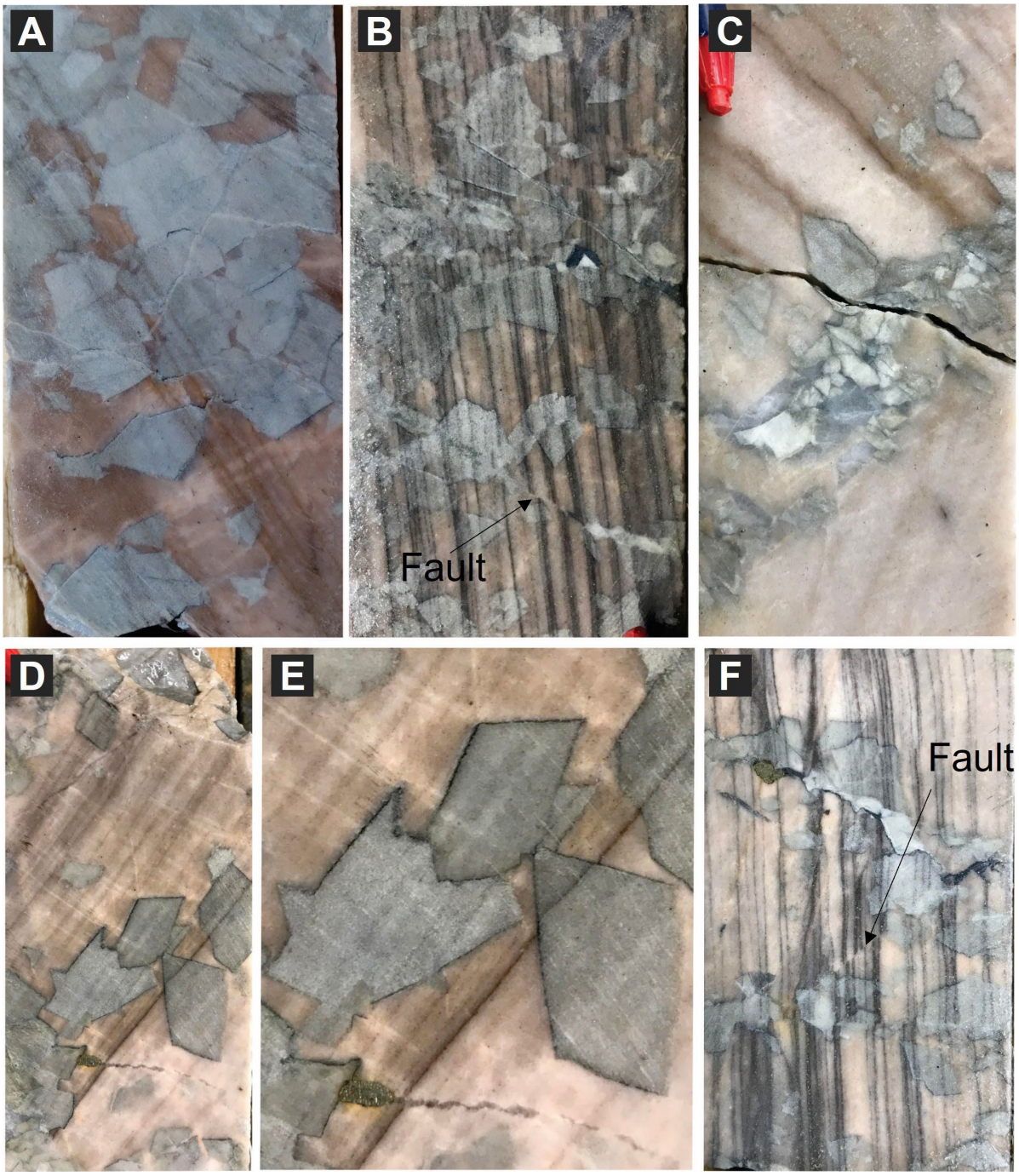

Photo 3. Coarse ferroan dolomite crystals overprinting albitized sedimentary rocks (from diamond-drill hole SM-19-024) associated with gold mineralization in the western extension of the Scadding deposit. All photos demonstrate the variable preservation of textures and changes in colour of ferroan dolomite locally. See text for additional explanation. All the diamond-drill core photos are of HQ core size with a diameter of 63.5 mm.

Two groups of metal associations occur in mineralization zones related to LT (Si,CO_2)-(Ca,Fe,Mg) alteration. The first association includes gold and cobalt in varied proportion and abundance as the primary metals but with consistently elevated arsenic and nickel, localized rare earth element anomalies and trace to absent copper. The best examples of gold, gold-cobalt and cobalt mineralization in the field trip area are the Palkovics trend, the Long trench showing (*see* Photo 1), the Bristol Breccia (*see* section "Examining Diamond-Drill Core at the Scadding Mine Core Shack", Cores 1, 3 and 4) and the zones of incipient cobalt mineralization at the Alwyn prospect (*see* section "Examining Diamond-Drill Core at the Scadding Mine Core Shack", Core 2). In zones of gold, gold-cobalt and cobalt mineralization, pyrite to arseniferous pyrite are the main sulfide minerals and are pervasively disseminated in the matrix of breccias as replacement fronts or as network of veins (*see* section "Examining Diamond-Drill Core at the Scadding Mine Core Shack", Cores 1, 2, 3 and 4).

The second association of metals includes silver, gold and copper as the primary metals, with cobalt and nickel being anomalous to absent, and arsenic being absent from the zones of mineralization. The best example of this mineralization type is at the Alwyn prospect and the Ashigami showing, both located along the McLaren Lake Fault System. In the vein networks of the Alwyn prospect, chalcopyrite with accessory to minor pyrite are the main sulfide minerals associated with silver-gold-copper mineralization. Chalcopyrite and pyrite are typically disseminated in the veins (*see* section "Examining Diamond-Drill core at the Scadding Mine Core Shack", Core 8) but also occur in veinlets that crosscut the ferroan-dolomite–quartz and quartz–ferroan-dolomite veins (*see* Photo 4).

For both metal associations, tabletop XRF images indicate that polymetallic mineralization and sulfide mineral deposition is associated with weak to moderate and localized to pervasive potassic alteration. Manganese also typically increases in areas of mineralization, either as haloes in ferroan-dolomite or in the replacement matrix associated with sulfide mineralization (*see* section "Examining Diamond-Drill Core at the Scadding Mine Core Shack", Cores 1, 2, 3, 4 and 8). At the Alwyn prospect and in the Palkovics trend, the spatial overlap between the two styles of mineralization suggests that they could be related to the compositional evolution of the same mineralization event, with gold-cobalt mineralization predating gold-copper mineralization.

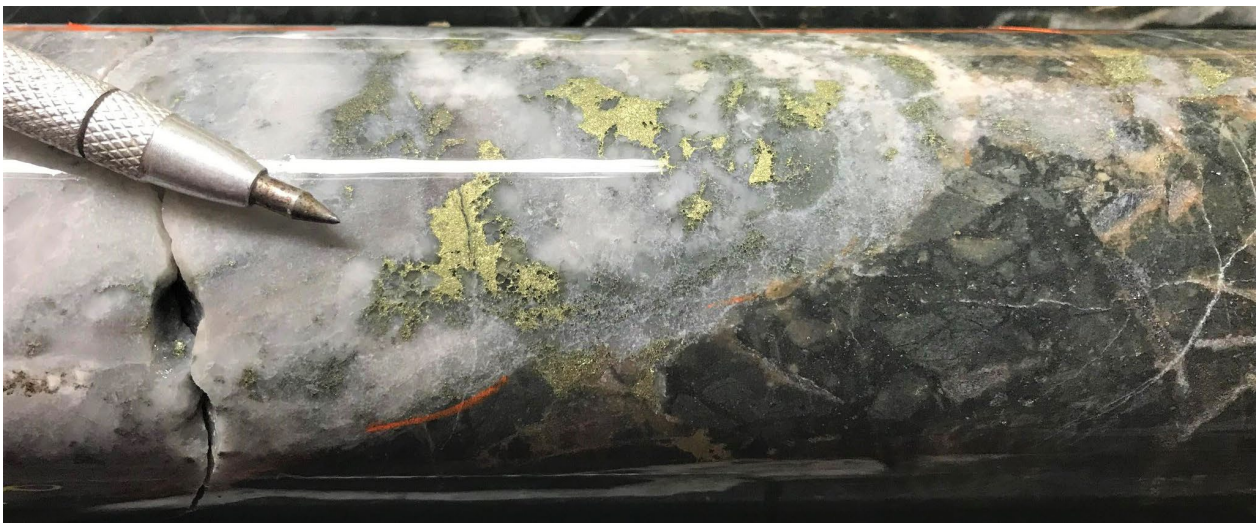

Photo 4. Chalcopyrite-pyrite mineralization associated with the LT (Si,CO_2)-(Ca,Fe,Mg) alteration facies that is forming a quartz-ferroan-dolomite vein at the Alwyn prospect. HQ core size with a diameter of 63.5 mm.

LT Mg-Si-(Na,K)-Fe Alteration Transitional to Si-(Fe,Mg) Alteration Associated with Au Mineralization

The LT Mg-Si-(Na,K)-Fe alteration facies is not spatially extensive in the field trip area. The facies consists of chlorite with accessory to absent pyrite and pyrrhotite, and absent to minor arseniferous pyrite (Photo 5A and 5B). In most cases, alteration replaced units of the Serpent Formation and intrusions of the Nipissing suite. A strong expression of that alteration facies occurs at the Scadding deposit and the Glade prospect; the facies is directly associated with significant gold mineralization and localized enrichment in silver, cobalt, copper and the rare earth elements. Incipient and unmineralized manifestation of the alteration facies also occurs in the Limestone trench area and the Palkovics trend. At the Scadding deposit, this facies is preferentially distributed in zones of selective replacement along certain beds, in breccia zones formed in deformed axial plane of folds, in fold hinges, along the Serpent–Espanola Formation contact and along networks of faults and fracture systems. In the Glade area, this facies is preferentially distributed along corridors of deformed and albitized Sudbury Breccia and along the Nipissing–Espanola Formation contact. It is not very strong at surface where the LT Si-(Mg,Fe) alteration facies is predominant.

The high abundance of chlorite as the primary expression of iron metasomatism results in iron silicate-gold mineralization. Within the Scadding deposit, some mineralogical variation can be observed in the replacement of the Serpent Formation toward the contact with the Espanola Formation. Notably, the proportion of magnetite formed with chlorite can increase, and in certain alteration zones formed very close to the Espanola Formation contact, gold-mineralized and magnetite-rich alteration has locally replaced the silty units of the Serpent Formation. This can locally form iron oxide-gold mineralization (Photo 5C).

In the Espanola Formation limestone unit at both the Scadding deposit and the Glade prospect, LT Mg-Si-(Na,K)-Fe alteration has variably formed stratabound magnetite, chlorite, epidote and pyrite and/or pyrrhotite replacement zones, as well as localized zones of magnetite veins and breccia. South of the Scadding deposit, rare earth element, copper, cobalt and nickel enrichment occurs in zones of strong magnetite and sulfide alteration in the Espanola Formation. In the Glade area, weak to moderate gold mineralization pervades into the Espanola Formation limestone unit in association with LT Mg-Si-Fe alteration. Gold mineralization occurs as very fine disseminations of pyrite to arseniferous pyrite and pyrrhotite that are selective to layers affected by iron alteration. At surface, gold was also observed to be spatially associated with parasitic folds corresponding to the main folding event in the area, a spatial relation that is comparable to the chlorite zones of the Scadding deposit.

At both the Scadding deposit and the Glade area, the LT Mg-Si-(Na,K)-Fe alteration facies exhibits a chemical evolution towards decreasing Fe/Si ratios. This evolution is marked by originally absent to low proportions of quartz associated with chlorite to progressively increasing modal proportions of quartz with chlorite. At the Villeneuve trench (Stop 5) and the eastern end of the East-West pit (Stop 4), located at the eastern limit of the Scadding deposit, LT Mg-Si-(Na,K)-Fe alteration (Fe-dolomite, silicification and albitization) transitions to the LT Si-(Mg,Fe) alteration facies (Fe-rich chlorite and quartz-chlorite breccia), where quartz becomes the primary mineral in the assemblage and continues to increase in proportion relative to chlorite (*see* Photo 5D). At Glade, the LT Si-(Mg,Fe) alteration facies predominates at surface where it is only locally observed to transition to LT Mg-Si-(Na,K)-Fe alteration (*see* Photo 5E). The LT Si-(Mg,Fe) alteration facies at Glade forms networks of gold-mineralized quartz-chlorite to quartz veins emplaced in fractures and in certain deformed corridors of Sudbury Breccia, in what is interpreted as the apical parts of that gold-mineralized system. Chlorite can be an important accessory phase or become completely absent in the gold-mineralized veins associated with the LT Si-(Mg,Fe) alteration facies (*see* Photo 5E and 5F).

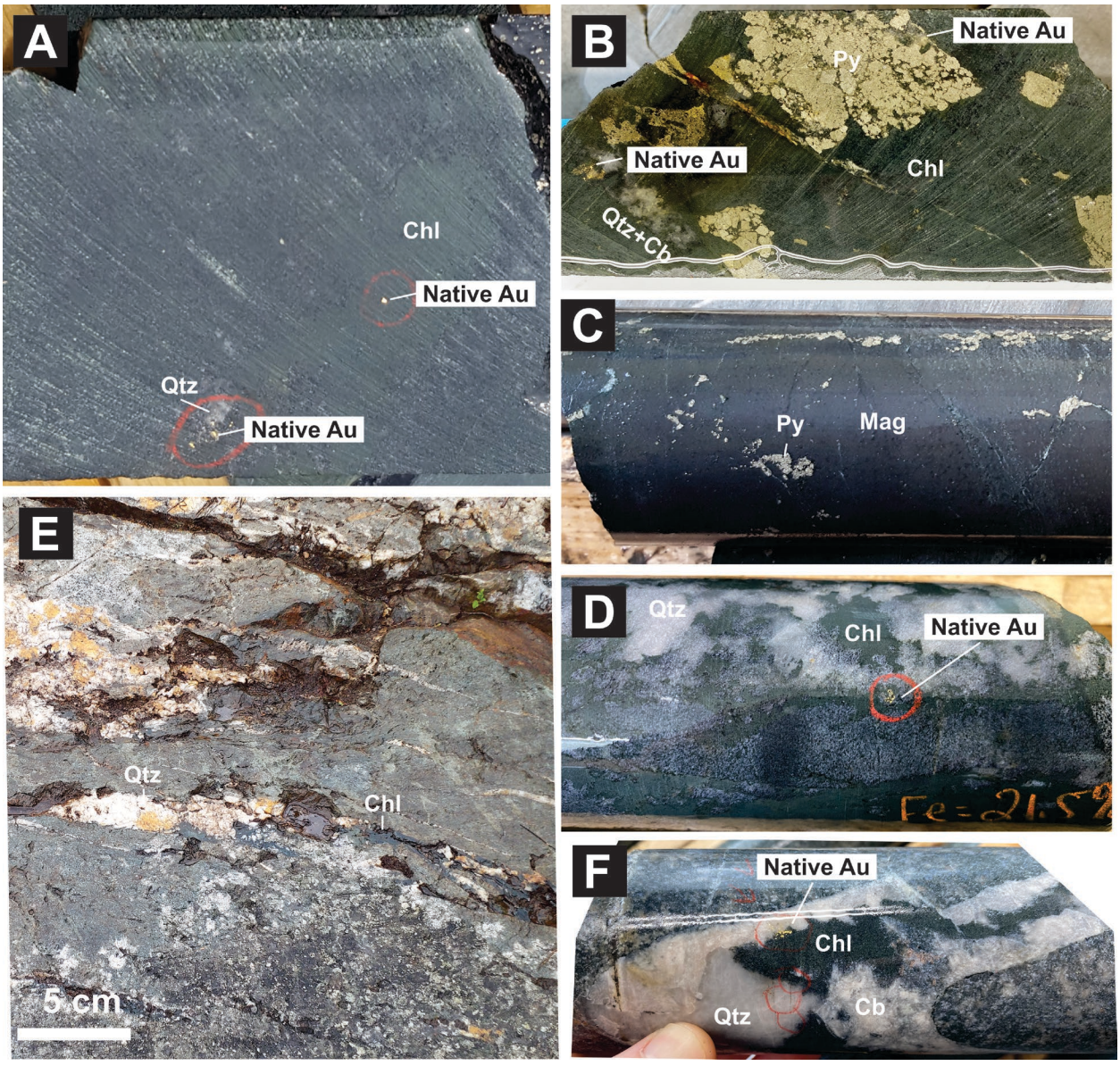

Photo 5. Varied expressions of the LT Mg-Si-(Na,K)-Fe alteration facies and its transition to the LT Si-(Mg,Fe) alteration facies in the Scadding and Glade areas. **A)** Strong chlorite alteration with accessory quartz and native gold mineralization. **B)** Strong chlorite alteration with pyrite selectively replacing ferroan dolomite with accessory quartz and native gold mineralization. **C)** Magnetite replacement corresponding to the LT Mg-Si-(Na,K)-Fe alteration facies developed in proximity to the Espanola Formation limestone unit in the Scadding deposit. **D)** Gold mineralization in the transition from the LT Mg-Si-(Na,K)-Fe alteration facies to the LT Si-(Mg,Fe) alteration facies at the eastern limit of the Scadding deposit. **E)** Quartz and quartz-chlorite veins with localized chlorite pods exposed at surface in the Glade area showing localized transition between the LT Si-(Mg,Fe) alteration facies and the LT Mg-Si-(Na,K)-Fe alteration facies. **F)** High-grade gold mineralization in the Glade area formed in a quartz-chlorite vein at the transition between the LT Si-(Mg,Fe) alteration facies and the LT Mg-Si-(Na,K)-Fe alteration facies. All the drill core pictures are from HQ core size with a diameter of 63.5 mm. Abbreviations: Au, gold; Cb, carbonate; Chl, chlorite; Mag, magnetite; Py, pyrite; Qtz, quartz.

LT (Ca,Mg)-K-Fe Alteration Transitional to Si-(Fe)-K Alteration Associated with Cu-Au Mineralization

At vertical depths exceeding 70 m in the Alwyn system, a gradual transition in the prevailing alteration facies is observed. Alteration associated with silver, gold and copper mineralization transitions from the (Si,CO_2)-(Ca,Fe,Mg) facies to a Si-(Fe)-K alteration facies. At depth in the Alwyn trend, Si-(Fe)-K alteration is expressed as very strong to locally complete silicification of a probable conglomerate of the Gowganda Formation, with areas of selective potassium-feldspar replacement (*see* Photo 6A and 6B). The full extent of that Si-(Fe)-K alteration facies in the Alwyn system is not currently known.

Locally and comparably to the transitions between the LT Mg-Si-(Na,K)-Fe alteration and Si-(Fe,Mg) alteration facies in the Scadding and Glade area, the LT Si-(Fe)-K alteration facies is seen to transition to a LT (Ca,Mg)-K-Fe and LT K-Fe alteration facies. Where present, the LT K-Fe alteration facies forms earthy to specular hematite veins with potassium feldspar, with the potassium feldspar located in certain veins or in haloes around the veins. Quartz can be abundant to absent in the veins with specular hematite and potassium feldspar. Chalcopyrite mineralization is spatially associated with potassium-feldspar alteration and with certain veins formed of specular hematite with variably developed quartz and with potassium-feldspar haloes (*see* Photo 6C). An amphibole-bearing variant of the LT Mg-Si-(Na,K)-Fe alteration facies was observed locally in the zone of strong silica replacement in the Alwyn region. This amphibole alteration is mineralized initially with pyrrhotite and pyrite and then by chalcopyrite, resulting in anomalous cobalt, copper and nickel contents. Tabletop XRF images and macroscopic observation indicate that the amphibole alteration is cut by and locally evolves to veins composed of earthy hematite with accessory potassium feldspar and carbonates (*see* Photo 6D and E).

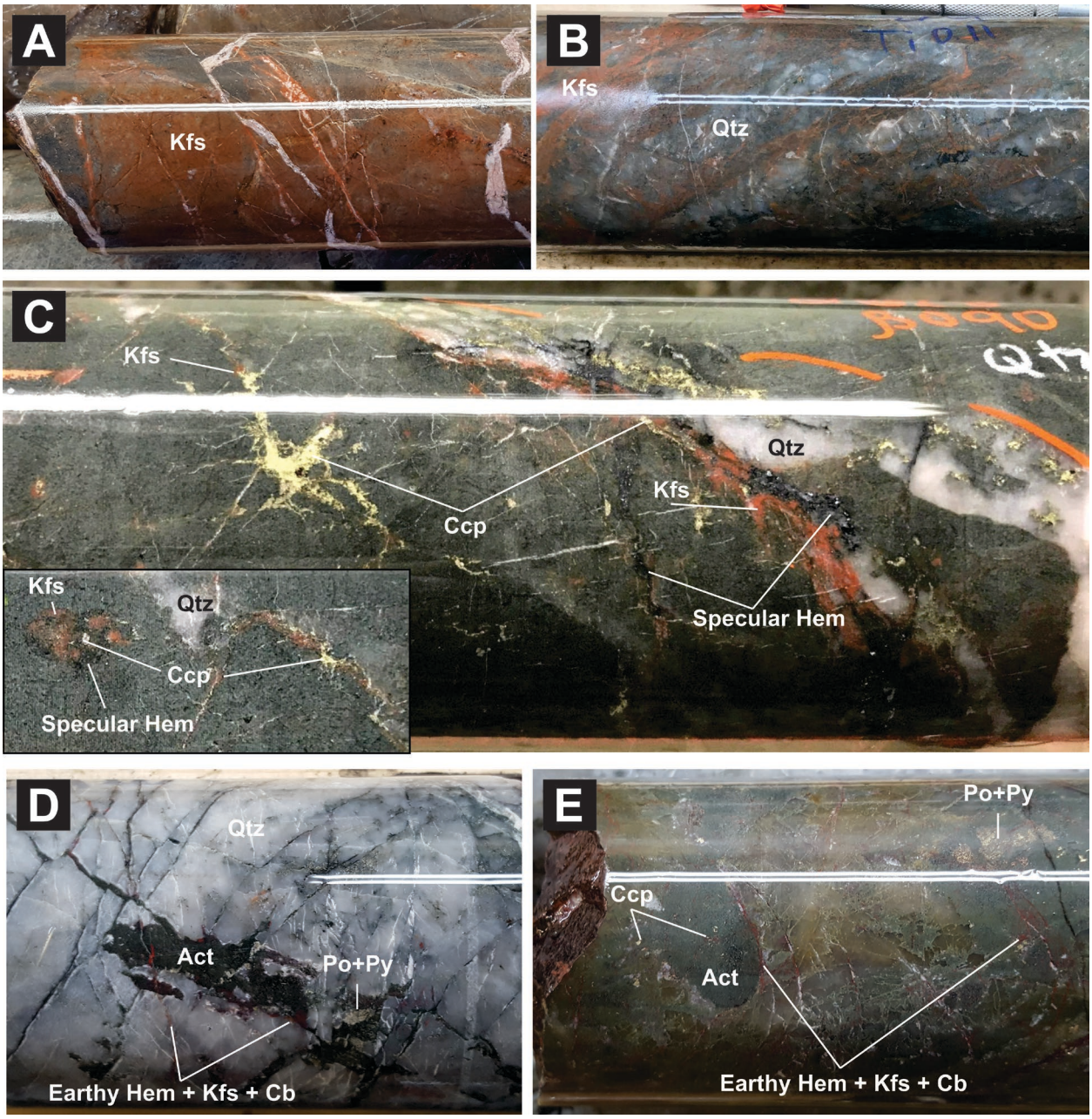

Photo 6. Pictures of the Si-(Fe)-K, LT Mg-Si-(Na,K)-Fe and LT K-Fe alteration facies associated with copper-gold mineralization at the Alwyn prospect. **A)** Potassium-feldspar alteration in the haloes of the zone of intense silicification of the host sedimentary unit. **B)** Intense silicification with selective potassium-feldspar alteration of certain layers and sporadic chalcopyrite mineralization. **C)** Quartz-specular hematite and specular hematite–potassium-feldspar associated with chalcopyrite mineralization. **D)** Actinolite vein with pyrrhotite and pyrite crosscutting the intensely silicified unit and cut by earthy hematite veins with accessory potassium-feldspar and carbonates. **E)** Actinolite vein and alteration front with pyrrhotite and pyrite associated with Co and Ni enrichments evolving to chalcopyrite mineralization crosscut by earthy hematite veinlets with accessory potassium-feldspar and carbonates (transitioning to LT K-Fe). All the drill core pictures are from HQ core size with a diameter of 63.5 mm. Abbreviations: Act, actinolite; Cb, carbonate; Ccp, chalcopyrite; Hem, hematite; Kfs, potassium feldspar; Po, pyrrhotite; Py, pyrite; Qtz, quartz.

This page left blank intentionally.

Road Log

Note: Caution should be taken when parking vehicles on the shoulders of roads and/or trails at the Scadding mine site to allow enough space for other motorists in the area to get by.

Universal Transverse Mercator (UTM) co-ordinates are provided using North American Datum (NAD) 83 in Zone 17.

DAY 1 AND DAY 2 OVERVIEW

Scadding Gold Deposit

The Scadding deposit (MDI41I10NE00012, Ontario Geological Survey 2023) represents one of the largest gold deposits of the Sudbury Gold Camp in addition to the Long Lake and the Norstar mines. The most prospective rock type in the Scadding deposit are breccias, replacement zones and networks of veins that are primarily composed of chlorite with varied amounts of pyrite, pyrrhotite, magnetite and quartz, which being coeval, collectively define a LT Mg-Si-(Na,K)-Fe alteration facies. The chlorite-rich assemblages associated with gold mineralization form iron silicate-gold mineralization, and the Scadding deposit could be tentatively classified as a Metasomatic Iron gold (MI-Au) deposit. LT Mg-Si-(Na,K)-Fe alteration is typically overprinting earlier sodic alteration and albitite that can become clasts in chlorite-cemented breccia zones. West of the Scadding deposit, LT Mg-Si-(Na,K)-Fe alteration transitions to ferroan-dolomite-quartz and quartz-ferroan-dolomite breccias and replacement zones associated with the LT (Si,CO_2)-(Ca,Mg,Fe) alteration facies. Gold and cobalt mineralization occurs in those breccias and replacement zones, particularly in the Bristol Breccia. The main host rocks for the mineralized zones of the Scadding deposit are the quartz sandstone and the basal siltstone of the Serpent Formation, but the alteration system and some gold mineralization extend into the underlying Espanola Formation.

Three structural trends have been identified that control emplacement of chlorite and mineralization: a series of subtle northwest- to northeast-striking (slightly variable) faults; dominantly east-trending (north-dipping) bedding; and east-northeast shallowly plunging fold hinges and the deformed axial zones of folds. It appears that fluid over-pressuring occurred in the north-trending faults and the east-northeast-plunging fold hinges, resulting in brecciation and open space filling of chlorite and sulfide minerals. Mineralization along the east-trending bedding is dominated by selective chlorite and sulfide mineral replacement along certain beds. Mineralized zones are semi-continuous at the Scadding mine site, as they pinch and swell.

In 2020, a series of trenches cleared by previous explorers on the property, as well as by MacDonald Mines personnel (2018–2019), were mapped and systematically sampled. This work was completed to gain a further understanding of the structural and geological controls on gold mineralization at the Scadding mine site. This field trip examines several of these mapped areas (Figure 6) to visualize the varied expression of iron metasomatism at the LT Mg-Si-(Na,K)-Fe alteration facies and to describe the structural controls on mineralization at the Scadding Mine.

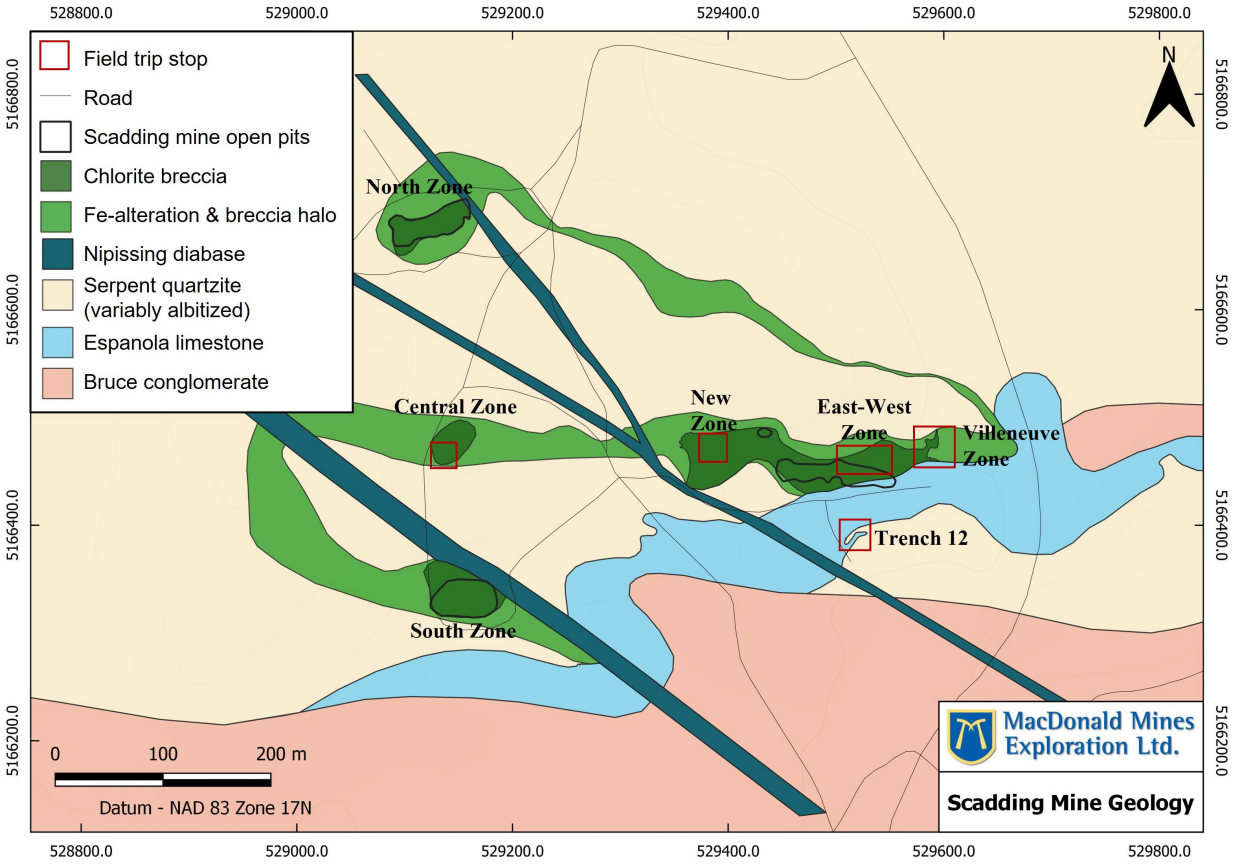

Figure 6. Geology and alteration map of the Scadding gold deposit showing the location of field trip stops.

Glade Gold Prospect

The Glade gold prospect (MDI41I10NE00052, Ontario Geological Survey 2023) is located 1 km south of the Scadding deposit and was investigated initially in 2020 because significant gold mineralization was detected at surface and in shallow diamond drilling at the Glade East (now AGT-21-002) and Glade West (now AGT-21-005/006) showings (Figure 7). Diamond-drilling data and surface mapping acquired in 2021 and 2022 illustrate that the Glade prospect represents the southern extension of the mineralized system that formed the Scadding deposit, and that a large gold system in the Nipissing intrusions and extending into the Espanola Formation limestone unit to the south is present at the Glade prospect (*see* Figure 7). At surface, the Glade East and West showings expose the apical part of the Scadding mineralized system. Gold mineralization is primarily related to extensional and variably sheared quartz veins with accessory to absent chlorite that are part of the LT Si-(Mg,Fe) alteration facies. In diamond-drill core from the Glade prospect, this alteration assemblage is observed to evolve to the chlorite-rich with accessory to absent quartz assemblages that are characteristic of the LT Mg-Si-(Na,K)-Fe facies. Mafic intrusions of the Nipissing suite are the primary hosts of the mineralized quartz veins of the Glade prospect. The Bruce Formation conglomerate occurs at the northern contact of the Nipissing intrusion, and the Espanola Formation limestone occurs at the southern contact. Mineralization, alteration and deformation extend and overprint the Espanola Formation limestone, but so far have not been observed in the Bruce Formation conglomerate. The stop AGT-21-007 exposes the intense to strong alteration and deformation at the Nipissing–Espanola contact, and zones of gold mineralization in the Espanola Formation limestone just below the contact (*see* Figure 7).

The Glade West showing at station AGT-21-005/006 and trench AGT-21-007 illustrates an intricate relation between pre-existing zones of Sudbury Breccia bodies in a Nipissing intrusion and the formation of the gold system developed in the Nipissing suite intrusions at Glade (*see* Photo 7). Trenching and drilling indicate that the main shear systems preferentially follow corridors of Sudbury Breccia that were likely deformed syn-alteration and syn-mineralization during the Yapavai Orogeny. The corridors of Sudbury Breccia are the main host for gold-mineralized quartz veins with variable chlorite abundance and zones of sodic alteration overprinted by gold-mineralized chlorite alteration mineralization. At surface and at depth, the original geometry of the Sudbury Breccia bodies is a primary control on the geometry of the zones of mineralization, and this is covered at the core shack stop on Day 2 of the field trip.

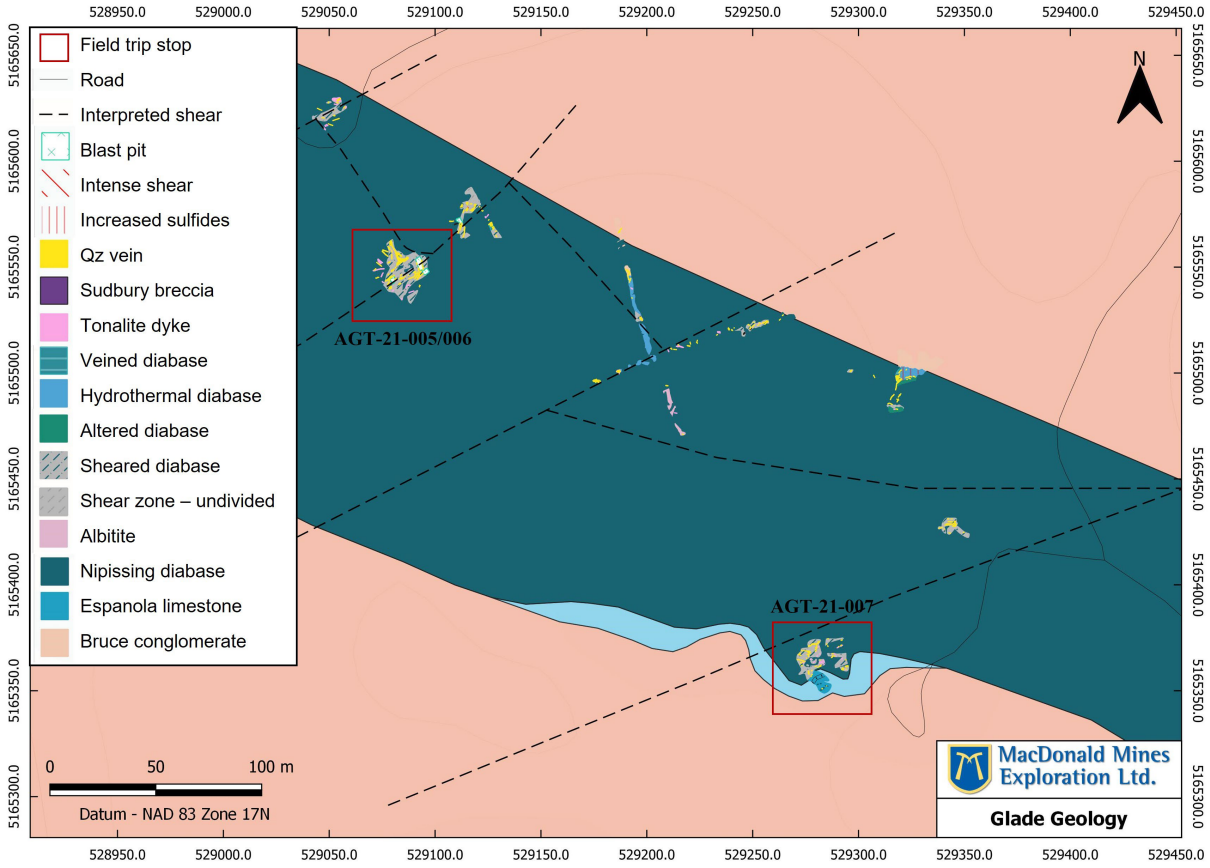

Figure 7. Geology map of Glade prospect. Abbreviation: Qz, quartz.

Photo 7. Corridors of deformed Sudbury Breccia in the Nipissing intrusion in the Glade prospect area. **A)** and **B)** are both from stations AGT-21-005/006; **C)** is from station AGT-21-007. Abbreviations. Bx, breccia; Db, diabase (Nipissing).

Alwyn Copper-Gold Prospect

The Alwyn copper-gold prospect (MDI41I10NE00047, Ontario Geological Survey 2023) is centred on the former Alwyn Mine (formerly Alwyn-Porcupine Mine and the Haultain Mine), which consists of 3 levels of underground workings developed in 1901. The Alwyn Mine produced 7,000 tons of strongly mineralized quartz-carbonate vein and breccia material hosted in siltstone and clast-poor conglomerate of the Gowganda Formation. Mineralization graded 3% copper and 0.20 oz/ton gold (Ontario Assessment File Database Report 41I10NE0154). Since then, there has been sporadic exploration conducted on the property, including some diamond drilling in the 1950s (Ontario Assessment File Database Report 41I10NE0158), dewatering of the underground workings and diamond drilling in the 1980s (Ontario Assessment File Database Reports 41I10NE0137, 41I10NE0139, 41I10NE0154, 41I10NE0170; Klondike Bay Resources 1999), and overburden stripping and mapping done in 2010 (Ontario Assessment File Database Report 20011267). Recent surface work in 2021 and 2022 showed that gold-copper mineralization is spatially related at surface to an intense shear zone parallel to the McLaren Lake Fault Zone (MLFZ) (Metcalf 2021). Copper-gold mineralization at surface is hosted within multidirectional

networks of quartz-carbonate-sulfide veins associated with the LT (Si,CO_2)-(Ca,Fe,Mg) facies that are developed around and within the shear zone (*see* Photos 4 and 6, and Stop 8). Mineralization in the veins and the shear zone consists of chalcopyrite, pyrite and trace malachite. Sodic alteration surrounds the shear zones, and weak and localized potassium-feldspar alteration fronts are visible at surface.

At depth, diamond drilling conducted in 2022 by MacDonald Mines Exploration Ltd. indicated that alteration and mineralization in the Alwyn system transitions from the LT (Si,CO_2)-(Ca,Fe,Mg) facies (quartz, Mn-dolomite, earthy hematite) to a Si-(Fe)-K alteration (quartz, earthy hematite, potassium feldspar) facies with incipient to weak manifestation of the LT (Ca,Mg)-K-Fe (actinolite, potassium feldspar, earthy to specular hematite) alteration facies that become primarily associated with copper-gold mineralization (*see* Photo 6 and section "Examining Diamond-Drill Core at the Scadding Mine Core Shack", Core 8).

DAY 1

0.0 km	Start at Laurentian University, outside of the RD Parker building. Paid day parking is available on Laurentian campus [*935 Ramsey Lake Rd, Sudbury, ON P3E 2C6*].
0.8 km	Follow University Road through campus and turn left onto Ramsey Lake Road (Greater Sudbury Regional Road 39).
3.1 km	Turn right onto Paris Street (Greater Sudbury Regional Road 80 N).
5.5 km	Turn right onto Brady Street (Greater Sudbury Regional Road 49).
6.05 km	Continue onto Lloyd Street (Greater Sudbury Regional Road 55) to the Kingsway (Greater Sudbury Regional Road 55).
20.8 km	Continue travelling east onto Trans-Canada Highway 17 until you reach the turnoff for Kukagami Road.
39.8 km	Turn left onto Kukagami Lake Road and travel north.
55.8 km	The entrance to the Scadding mine site is approximately 700 m past the turn for Ashigami South Shore Road, after the 16 km marker. The entrance is marked with an orange pilon on the left-hand side of the road. There is a large area to park as soon as you turn left; someone from MacDonald Mines Exploration Ltd. will meet you at this point to guide you for the rest of the way to the first stop.

Stop 1. Scadding Mine – Central zone

UTM 529142E 5166476N (NAD83, Zone 17)

The outcrop directly beside the core shack marks one of the main discovery outcrops for the Central zone of the Scadding deposit. The Central zone was mined underground in the 1980s using a now rehabilitated portal and was the main center of gold production from the Scadding deposit. The outcrop demonstrates intense Fe-rich chloritization, characterized by the dark green colouration of strongly albitized Serpent Formation quartzite (also referred to as albitite in zones of stronger albitization). Nearest to the two drill collars completed in 2020 (SM-20-065 and SM-20-009), the rock demonstrates strong brittle deformation and/or brecciation, with Fe-chlorite and minor magnetite infilling the matrix (Photo 8A). Potentially two episodes of albitization can be observed. The first early phase of albitization affects the whole Serpent Formation quartzite giving the rock a light pink and/or bleached background colour (fragments in Photos 8A-C). The second phase occurs syn- to post-chloritization as moderate to strong albitized halos (light

white to pink) surrounding chlorite (Photos 8A-C). Northward across the outcrop, alteration decreases in intensity, and some Fe-chlorite-quartz zones can be observed (Photo 8D). Patches of more intense sulfide mineralization occur throughout the outcrop, but also decrease in abundance northward. These mineralized patches consist predominantly of pyrite and pyrrhotite; visible gold occurs separate from these sulfide patches, associated with zones of intense chloritization, but is very nuggety. Several intense shears and minor faults can also be observed across the outcrop.

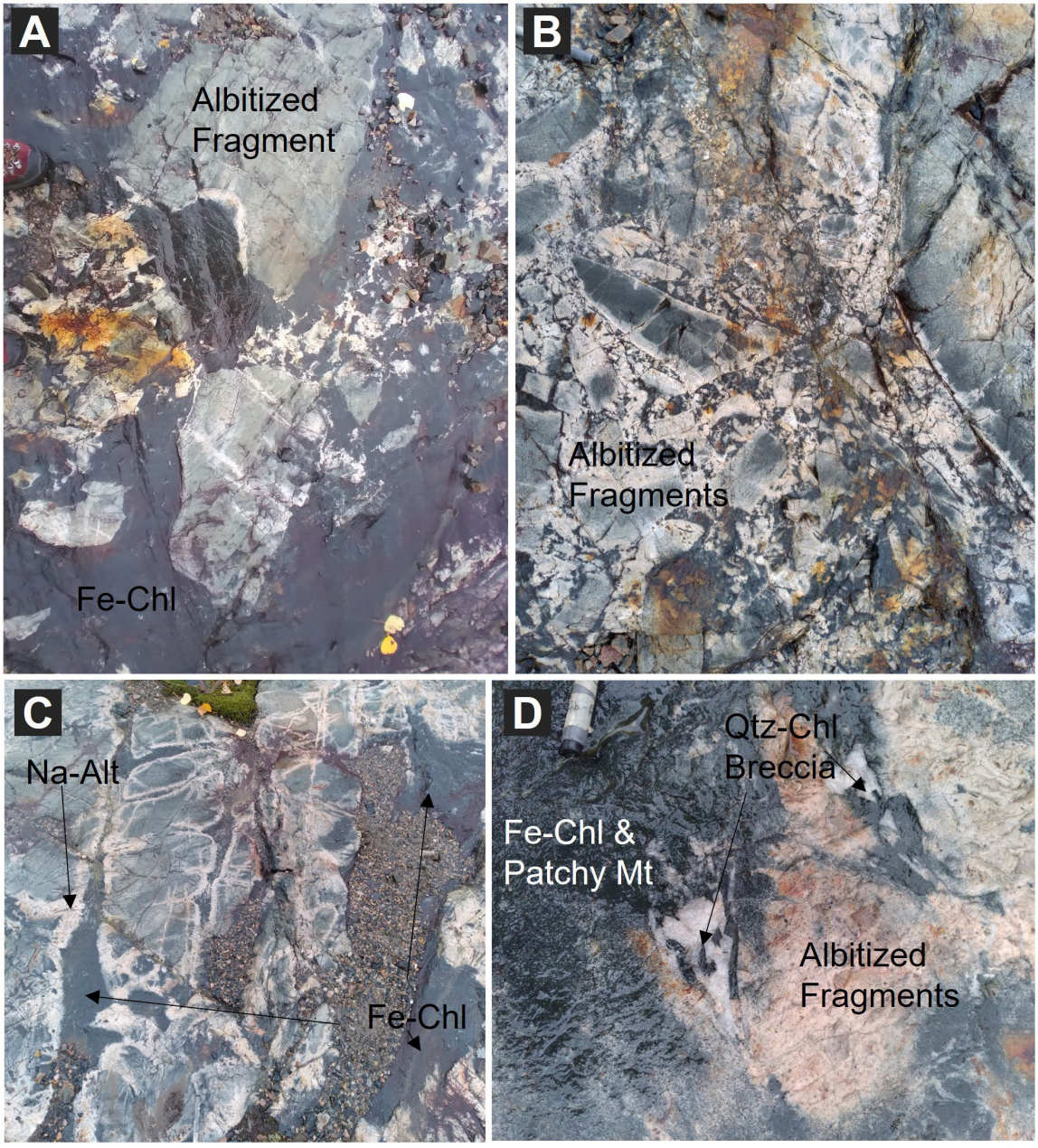

Photo 8. Intense Fe metasomatism and albitization of Serpent Formation quartzite at the Scadding core shack outcrop (Central zone) (Stop 1). **A)** and **B)** Breccia infilled by Fe-rich chlorite. **C)** Fe-rich chlorite infiltrating Serpent Formation quartzite along fractures with strong halos of albitization. **D)** The mineral assemblages within the triangular void infills demonstrate the transition to chlorite-quartz breccias and alteration associated with the Scadding system. Abbreviations: Alt, alteration; Chl, chlorite; Fe, iron; Mt, magnetite; Na, sodium; Qtz, quartz.

Stop 2. Scadding Mine – Currie Rose New Zone

UTM 529361E 5166474N (NAD83, Zone 17)

In 1997, Currie Rose discovered a mineralized zone between the East-West pit and the underground workings used to mine the Central zone of the Scadding deposit. They termed the discovery the "New Zone" and stripped an area in the interpreted surface projection. MacDonald Mines Exploration Ltd. mapped the New Zone outcrop in 2020 since there was no known map from the previous work (Figure 8).

The geology is typical of the Scadding deposit, consisting of strongly albitized Serpent Formation quartzite with locally brecciated domains. A zone of strong chlorite alteration occurs in the middle of the exposure. The breccia matrix is composed primarily of chlorite with a lesser iron carbonate component. The outcrop is structurally complex and includes faulting and folding. Much of the chlorite is contained within a prominent north-south fault and/or breccia zone that cuts through the centre of the outcrop. However, chlorite is also concentrated within fold hinges. The dominant fold hinge is oriented at 079°/19° (trend/plunge) within an axial plane of 260°/86° (strike/dip). Folding was based on various bedding domains that typically strike easterly but with varied dip direction (north and south). Diamond-drill testing of the fold hinge in 2020 in hole SM-20-041 revealed a strong association between fold hinges and high-grade gold mineralization.

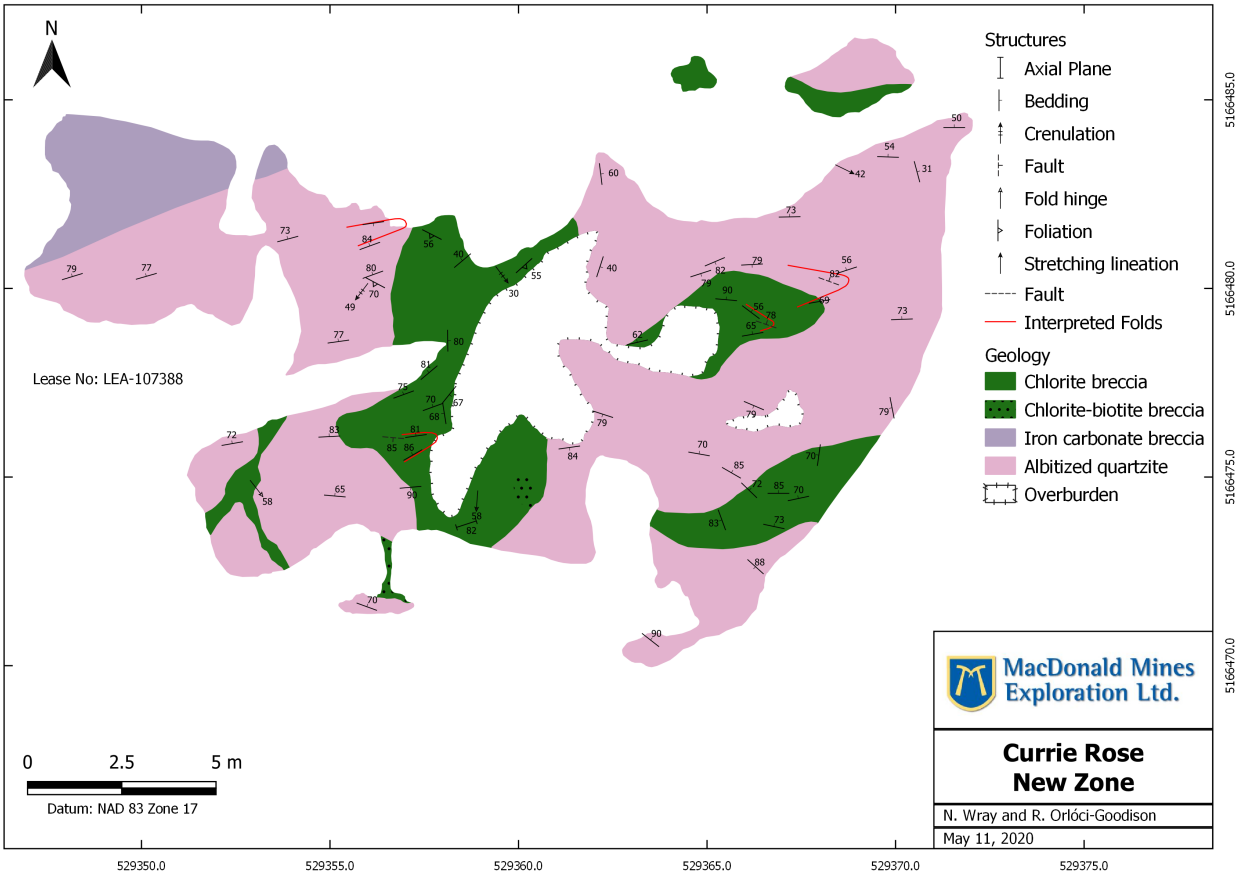

Figure 8. Geology map of Currie Rose New Zone (Stop 2).

Stop 3. Scadding Mine – SMT-20-012

UTM 529511E 5166387N (NAD83, Zone 17)

SMT-20-012 (Figure 9) was first uncovered in the 1980s by Northgate Exploration Ltd. The outcrop was found while attempting to find a Yavapai fold at the Serpent–Espanola formation contact associated with strong chlorite alteration and gold mineralization comparable to the one associated with the East-West zone located 50 m to the north. Although no significant chlorite zones were found at surface, the stripped outcrop illustrates the relation between Yavapai deformation and folding, alteration and brecciation that occurred along the Espanola–Serpent formation contact. Zones of brecciation can be observed to be preferentially developed in the hinge of the main east-trending folds in the Serpent Formation. Sodic alteration in the outcrop can be observed to selectively alter folded beds of the Serpent Formation, but fronts of sodic alteration also are cutting through the folds, suggesting a syn-deformation timing for sodic alteration. The rheological difference between the quartzite and the limestone is very apparent on the outcrop. Deformation in the limestone is dominantly expressed as folding, whereas brecciation and faulting is more common in the more competent quartzite. The presence of a sheath fold at the contact between the two units suggests a high level of strain partitioning at the contact. The undulating shape of the limestone–quartzite contact that also affects peak-deformation folds suggests a late-stage secondary north-northwest folding component.

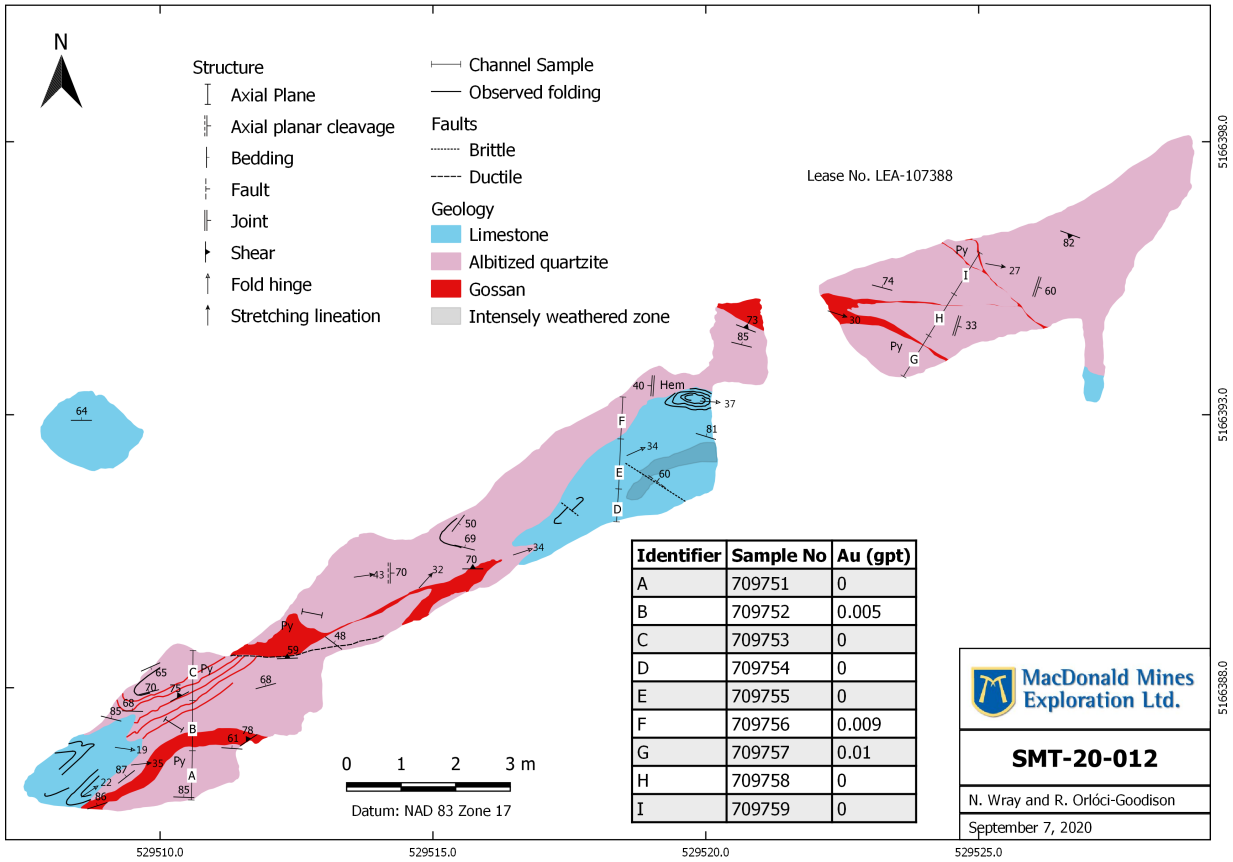

Figure 9. Geology map with channel sampling results from stripped area SMT-20-012 (Stop 3). Abbreviations: gpt, grams per tonne; Hem, hematite; Py, pyrite.

Stop 4. Scadding Mine – East-West zone

UTM 529512E 5166458N (NAD83, Zone 17)

Special caution is to be taken at this stop because the rock face drops down very steeply. During this stop participants are asked to stay a minimum of 10 feet (3 m) from the edge of the pit at all times. To allow for proper distancing, participants will be divided into smaller groups before being led up to the outcrop. Slips, trips and fall hazards are also possible along the walking path up to the top of the pit. Please do not attempt to walk at the base of the outcrop along the lake.

The East-West pit was mined from 1983–1984 by Westfield Minerals Ltd. as part of a test mining project for the Scadding Mill. A total of 24,018 tons of ore were milled from the three small pits at the Scadding mine site, including the North, South and East-West pits. The orientation of the East-West pit follows a large fold hinge (Photo 9) that is shallowly plunging to the east and west within the Serpent Formation at

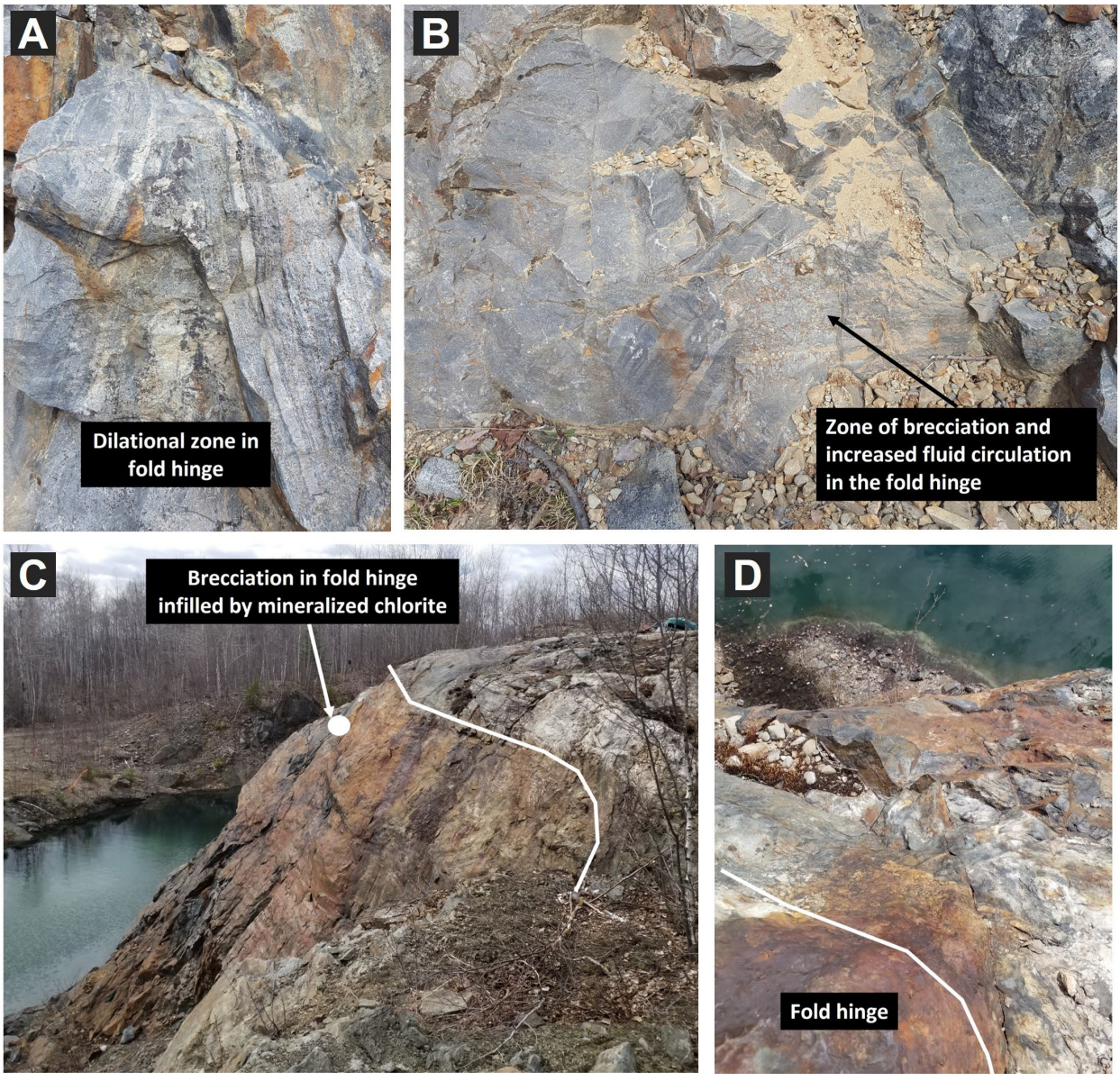

Photo 9. Photos of folding in Serpent Formation quartzite at the East-West pit (Stop 4). See text for additional explanation.

its contact with the Espanola Formation limestone. Similar to Stop 3, because of the hardness of the albitized quartzite, folding of this unit results in the creation of breccia zones and brittle faulting that make the fold hinges primary conduits for fluid migrations and mineralization across the Scadding mine site. This exposure also illustrates the preferential formation of breccia zones during deformation in the Serpent Formation at its contact with the Espanola Formation. This feature is exposed at the eastern end of the East-West pit. This stop will take place at the top of the pit wall, where variations in albitization and chlorite alteration in the Serpent Formation quartzite can be observed. Several examples of tight to isoclinal folding with brecciated fold hinges associated with mineralization can be observed at this location (*see* Photo 9).

Stop 5. Scadding Mine – Villeneuve zone

UTM 529588E 5166469N (NAD83, Zone 17)

In 2011, Trueclaim Exploration Inc. exposed an outcrop to the east of the East-West pit. They took three samples, the highest of which returned 0.626 g/t gold. A detailed structural analysis by MacDonald Mines Exploration Ltd. and grab sampling (Sample 802357: 8.62 g/t gold) identified potential for expansion of the mineralized zone. The area was mechanically stripped, exposing a zone of chlorite and sulfide minerals that is now called the Villeneuve Zone (Figure 10). The stripped area is characterized by zones of strong Fe-alteration and intense brecciation at the Serpent–Espanola Formation contact. This outcrop illustrates the close spatial relation and the evolution of alteration in the Scadding deposit, from LT Mg-Si-(Na,K)-Fe alteration facies (ferroan-dolomite, silicification, albitization) to the LT Si-(Mg,Fe) alteration facies (quartz-chlorite breccia, Fe-rich chlorite). The contact between the Espanola Formation limestone and the Serpent Formation quartzite occurs at the south end of the trenched area. Strong ductile deformation is observed within the Espanola Formation limestone as observed at trench SMT-20-012 (*see* Stop 3), along with selective layers of magnetite and chlorite replacement. On the Serpent Formation quartzite side of the contact, strong brittle deformation associated with extensive brecciation is observed. The breccias are cemented by ferroan-dolomite and quartz associated with the LT (Si,CO_2)-(Ca,Mg,Fe) facies that is locally overprinted by chlorite associated with the LT Mg-Si-(Na,K)-Fe facies. Northward along the outcrop, the fragments in the breccia increase in size and display less rotation within the breccia matrix; gradually the brecciated areas become more localized. The changes in bedding orientation are interpreted as a sign that the zone of brecciation is developed within the hinges of tight to isoclinal folds in the quartzite.

Northward along the outcrop, LT (Si,CO_2)-(Ca,Mg,Fe) alteration progressively transitions to a zone of strong to intense chlorite alteration. Chlorite alteration is distributed within the same fold system. It is very strong in the axial zone of the fold and expands outside of the axial zone as selective replacement fronts replace beds in the Serpent Formation. Toward the east, the quartz content gradually increases to a point where quartz predominates completely over chlorite, marking at surface the transition between the LT Mg-Si-(Na,K)-Fe and the LT Si-(Mg,Fe) facies. Mineralization occurs as patchy pyrite, pyrrhotite and trace chalcopyrite. Locally visible gold is associated with the strong chlorite alteration, and the channel sample with the highest gold grade was located in the main zone of transition between the LT Mg-Si-(Na,K)-Fe and the LT Si-(Mg,Fe) facies.

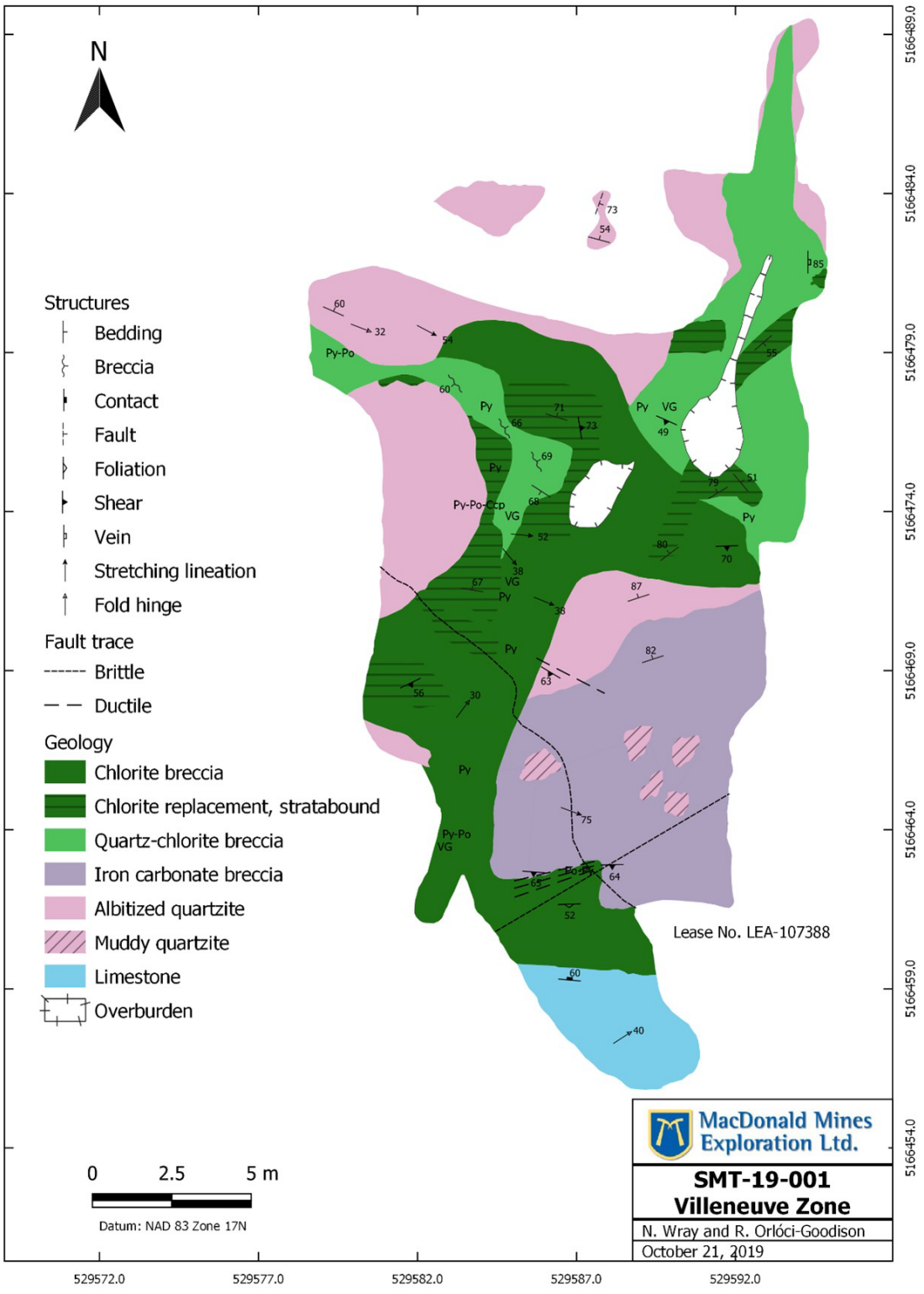

Figure 10. Geology map of Scadding Mine's Villeneuve zone (Stop 5). Abbreviations: Ccp, chalcopyrite; Po, pyrrhotite; Py, pyrite; VG, visible gold.

Return to vehicles and follow the mine road out of the Scadding mine site.

0.0 km	Turn right onto Kukagami Road from the entrance of the Scadding mine site.
16.0 km	Turn right onto Trans-Canada Highway 17. Continue travelling west until you enter the city of Greater Sudbury, where Highway 17 becomes the Kingsway (Regional Road 55).
49.75 km	Keep right and continue onto Lloyd Street (Regional Road 55). Then continue straight onto Brady Street (Regional Road 49).
50.25 km	Turn left onto Paris Street (Regional Road 80).
52.7 km	Turn left onto Ramsey Lake Road (Regional Road 39).
55.0 km	Turn right onto University Road. After 650 m turn left and head another 200 m to the RD Parker building.

DAY 2

0.0 km	Start at Laurentian University, outside of the RD Parker building. Paid day parking is available on Laurentian campus [*935 Ramsey Lake Rd, Sudbury, ON P3E 2C6*].
0.8 km	Follow University Road through campus and turn left onto Ramsey Lake Road (Greater Sudbury Regional Road 39).
3.1 km	Turn right onto Paris Street (Greater Sudbury Regional Road 80 N).
5.5 km	Turn right onto Brady Street (Greater Sudbury Regional Road 49).
6.05 km	Continue onto Lloyd Street (Greater Sudbury Regional Road 55) to the Kingsway (Greater Sudbury Regional Road 55).
20.8 km	Continue travelling east onto Trans-Canada Highway 17 until you reach the turnoff for Kukagami Road.
39.8 km	Turn left onto Kukagami Road and travel north.
55.8 km	The entrance to the Scadding mine site is approximately 700 m past the turn for Ashigami South Shore Road, after the 16 km marker. The entrance is marked with an orange pilon on the left-hand side of the road. There is a large area to park as soon as you turn left; someone from MacDonald Mines Exploration Ltd. will meet you at this point to guide you for the rest of the way to the first stop.

Stop 6. Glade – AGT-21-007

UTM 529284E 5165361N (NAD83, Zone 17)

AGT-21-007 (Figure 11) was mechanically stripped and cleaned by MacDonald Mines Exploration Ltd. in 2021. This area was chosen to test the contact between Espanola Formation limestone and the Nipissing diabase in the Glade area, which has proven to be a significant trap for mineralization elsewhere in the camp. The spatial relation between the Espanola Formation and mineralization is observed at Long trench in the Powerline area, and at both Scadding (Stop 1) and Glade (Stop 6). The outcrop consists of strongly deformed Espanola Formation limestone in contact with Nipissing diabase on the southeast side, which is also significantly sheared and deformed proximal to the contact in a southwesterly orientation from 208-234°/68-70°. The limestone at this trench has at least two generations

of folding, where F_1 plunges moderate to strongly to the northeast from 030-065°/55-72° (trend/plunge), and F_2 plunges moderately to the west from 276-280°/44-48° (trend/plunge) (Photo 10). Alteration in the limestone consists of abundant carbonate (ankerite + calcite and/or dolomite), minor to moderately abundant chlorite in foliation and selective layers, and patches of trace hematite. Of significance at this trench, is that channel and grab samples through the northeast-plunging fold hinges contain low-grade gold from 0.055 to 0.403 g/t, associated with very fine-grained pyrite, pyrrhotite and arseniferous pyrite. Although the mineralization at this trench is low grade, with weaker alteration intensities than those observed elsewhere in the Glade region, this location is significant in demonstrating the structural controls on mineralization in the Espanola Formation limestone and the presence of gold mineralization in the limestone even when there are very weak visual indicators.

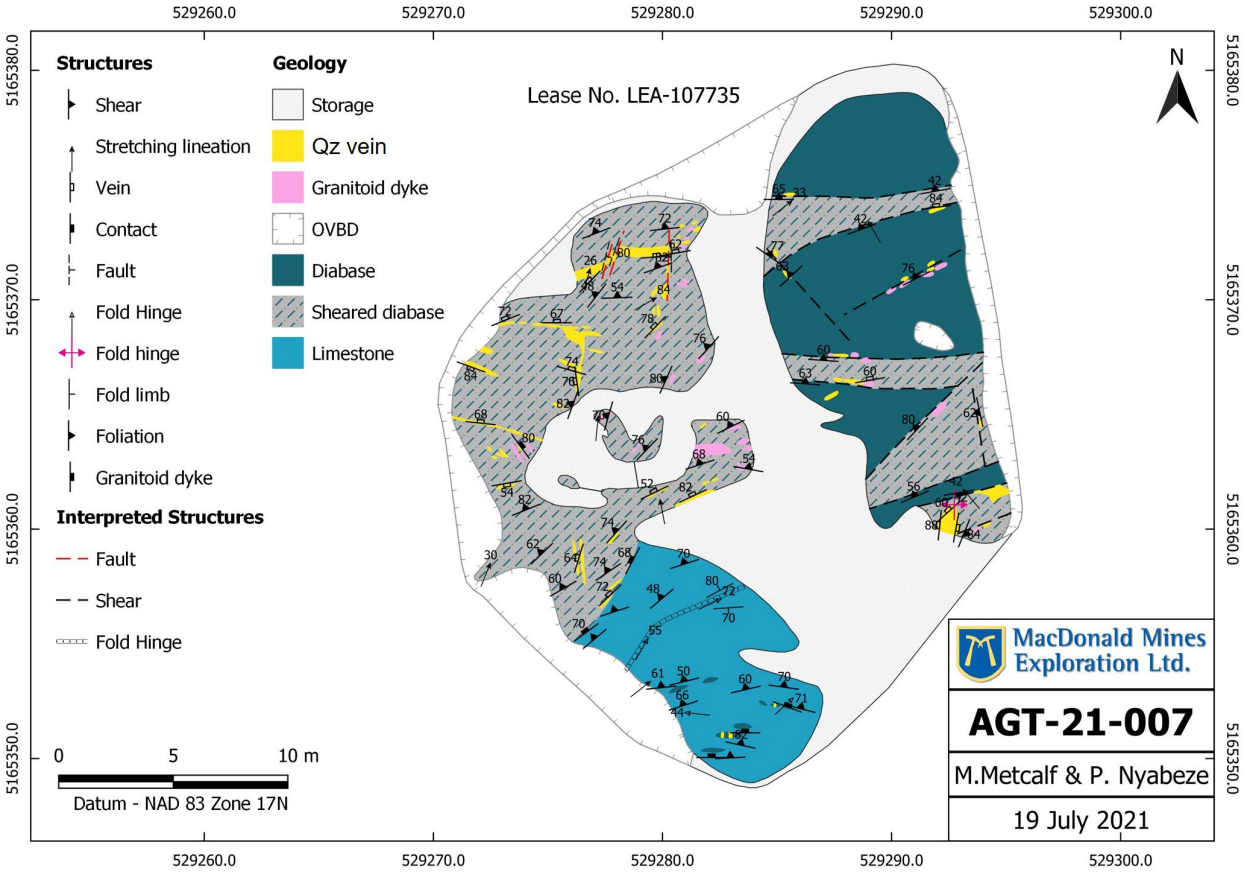

Figure 11. Geology map of AGT-21-007 (Stop 6). Abbreviations: OVBD, overburden; Qz, quartz.

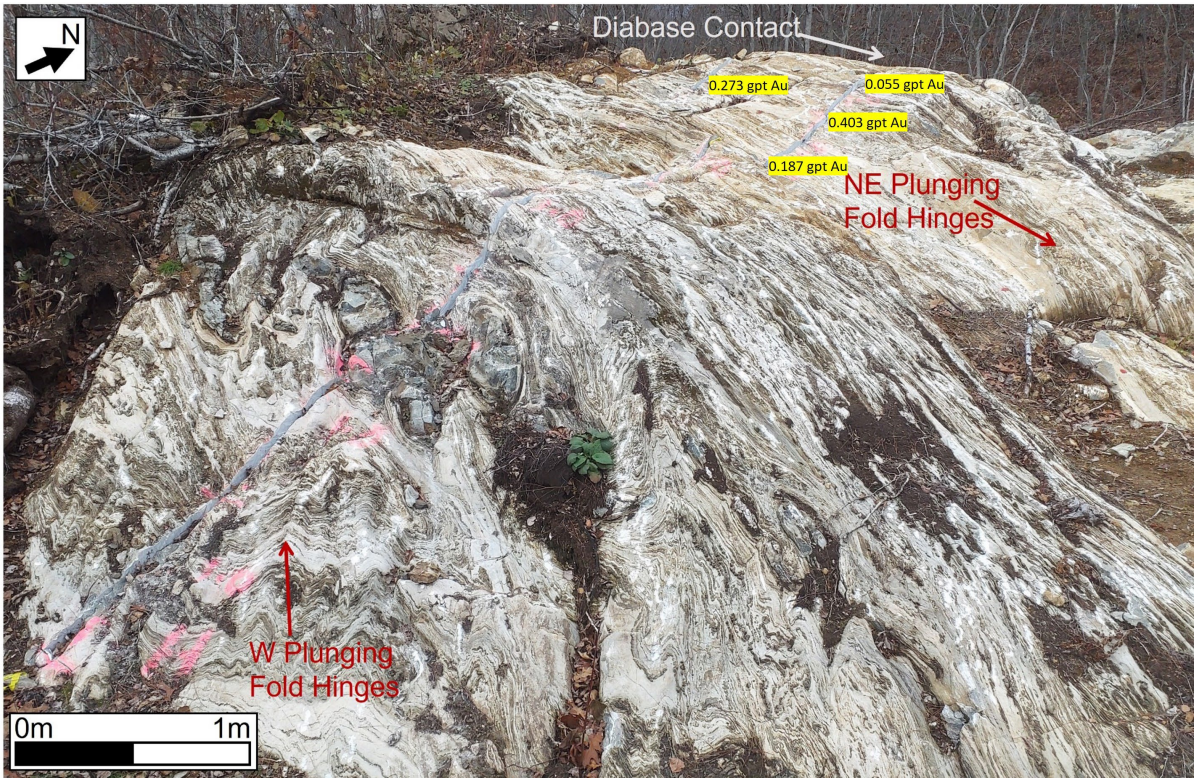

Photo 10. Folding and mineralization in Espanola Formation limestone at AGT-21-007 (Glade) (Stop 6). Abbreviations: Au, gold; gpt, grams per tonne; NE, northeast; W, west.

Following completion of the 2022 diamond-drilling program by MacDonald Mines Exploration Ltd. at Glade and reviewing surface geology, the presence of Sudbury Breccia has become increasingly recognized in the Glade area. At this trench, networks of chloritized Sudbury Breccia veinlets with fragments of felsic intrusive rocks occur in patches throughout shear zones in the Nipissing diabase, typically associated with gossanous patches of pyrite, pyrrhotite and minor chalcopyrite. The significance of Sudbury Breccia will be examined in greater detail at trench AGT-21-005/006 (Stop 7).

Stop 7. Glade – AGT-21-005/006

UTM 529079E 5165551N (NAD83, Zone 17)

This trench is fairly steep and can be slippery when wet. Participants should be careful walking up the outcrop and are encouraged to use the trail on the west side of the trench to walk down the outcrop if it is wet. Additionally, there are two small blast pits at the top of the trench; as a safety precaution, please keep a minimum distance of 5 ft (1.5 m) from the edge of these pits.

AGT-21-005/006 (Figure 12), also known as the Glade West showing, consists of a stripped area and two blasted pits of unknown origin. In 2021, the historically stripped area was extended for detailed structural and alteration mapping around the two blast pits to gain a better understanding of the vein system and the structural controls on the location of the veins and mineralization. The outcrop consists of deformed quartz ± iron-rich chlorite veins hosted in sheared Nipissing diabase. The trench demonstrates that the two preferential orientations of shearing observed are parallel to pre-existing corridors of Sudbury Breccia. Each deformed corridor of Sudbury Breccia hosts networks of quartz veins with varied chlorite content

that are also variably deformed by shearing. The dominant orientation of the Sudbury Breccia corridors and shearing trends southwesterly at 239°/74° and is observed throughout the Nipissing intrusions in the Glade area. This orientation is parallel to the dominant quartz vein orientation at 232°/76°NW (strike/dip). A second less pervasive orientation of shearing trends northwesterly at 329°/71°.

Pinching and swelling is very common in the quartz veins along the deformed corridors of Sudbury Breccia, and zones of swelling of veins are observed at the intersection of corridors of deformed Sudbury Breccia. One of these intersections at station AGT-21-005/006 corresponds to an area of higher-grade gold mineralization as determined by channel sampling (sample 265910 – 17.1 g/t gold), whereas another intersection corresponds to the location of the historical pit. Mineralization occurs as pyrite and gold near the margins of the vein where the quartz is interlayered with iron-rich chlorite. This style of mineralization is similar to the mineralization at the northeastern end of the Villeneuve zone (Stop 5), where the quartz-rich breccias, with lesser iron-rich chlorite, are the host to some of the trench's mineralization. At depth, the main corridor of deformed Sudbury Breccia observed at station AGT-21-005/006 is strongly albitized and altered by gold-mineralized chlorite. This forms a mineralization assemblage comparable to the chlorite zones of the Scadding deposit and suggests that the system transitions from the LT Si-(Mg,Fe) facies that predominates at surface to the LT Mg-Si-(Na,K)-Fe facies at depth.

This station also exposed centimetres- to metres-wide felsic intrusions cutting across the prevailing Nipissing intrusions. Fragments of felsic intrusive rock are present in most of the Sudbury Breccia corridors developed in the Nipissing intrusions in the Glade area. These originally linear zones of rheological contrasts between mafic and felsic intrusions in the Nipissing intrusions may have preferentially partitioned the stress of the impact in linear corridors that were then variably deformed and altered during the Yavapai Orogeny.

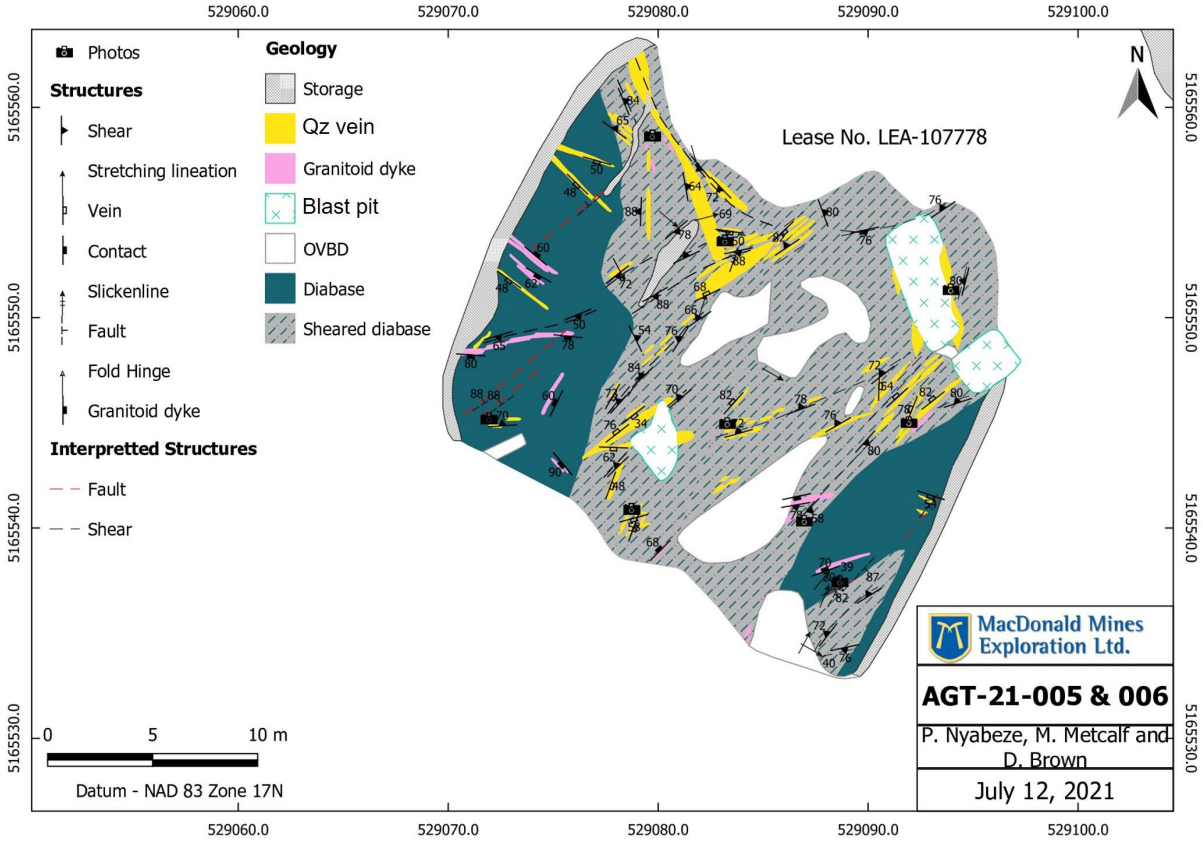

Figure 12. Geology map of AGT-21-005/006 (Stop 7). Abbreviations: OVBD, overburden; Qz, quartz.

Stop 8. Alwyn Mine – AWT-21-001

UTM 528257E 5172114N (NAD83, Zone 17)

The historical Alwyn Mine shaft is just off the trail that leads up to this stop. Caution tape marks the location of the shaft, but participants are asked to stay on the marked trail to ensure safety, as well as to reduce the potential for slips, trips and fall hazards going up the hill to the stop.

This stop covers the main Alwyn Mine trench and showing, AWT-21-001 (Figure 13), located 72 m northwest of the historical Alwyn Mine shaft. The trench consists of strongly sheared and/or strained Gowganda Formation, clast-poor conglomerate and siltstone, with moderate to high density veining. A very intense, approximately 1 m wide shear zone occurs on the western side of the trench striking northwesterly at 316°/82°NE (strike/dip) that is parallel to the regional McLaren Lake Fault Zone (MLFZ). Along the northeastern margin of this shear zone exists a strong strain corridor with an albitized alteration halo; within this corridor the rock is moderate to strongly jointed with common anastomosing shear bands (Photo 11). Approximately 3 m northeast of the shear zone, the rock becomes slightly more massive, with less frequent jointing and narrow shears.

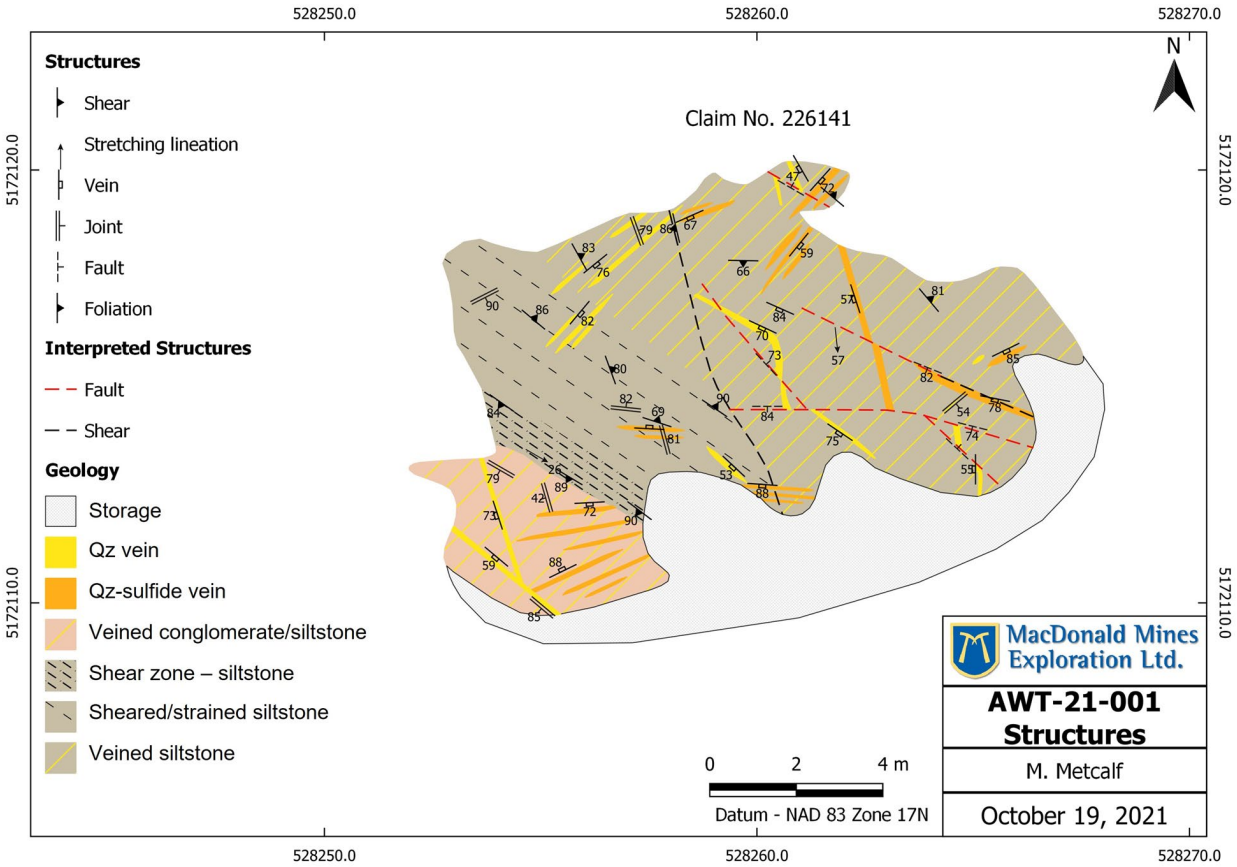

Figure 13. Geology map of AWT-21-001 (Stop 8). Abbreviation: Qz, quartz.

Quartz-carbonate ± sulfide mineral veining associated with copper-gold mineralization occurs at three dominant orientations. The dominant vein set is orientated at 053°/73°SE (strike/dip – most abundant set), with secondary vein sets orientated at 089°/75°S (strike/dip – least abundant set), and 141°/62°SW (strike and dip). All three vein orientations are variably mineralized with chalcopyrite, pyrite and malachite staining, as well as earthy, red hematite surrounding sulfide mineralization. Although no specular hematite or potassium feldspar is observed at this trench, at depth through the 2022 diamond-drilling program, as well as farther along the Alwyn copper-gold trend, quartz-carbonate veins also can be associated with specular hematite and potassium feldspar. Across all trenches there is evidence of crosscutting relationships that indicate the veins are contemporaneous; this observation is further supported by diamond drilling completed in May 2022 by MacDonald Mines Exploration Ltd. Conversely, there is good evidence that the primary shear zone postdates veining, as it completely cuts off veins on the southwest side of the exposed area and has incorporated fragments of both mineralized and unmineralized quartz veins. Although this shear zone appears to postdate veining at AWT-21-001 (Stop 8), it is still likely that one or more of the structures associated with the MLFZ played a crucial role in facilitating the migration of fluids during the mineralization event at Alwyn Mine; however, additional work will be needed to determine the extent of the influence of the MLFZ.

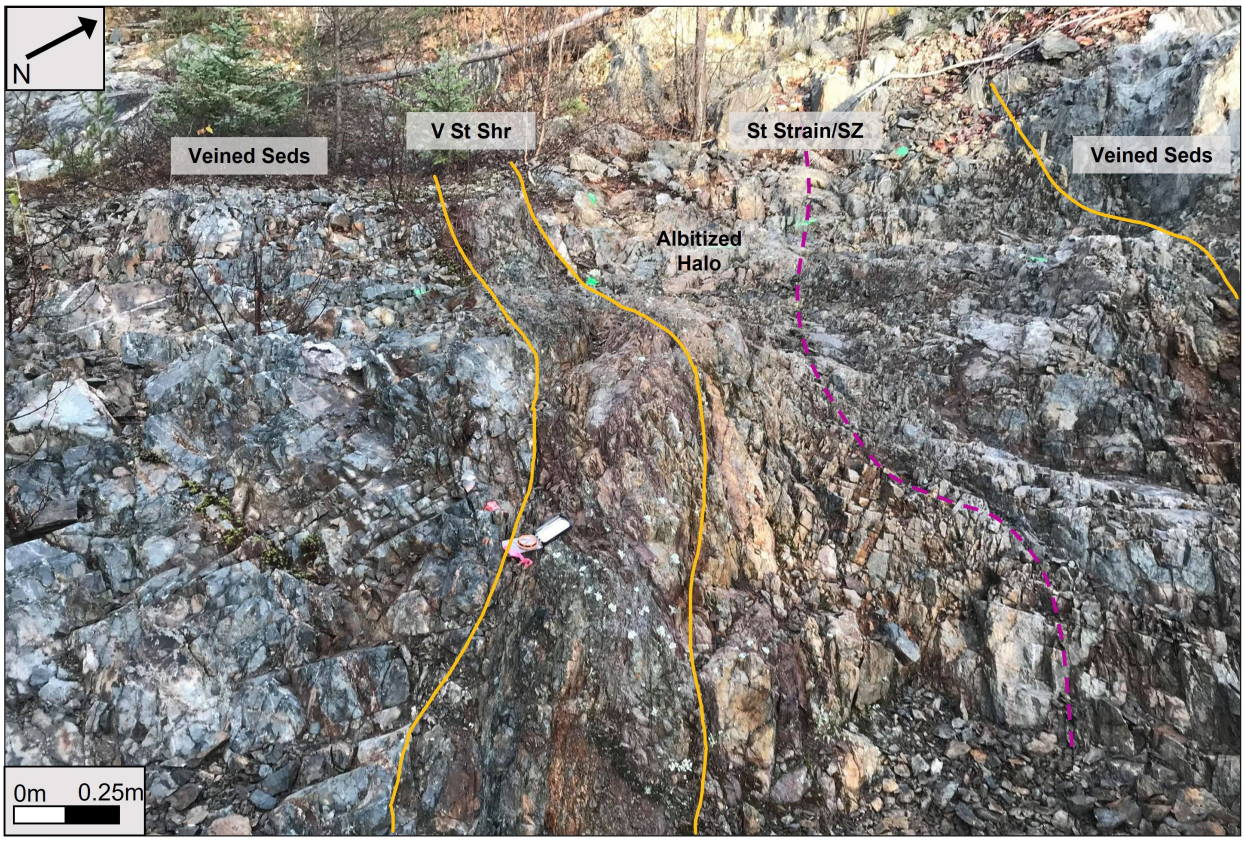

Photo 11. Intense shear zone present in trench AWT-21-001 at the Alwyn Mine (Stop 8). Abbreviations: Seds, sediments; St Strain/SZ, strong strain and/or shear zone; V St Shr, very strong shear zone.

Stop 9. Examining diamond-drill core at the Scadding Mine core shack

UTM 529111E 5166455N (NAD83, Zone 17)

The second portion of this field trip will focus on reviewing highlighted diamond-drill hole intervals from the Scadding Mine, Glade, Alwyn and Jovan areas. This core will demonstrate characteristic alteration facies and iron-rich to iron-poor mineralization associated with MIAC systems. Figure 14 shows the locations of the 9 diamond-drill holes selected for the field trip. For each drill hole, high-resolution tabletop XRF images were acquired to illustrate the mineralogy and certain characteristic element associations of the presented alteration facies.

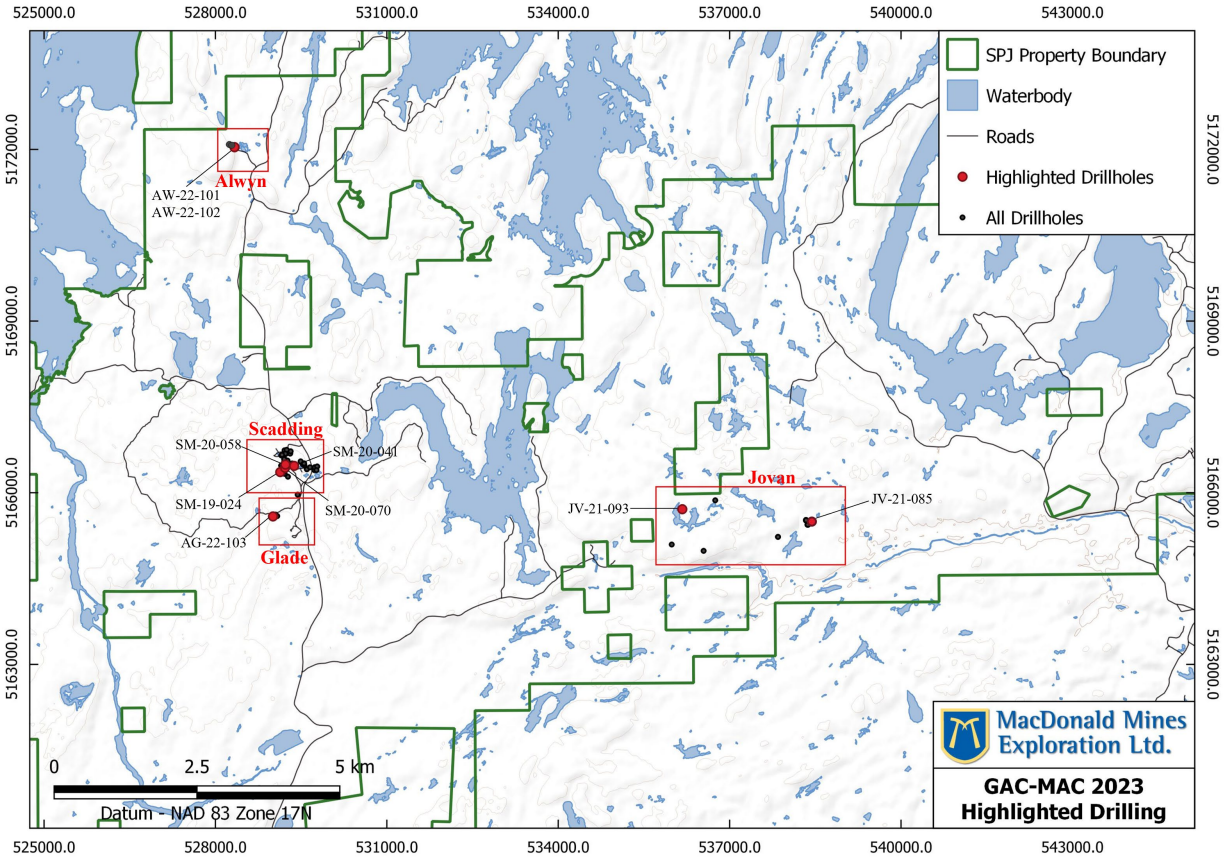

Figure 14. Location map showing the location of drill holes to be examined at the Scadding Mine core shack.

Core 1 – SM-19-024 – Regional sodic alteration overprinted by iron-dolomite associated with the LT CO_2-(Ca,Mg,Fe)-Si alteration facies

This interval of core from SM-19-024 (184.8 – 211.0 m) displays the shoulders of the Bristol Breccia where LT CO2-(Ca,Mg,Fe)-Si alteration overprints an albitite and forms very coarse-grained iron-dolomite crystals, which exhibit oscillatory zoning (highlighted by iron in Photo 12), with accessory quartz. The LT CO2-(Ca,Mg,Fe)-Si and Na alteration facies are regionally present in the field trip area and are very common in the alteration haloes, or are directly hosting many zones of mineralization. In the sample analyzed by tabletop XRF, LT CO2-(Ca,Mg,Fe)-Si alteration overprints an albitite formed after layered units of the Serpent Formation (displayed in Photo 12). The micro-XRF images and macroscopic

textures indicate that the primary laminations of the sedimentary precursor extend into the very coarse-grained dolomite crystals that are overprinting the albitite (best demonstrated by titanium in Photo 12). These textural relations demonstrate that Fe-dolomite formed by dissolution-precipitation of the albitite at constant volume and illustrate the potential of metasomatism to completely recrystallize and change the original textures of rock units (best demonstrated by titanium in Photo 12).

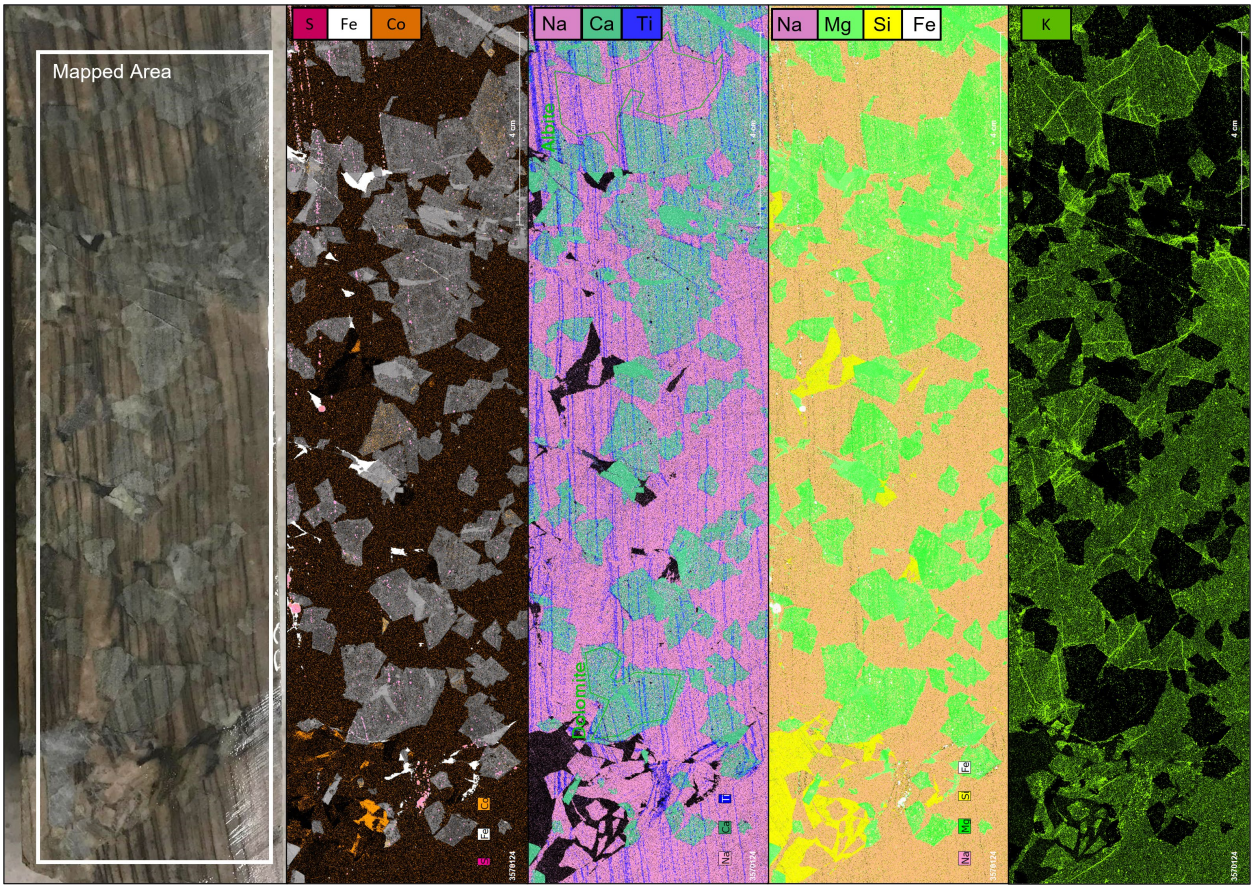

Photo 12. False colour micro-XRF elemental distribution maps of core from SM-19-024 (Core 1) (XRF Sample 2 – 206.1 m; left photograph) demonstrating strong pervasive sodic (Na – pink) and moderate potassic (K – green) alteration, very coarse-grained iron-dolomite (Fe-Dol) rhombs (Fe – white; Mg – yellow-green) with original laminations of precursor sedimentary unit preserved (demonstrated chemically by titanium – blue).

Core 2 – AW-22-101 – Incipient cobalt mineralization at the Alwyn prospect

This interval of core (76.5 – 103 m) from Alwyn demonstrates pervasive low-grade cobalt mineralization associated with the LT CO_2-(Ca,Mg,Fe)-S facies that overprints earlier, pervasive sodic alteration (up to 5 weight % Na in core samples in the zone; Photo 13). This represents the first observation of this style of mineralization in the Alwyn area. The broader zone mineralization contains 153 ppm Co over 26.5 m and is hosted in fine-grained siltstone of the Gowganda Formation which contains the occasional polymictic clasts. Cobalt mineralization can be related to pervasive dissemination of arseniferous pyrite coupled with manganese enrichment and pervasive potassic alteration (Photo 14). This chemical association detected with the tabletop XRF may represent, at lower intensity, alteration and cobalt mineralization that are comparable to the Palkovics area (*see* Core 3) and the Bristol Breccia (*see* Core 4).

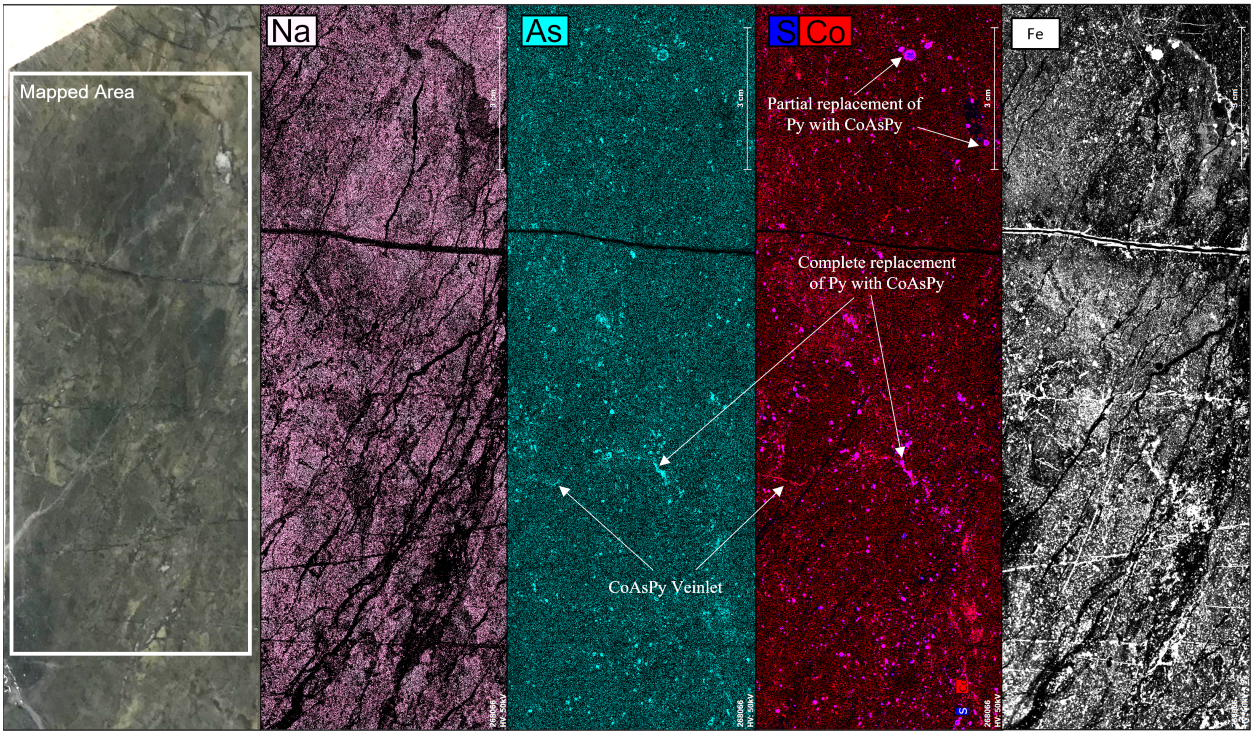

Photo 13. False colour micro-XRF elemental distribution maps of core from AW-22-101 (Core 2) (XRF Sample 3 – 84.6 m; left photograph) demonstrating strong pervasive sodic alteration (Na – pink), with progressive replacement of pyrite by cobalt-bearing and arseniferous pyrite (CoAsPy; As – light blue, S – navy blue, Co – red, Fe – white).

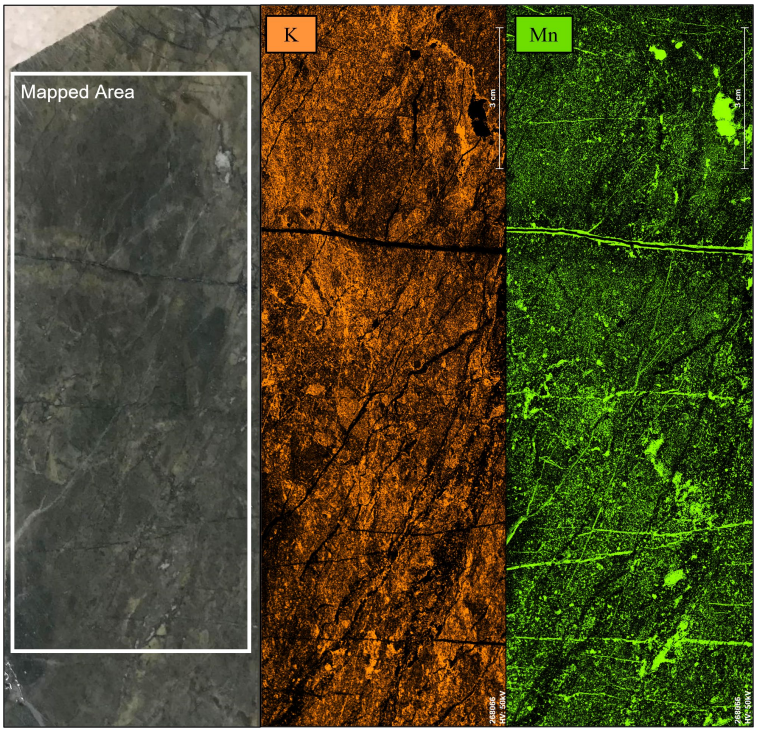

Photo 14. False colour micro-XRF elemental distribution maps of core from AW-22-101 (Core 2) (XRF Sample 3 – 84.6 m; left photograph) demonstrating moderate potassic alteration (K – orange) and weak to moderate manganiferous (Mn – yellow-green) alteration comparable to Bristol Breccia (Scadding (Core 4)) and Palkovics (Core 3).

Core 3 – JV-21-093 – Cobalt and gold mineralization at the Palkovics prospect

This hole was completed in the winter of 2021 to test the lateral and western extension of gold-cobalt-copper mineralization observed on the Palkovics 1 trench, sampled in 2018 to 2020. This hole successfully tracked gold and cobalt mineralization hosted within a strongly albitized conglomerate host unit.

Sample 4 (Photos 15 and 16) illustrates a zone of cobalt mineralization associated with the LT CO_2-(Ca,Mg,Fe)-Si facies that contain 1640 ppm Co over a length of 1.32 m. This zone was intersected between 161.56 and 162.88 m in JV-21-093. In that sample, tabletop XRF images illustrate pervasively disseminated cobalt-bearing arseniferous pyrite associated with weak potassic alteration with Mn and

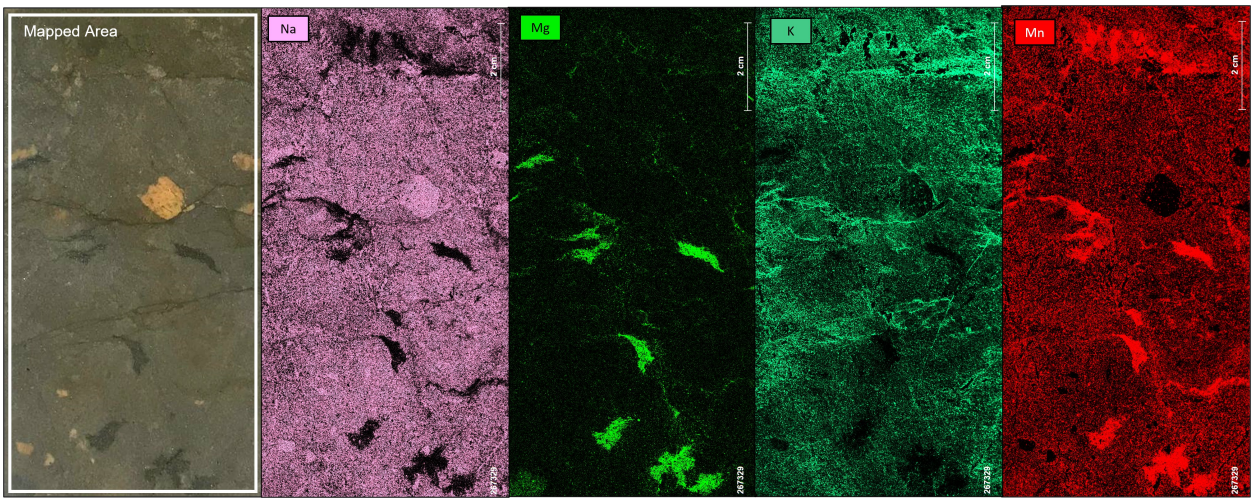

Photo 15. False colour micro-XRF elemental distribution maps of core from JV-21-093 (Core 3) (XRF sample 4 – 162.6 m, left photograph) showing strong pervasive sodic (Na – pink) alteration, patchy Fe-dolomite (Mg – yellow-green) replacement and moderate potassic (K – green) alteration. Dolomite is relatively rich in manganese (Mn – red).

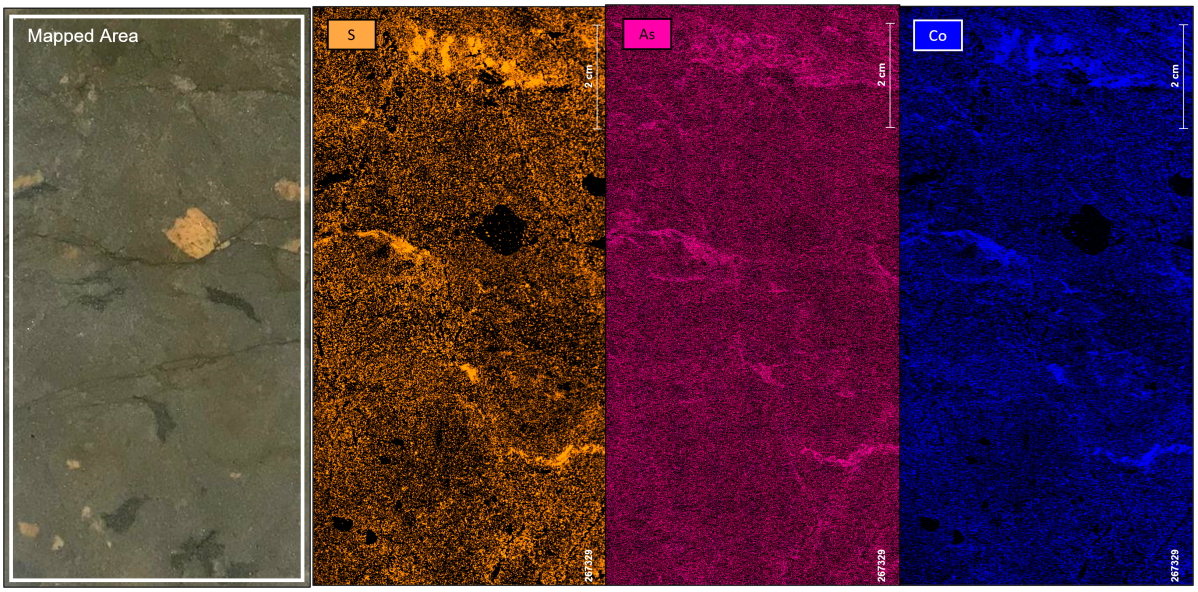

Photo 16. False colour micro-XRF elemental distribution maps of core from JV-21-093 (Core 3) (XRF sample 4 – 162.6 m, left photograph) showing the association between Fe, S, As and Co that indicate the association between cobalt mineralization and the formation of cobalt-bearing arseniferous pyrite (Co-As-Py).

pervasive Fe-Dol + Qtz alteration that overprints an albitized conglomerate (*see* Photos 15 and 16). This zone of cobalt mineralization at the Palkovics showing (Core 3) is comparable, but more developed, to the one observed at the Alwyn prospect (Core 2).

Sample 5 (Photos 17 and 18) illustrates a zone of iron-poor gold mineralization associated with the LT CO_2-(Ca,Mg,Fe)-Si facies that contains 2.66 g/t gold over 0.96 m. This sample is part of a larger zone of gold mineralization that contains 0.88 g/t gold over 6.25 m that is developed in an altered conglomerate and a small Sudbury Breccia body. Tabletop XRF images shown in Photo 17 illustrate strong and pervasive sodic alteration in the conglomerate unit. Sodic alteration is also overprinting the Sudbury Breccia veinlet but is weaker than in the conglomerate. The albitized conglomerate and Sudbury Breccia are both replaced by a mineral assemblage of the LT CO_2-(Ca,Mg,Fe)-Si facies composed of pervasive and fine- to coarse-grained iron-dolomite (Fe-Dol) with accessory quartz and pyrite. The tabletop XRF images indicate a weak to moderate potassic alteration with manganese that is associated with Fe-Dol alteration. In the conglomerate, Photo 18 demonstrates that arseniferous pyrite, interpreted to be related to the gold mineralization, is preferentially formed around the crystals of Fe-Dol, whereas arseniferous pyrite is spotted in the Sudbury Breccia. Of interest, disseminated nickel is hosted in Sudbury Breccia.

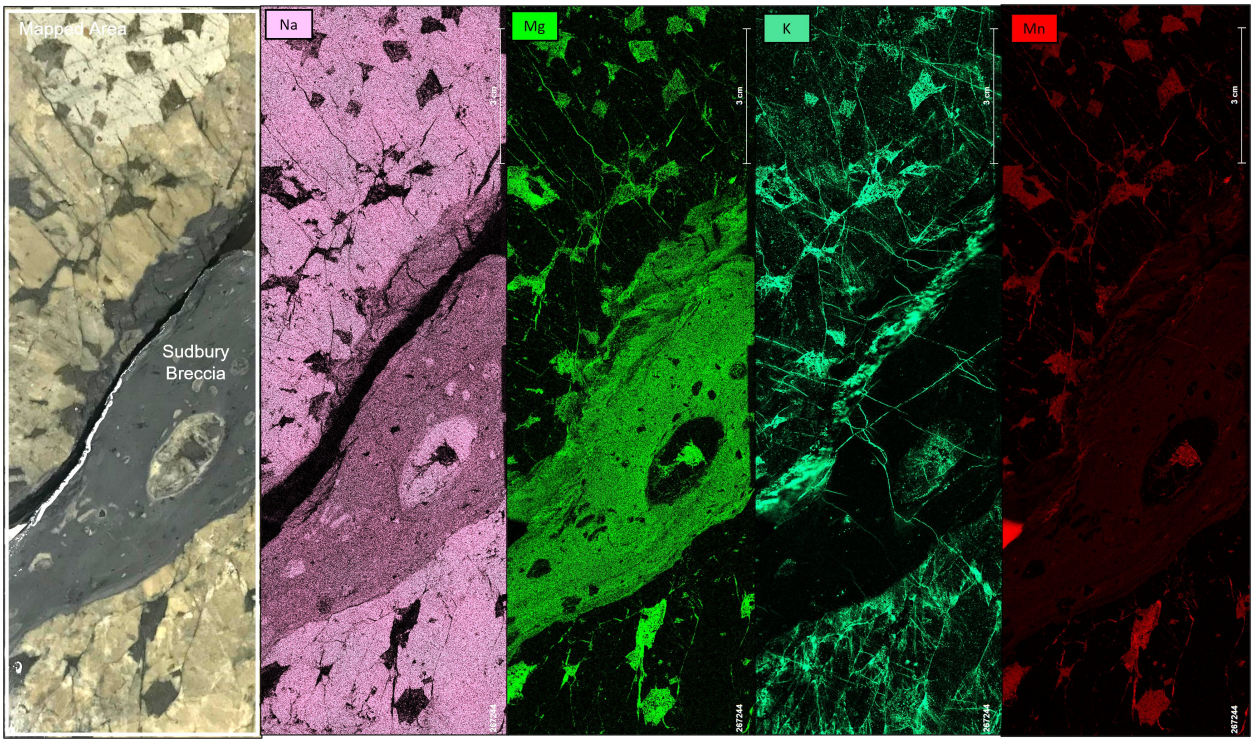

Photo 17. False colour micro-XRF elemental distribution maps of core from JV-21-093 (Core 3) (Sample 5 – 93.1 m; left photograph) demonstrating strong pervasive sodic alteration (Na – pink), weak Fe-dolomite (Mg – yellow-green) replacement with a weak Mn signature (Mn – red), and moderate potassic replacement (K – green).

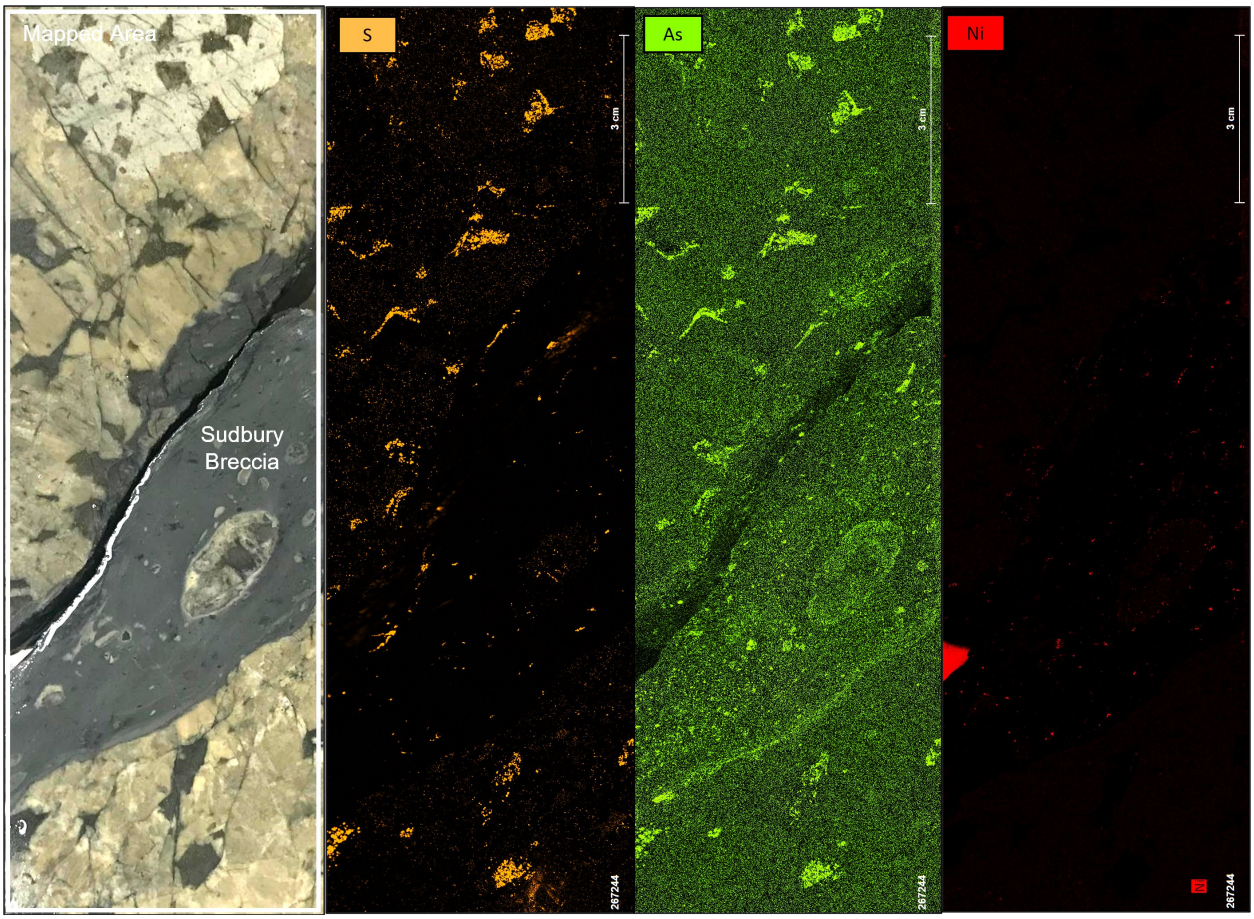

Photo 18. False colour micro-XRF elemental distribution maps of core from JV-21-093 (Core 3) (Sample 5 – 93.1 m; left photograph) demonstrating the replacement of Fe-dolomite with some cobalt-bearing arseniferous pyrite and pyrite (S – orange, As – green). Also note the disseminated nickel (Ni – red) within the Sudbury Breccia vein.

Core 4 – SM-20-058 – Gold-cobalt mineralization in the Bristol Breccia

The interval (145.95 – 190.12 m) from SM-20-058 displays the Bristol Breccia west of the Central zone of the Scadding deposit that contains 0.63 g/t gold and 94 ppm Co over 25.77 m. The Bristol Breccia is a silica-rich brecciated unit formed after strong to intense albitization of rocks of the Serpent Formation. Gold with accessory cobalt mineralization is associated with arseniferous pyrite alteration fronts that evolved from the Qtz-Fe-Dol (LT Si-(Ca,Mg,Fe)-CO_2) cement in the breccia (Photo 19). The arseniferous pyritic fronts overprint both the clasts and matrix, and are associated with a K and Mn signature (Photo 20). This unit represents gold-cobalt mineralization and alteration assemblages that are comparable to gold and cobalt mineralization at Palkovics (Core 3) and cobalt mineralization at Alwyn (Core 2), although they are texturally different.

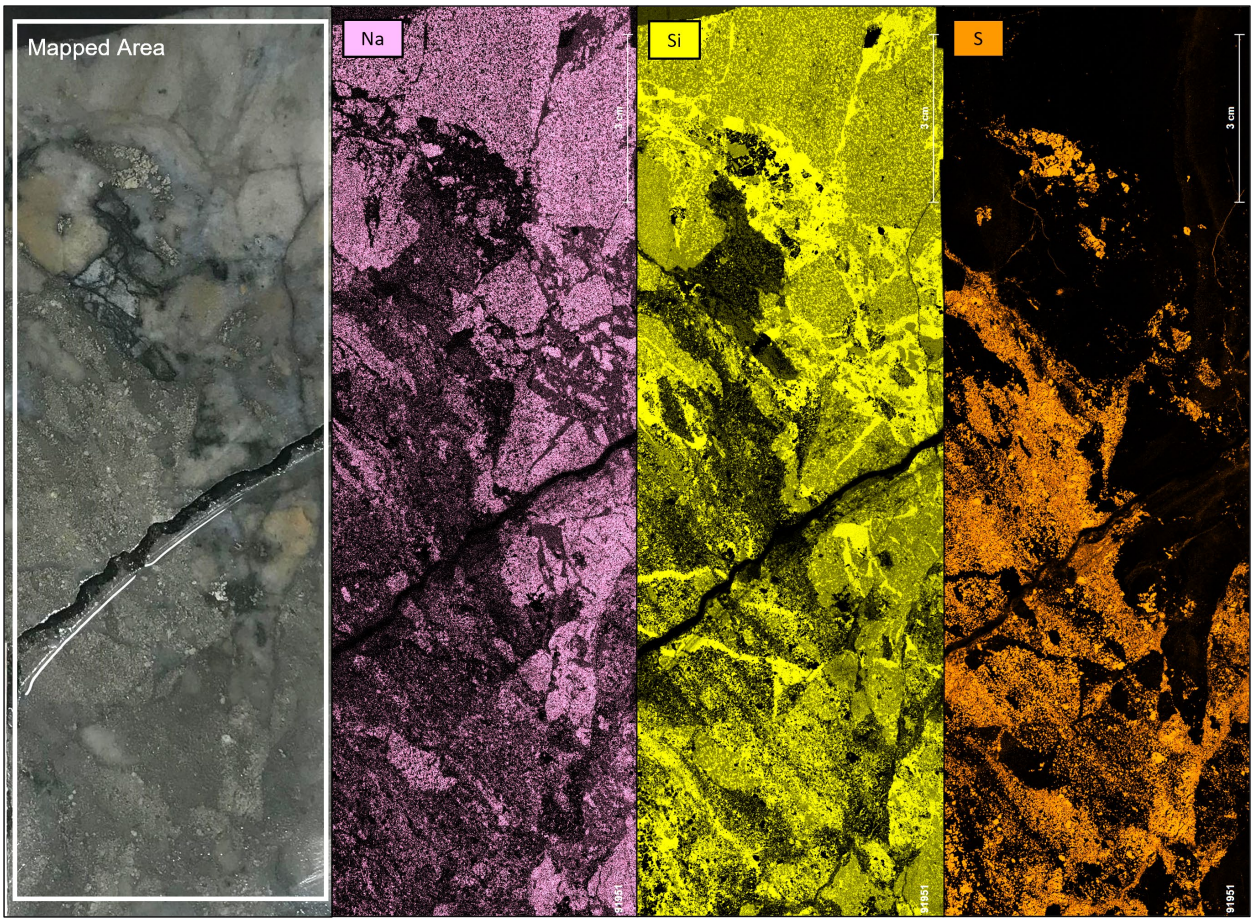

Photo 19. False colour micro-XRF elemental distribution maps of core from SM-20-058 (Core 4) (XRF Sample 6 – 157.3 m; left photograph) demonstrating strong pervasive sodic alteration of host rock (Na – pink), which has been brecciated and infilled with strong siliceous cement (Si – yellow). Disseminated pyrite overprints the matrix of the breccia (S – orange).

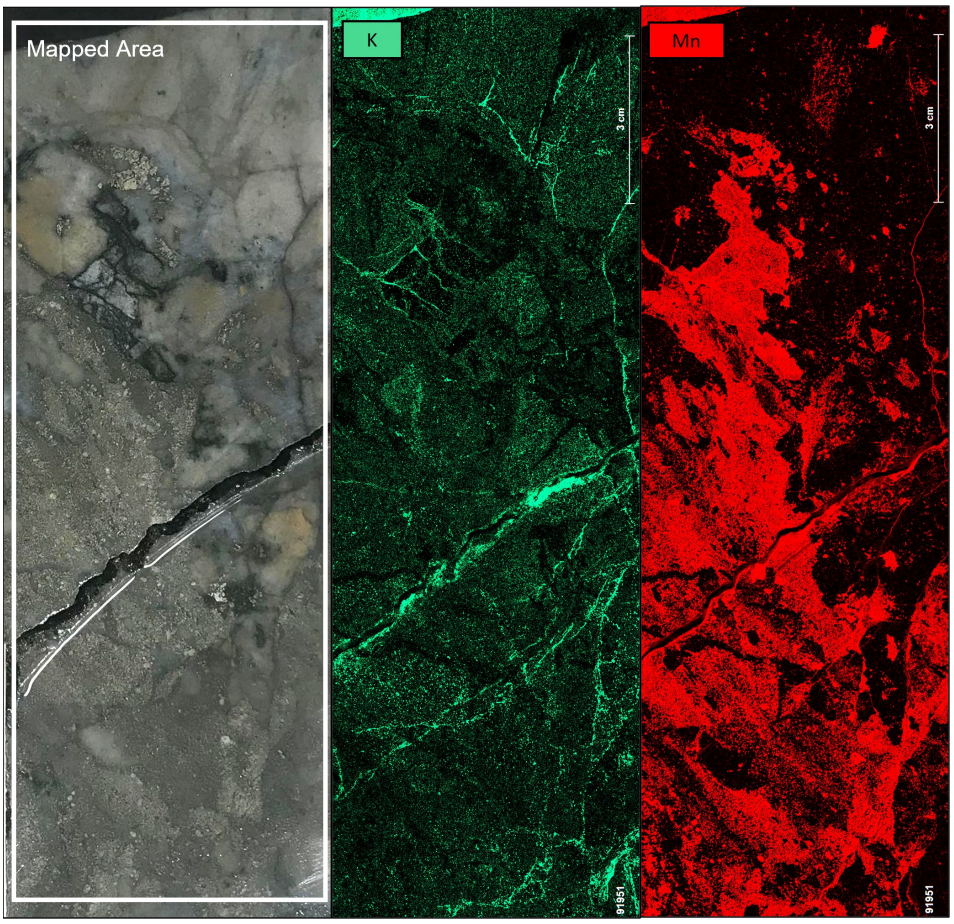

Photo 20. False colour micro-XRF elemental distribution maps of core from SM-20-058 (Core 4) (XRF Sample 6 – 157.3 m; left photograph) demonstrating weak potassic (K – green) and strong manganiferous (Mn – red) alteration comparable to Bristol Breccia (Scadding (Core 4)) and Palkovics (Core 3).

Core 5 – SM-20-070 – Chlorite with variable magnetite alteration related to gold and gold-cobalt mineralization at the Scadding deposit

The interval (70.18 – 105.56 m) from SM-20-070 demonstrates typical Scadding mine gold mineralization with accessory and localized cobalt enrichments associated with the LT Mg-(Na,K)-Fe alteration facies. The upper zone of mineralization in that interval contains 1.74 g/t gold and 170 ppm Co over 7.33 m, whereas the lower zone of mineralization contains 2.04 g/t gold over 12.03 m without significant Co. The sample analyzed with the tabletop XRF is a gold-rich sample that contains 11 g/t gold. Characteristic of the Scadding deposit, the Serpent Formation quartzite has been strongly albitized and then progressively iron altered by hydrothermal fluids, which completely obliterates original textures of the quartzite (Photo 21). This alteration is represented by strong zones of Fe-rich chlorite (white), magnetite and/or sulfide minerals (pyrite, pyrrhotite and minor chalcopyrite). The micro-XRF maps also indicate that potassic alteration occurred with chloritic alteration and is spatially associated with mineralization.

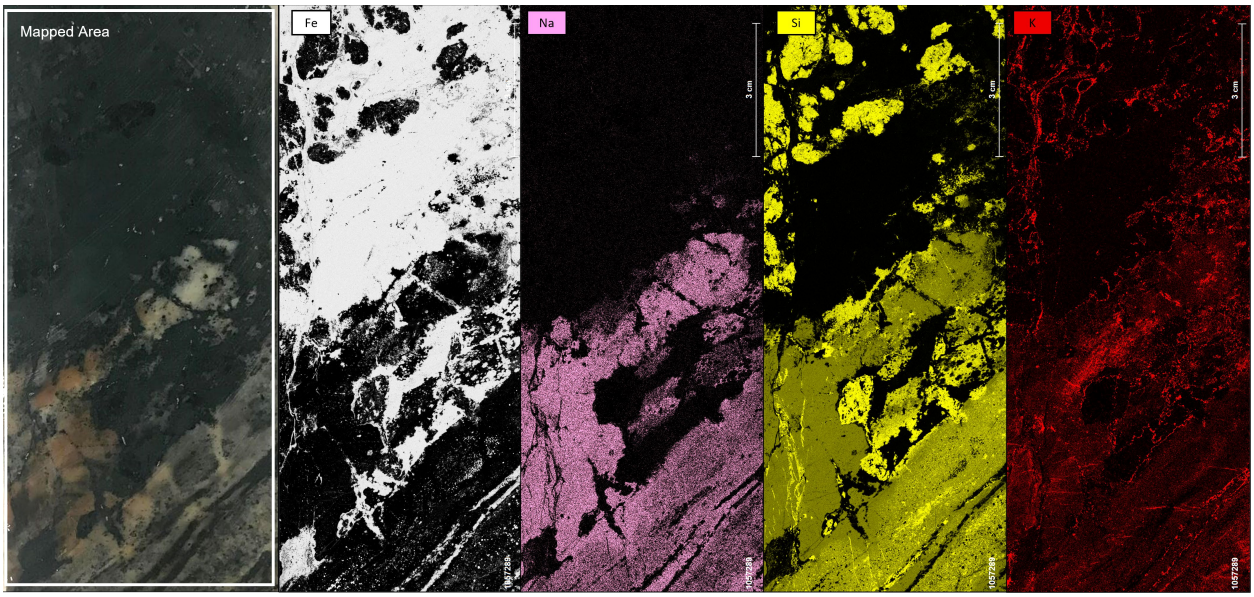

Photo 21. False colour micro-XRF elemental distribution maps of core from SM-20-070 (Core 5) (XRF Sample 10 – 98.7 m; left photograph) demonstrating strong pervasive sodic alteration (Na – pink) of host rock, overprinted by strong Fe-rich chlorite alteration (Fe – white) which destroyed original fabric and weak pervasive potassic alteration (K – red).

Core 6 – SM-20-041 – High-grade gold mineralization of the Scadding deposit

This interval (11.76 – 16.89 m) demonstrates the evolution of the MIAC alteration facies of the Scadding deposit from the early sodic alteration (albitized intervals and fragments) to carbonate-quartz alteration, and then to gold mineralized Fe-rich chlorite alteration with sulfide minerals (pyrrhotite and pyrite). This interval represents an example of the high-grade gold mineralization zones that are present in the Scadding deposit and that formed in the hinges of folds. The interval contains 27.17 g/t gold over 5.13 m, including 79.3 g/t gold over 1.03 m in the sample analyzed with the tabletop XRF. Gold is almost always observed with Fe-chlorite in this system where chlorite forms either massive replacement zones or the cement between brecciated fragments. When present, native gold precipitated along the margins of veins and within the chlorite replacement fronts or breccia cements. Photo 22 demonstrates the relationship between each alteration facies involved in the hydrothermal history of the Scadding deposit and provides excellent context for examining core from the Glade gold system (Core 7). The micro-XRF maps also indicate a weak potassic alteration spatially associated with chlorite alteration and old mineralization in the Scadding deposit.

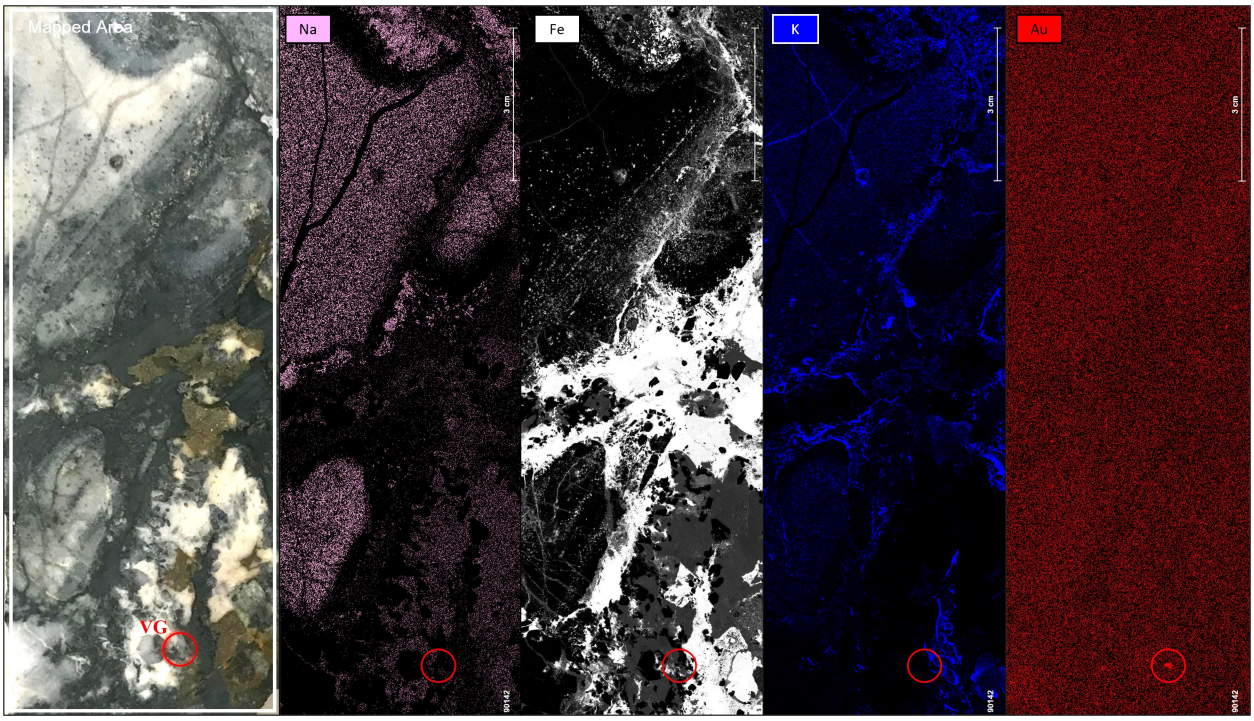

Photo 22. False colour micro-XRF elemental distribution maps of core from SM-20-041 (Core 6) (XRF Sample 9 – 16.5 m; left photograph) demonstrating the complex relationship between moderate albitization (Na – pink), weak to moderate carbonate-quartz alteration, weak potassic (K – blue), and strong Fe-rich alteration (chlorite and sulfide minerals; Fe – white). Visible gold (Au – red) is observed along the contact between Fe-rich chlorite and a fragment of a carbonate-quartz vein.

Core 7 – AG-22-103 – Gold mineralization associated with the LT Mg-Si-(Na,K)-Fe facies in the Glade area

Diamond-drill hole AG-22-103 (from 102.75 – 200.5 m) from the Glade area displays a succession of gold mineralization zones formed in the LT Mg-Si-(Na,K)-Fe facies in a composite Nipissing intrusion and the Espanola Formation limestone. The upper zone of mineralization extends from 102.75 to 113.1 m and contains 0.71 g/t gold over 10.35 m. The lower zone of mineralization straddles the Nipissing–Espanola Formation contact, extends from 144.5 m to 185 m and contains 0.82 g/t gold over 40.5 m, including 7.76 g/t gold over 2.9 m. The two zones of gold mineralization are separated by a zone of low-grade magmatic nickel-copper-PGE mineralization in a more primitive phase of the Nipissing intrusion (125.1 – 129.1 m).

In the Nipissing intrusions in general, chlorite alteration associated with gold mineralization preferentially overprints variably albitized corridors of Sudbury Breccia that were visited at surface at Stops 6 and 7 (Photo 23). Gold mineralization is associated with accessory and disseminated chalcopyrite-pyrrhotite-pyrite with possible arseniferous pyrite occurring as veins or disseminations. The association between gold mineralization and pervasive Fe-rich chlorite alteration is comparable to the iron-rich nature of chlorite in the Scadding deposit.

In the Espanola Formation limestone below its contact with the Nipissing intrusion, LT Mg-Si-(Na,K)-Fe alteration occurs as selective and stratabound alteration fronts of varied intensity. LT Mg-Si-(Na,K)-Fe alteration consists of Fe-rich chlorite with accessory to absent magnetite and with finely disseminated pyrite and arseniferous pyrite. These alteration and mineralization assemblages are comparable to those observed in the Sudbury Breccia corridors in the Nipissing intrusion. Zones of higher grade gold

mineralization in the Espanola Formation limestone typically correspond to strong LT Mg-Si-(Na,K)-Fe alteration of the Espanola Formation limestone (1.05 g/t gold from 181.5 – 185.0 m). The presence of the LT Mg-Si-(Na,K)-Fe facies at depth at Glade demonstrates that the system evolves from the LT Si-(Mg,Fe) facies prevailing at surface that was observed at Stop 7 to Scadding-like mineralization at depth.

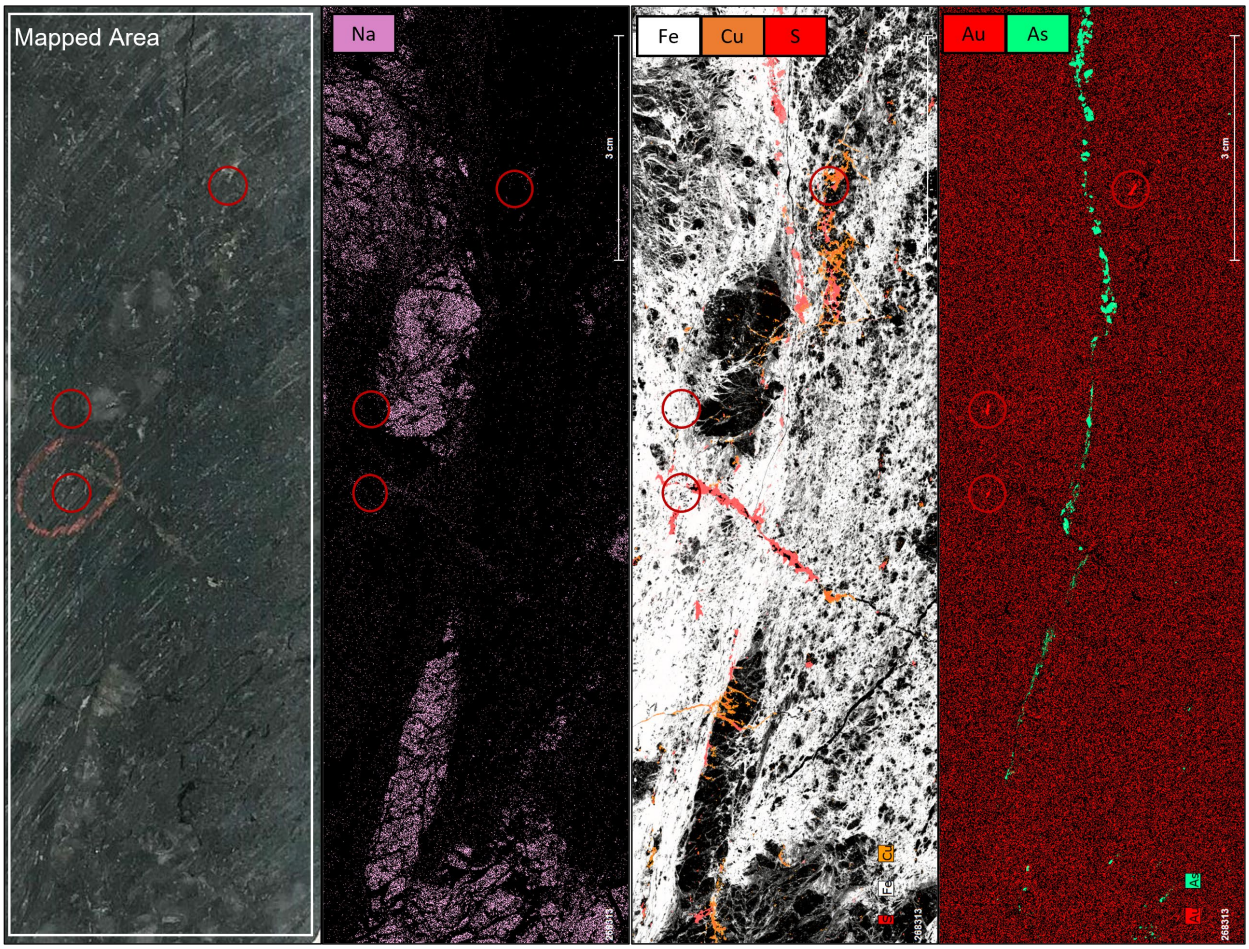

Photo 23. False colour micro-XRF elemental distribution maps of core from AG-22-103 (Core 7) (XRF sample 11 – 106.1 m; left photograph). Visible gold (Au – red) associated with moderate sodic (Na – pink) and strong Fe-rich chlorite alteration (Fe – white) in brecciated diabase (intrusive breccia unit).

Core 8 – AW-22-102 – Copper-gold mineralization associated with the LT (Si-CO_2)-(Ca,Mg,Fe), LT Si-(Fe)-K and LT (Ca,Mg)-Si-K-Fe alteration facies at the Alwyn prospect

The core interval (24.9 – 134.3 m) displayed from Alwyn demonstrates the transition from copper-gold mineralization associated with the LT (Si-CO_2)-(Ca,Mg,Fe) alteration facies (Photo 24) to copper-gold mineralization associated with the LT Si-(Fe)-K and LT (Ca,Mg)-Si-K-Fe alteration facies (Photos 25 and 26). The precursor units in all the displayed core interval are siltstones and clast-poor conglomerate of the Gowganda Formation. The upper interval consists of a large and composite quartz–Fe-dolomite vein formed as part of the LT (Si-CO_2)-(Ca,Mg,Fe) alteration facies that is pervasively mineralized by chalcopyrite with accessory pyrite. Micro-XRF maps indicate that copper-gold mineralization is

associated with Mn enrichments in the Fe-dolomite crystal located in the shoulders of copper-gold mineralization. Traces of a possible potassic alteration overprint associated with copper-gold mineralization are also visible on the micro-XRF maps.

The lower interval from AW-22-102 (Photos 25 and 26) demonstrates intense metasomatic replacement of the host rock and quartz veining resulting in the formation of the LT Si-(Fe)-K alteration facies (quartz, potassium feldspar, hematite) which is closely associated with copper-gold mineralization. Intense silicification completely obliterates the original textures and forms Fe-poor metasomatic alkali-calcic copper-gold mineralization, whereas potassium-feldspar altered certain relicts of the sedimentary precursor unit. The lowermost parts of AG-22-102 illustrate the incipient to weak development of the LT (Ca,Mg)-Si-K-Fe alteration facies (actinolite, quartz, potassium feldspar, hematite) that is also associated with copper-gold mineralization, and an earlier event of cobalt-nickel mineralization. Two different assemblages of minerals are associated with the LT (Ca,Mg)-Si-K-Fe facies. The earliest mineral assemblage consists of actinolite with disseminated pyrrhotite and pyrite associated with incipient cobalt-nickel mineralization. This assemblage has been overprinted by hematite veins with variable potassium feldspar and carbonate contents associated with copper mineralization. This is the most intense zone alteration observed in the Alwyn Mine area to-date and occurs outside of the historical footprint of the mine. This observation is very significant for the system, as it demonstrates increasing intensity southeastward that may vector toward the core zone of the mineralized system.

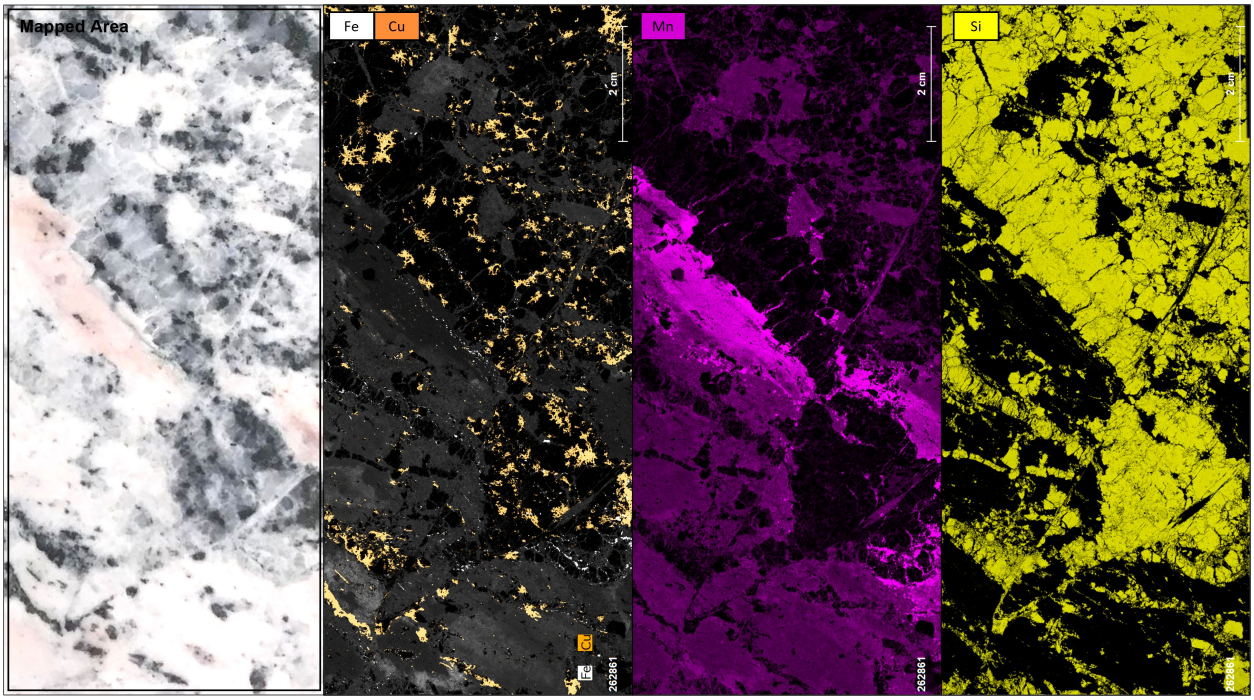

Photo 24. False colour micro-XRF elemental distribution maps of core from AW-22-102 (Core 8) (XRF Sample 12 – 50.0 m; left photograph) that show strong Mn enrichments (Mn – purple) in Fe-dolomite (Fe – white) in the haloes of copper-gold mineralization (Cu – orange) formed by clusters and fracture filling of chalcopyrite with accessory pyrite.

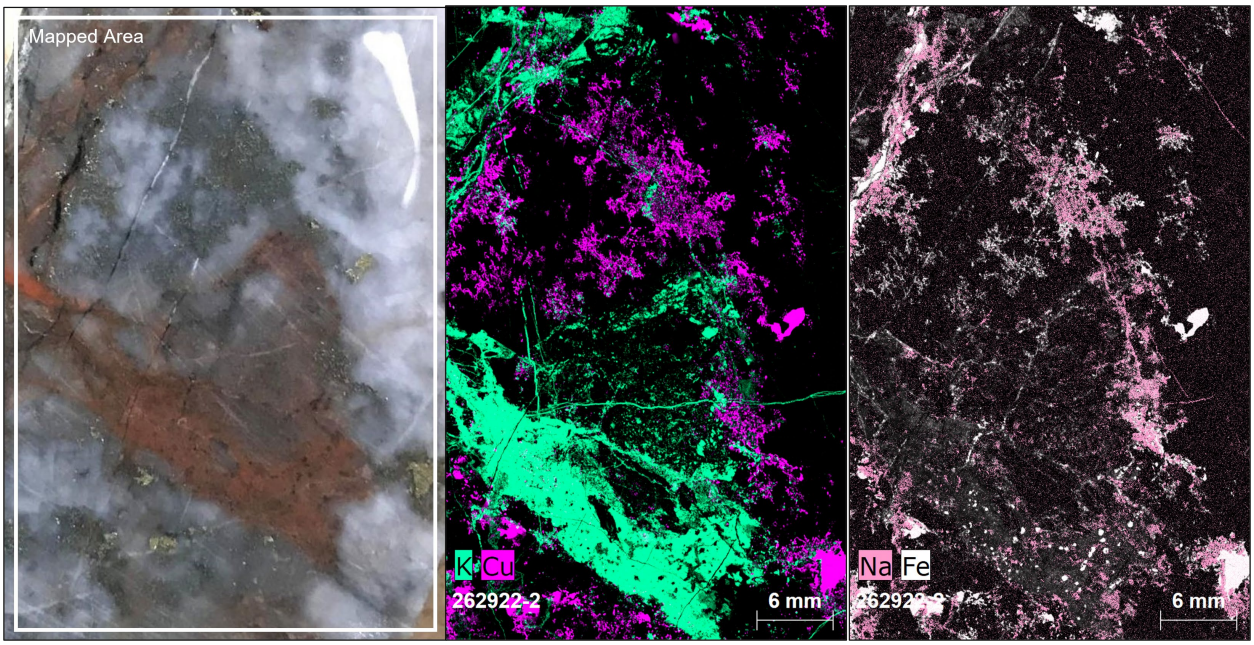

Photo 25. False colour micro-XRF elemental distribution maps of core from the lower zone of AW-22-102 (Core 8) (XRF Sample 7 – 126.3 m; left photograph) demonstrating strong potassic (K – green) and weak to moderate sodic (Na – pink) alteration associated with copper-gold mineralization (Cu – purple) in the zone of extreme silicification.

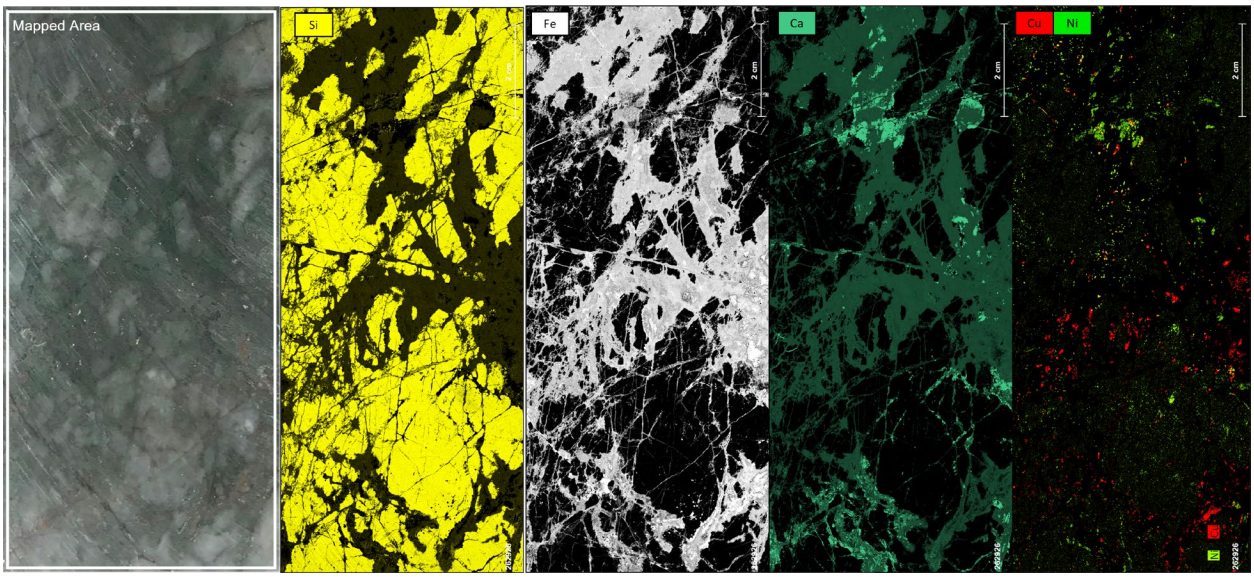

Photo 26. False colour micro-XRF elemental distribution maps of the lower zone of AW-22-102 (Core 8) (XRF Sample 8 – 129.3 m; left photograph) demonstrating intense Fe metasomatism (chlorite-amphibole; Fe – white; Ca – teal) of massive quartz veining and/or silicified interval (Si – yellow), associated with copper-gold mineralization (Cu – red) and accessory nickel (Ni – green).

Core 9 – JV-21-085 – Nickel-PGE mineralization associated with the HT Ca-(Mg)-Fe alteration at the Limestone prospect

Thus far, all outcrops and core observed have demonstrated low temperature MIAC alteration facies. This interval (202.61 – 230.66 m) of core from the Limestone trenches on the eastern portion of the SPJ property, the Jovan area, was selected to illustrate HT nickel-copper-PGE mineralization associated with the sulfide-rich variant of the HT Ca-(Mg)-Fe facies. In this core, high temperature metasomatism of Espanola Formation limestone has resulted in the formation of semi-massive sulfides (pyrrhotite with lesser chalcopyrite) with strong magnetite alteration. Actinolite and variable red apatite complement pyrrhotite or magnetite in the alteration assemblage halos. Photo 27 demonstrates that HT Ca-Fe alteration overprinted a pre-existing pervasive sodic alteration of the Espanola Formation limestone.

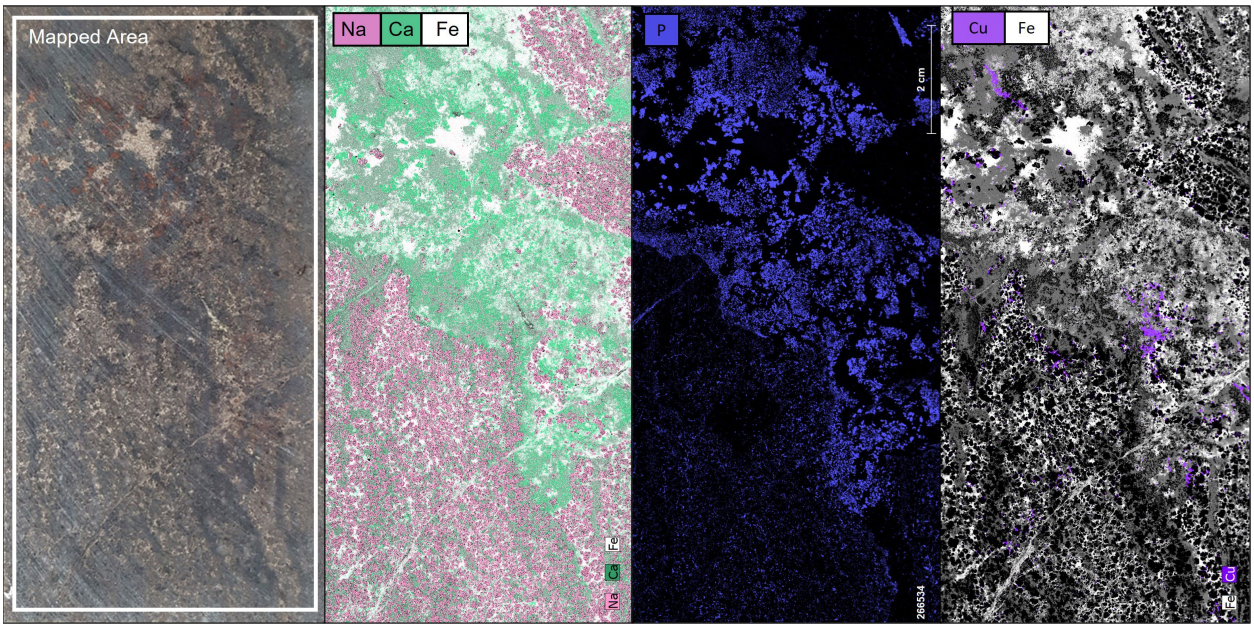

Photo 27. False colour micro-XRF elemental distribution maps of core from JV-21-085 (Core 9) (XRF Sample 1 – 210.1 m; left photograph) demonstrating sulfide mineralization (Cu – purple; Fe – white) in altered sedimentary rocks with moderate pervasive sodic alteration (Na – pink), moderate Fe-Ca-Mg alteration (actinolite; Ca – teal; Fe – white), and moderate phosphorus alteration (red apatite grains in left photograph; P – blue).

Return to vehicles and follow the mine road out of the Scadding mine site.

0.0 km	Turn right onto Kukagami Road from the entrance of the Scadding mine site.
16.0 km	Turn right onto Trans-Canada Highway 17. Continue travelling west until you enter the city of Greater Sudbury, where Highway 17 becomes the Kingsway (Regional Road 55).
49.75 km	Keep right and continue onto Lloyd Street (Regional Road 55). Then continue straight onto Brady Street (Regional Road 49).
50.25 km	Turn left onto Paris Street (Regional Road 80).
52.7 km	Turn left onto Ramsey Lake Road (Regional Road 39).
55.0 km	Turn right onto University Road. After 650 m turn left and head another 200 m to the RD Parker building.

End of road log.

Acknowledgments

The authors thank Delaney Carter, Research Assistant at Saint Mary's University for running micro-XRF analyses and Dr. Pierre-Marc Godbout (Geological Survey of Canada) and Dr. Bruno Lafrance (Laurentian University), Dr. Mike Easton (Ontario Geological Survey), and Marg Rutka (Ontario Geological Survey) for their thorough review of the manuscript. The authors also thank Shirley Péloquin (Sudbury District Geologist) for her input and ideas discussed while preparing this field trip. The research was in part funded by the Targeted Geoscience Initiative program of the Geological Survey of Canada (Natural Resources Canada) in collaboration with MacDonald Mines Exploration Ltd. This is Natural Resources Canada contribution 20220553.

References

Adlakha, E., Corriveau, L., Neyedley, K., Conliffe, J. and Piette-Lauzière, N. (organizers) 2022. Metasomatic iron and alkali-calcic (MIAC) systems with IOCG and associated critical mineral deposits: Prospectivity of the Canadian Appalachian Orogen; Geological Association of Canada – Mineralogical Association of Canada – International Association of Hydrogeologists – Canadian National Committee – Canadian Society of Petroleum Geologists (GAC-MAC-IAH-CNC-CSPG) Annual Meeting, Workshop SCW-A1, Halifax, Nova Scotia, May 15–18, 2022.

Al-Hashim, M.H. 2016. Sedimentology and geochemistry of the mixed carbonate-siliciclastic Espanola Formation, Paleoproterozoic Huronian Supergroup, Bruce Mines-Elliot Lake area, Ontario, Canada; unpublished PhD thesis, University of Western Ontario, London, Ontario, 287p.

Austin, J.R. and Blenkinsop, T.G. 2008. The Cloncurry Lineament: Geophysical and geological evidence for a deep crustal structure in the Eastern Succession of the Mount Isa Inlier; Precambrian Research, v.163, p.50-68.

Babo, J., Spandler, C., Oliver, N., Brown, M., Rubenach, M. and Creaser, R.A. 2017. The high-grade Mo-Re Merlin deposit, Cloncurry District, Australia: Paragenesis and geochronology of hydrothermal alteration and ore formation; Economic Geology, v.112, p.397-422.

Bailey, J., Lafrance, B., McDonald, A.M., Fedorowich, J.S., Kamo, S. and Archibald, D.A. 2004. Mazatzal–Labradorian-age (1.7–1.6 Ga) ductile deformation of the South Range Sudbury impact structure at the Thayer Lindsley Mine, Ontario; Canadian Journal of Earth Sciences, v.41, p.1491-1505.

Bain, W.M., Steele-MacInnis, M., Li, K., Li, L., Mazdab, F.K. and Marsh, E. 2020. A fundamental role of carbonate-sulfate melts in formation of iron oxide-apatite deposits; Nature Geoscience, v.13, p.751-757, https://doi .org/10.1038/s41561-020-0635-9.

Bekker, A., Kaufman, A.J., Karhu, J.A. and Eriksson, K.A. 2005. Evidence for Paleoproterozoic cap carbonates in North America; Precambrian Research, v.137, p.167-206.

Bennett, G., Dressler, B.O. and Robertson, J.A. 1991. The Huronian Supergroup and associated intrusive rocks; *in* Geology of Ontario, Ontario Geological Survey, Special Volume 4, Part 1, p.549-592.

Bleeker, W. and Kamo, S.L. 2022. The Sudbury structure, Earth's largest (partially) preserved impact crater—A review; *in* 68th Institute on Lake Superior Geology Annual Meeting, Proceedings, Part 1, p.5-6.

Bleeker, W., Kamo, S.L., Ames, D.E. and Davis, D. 2015. New field observations and U-Pb ages in the Sudbury area: Toward a detailed cross-section through the deformed Sudbury Structure; *in* Targeted Geoscience Initiative 4: Canadian Nickel-Copper-Platinum Group Elements-Chromium Ore Systems—Fertility, Pathfinders, New and Revised Models, Geological Survey of Canada, Open File 7856, p.151-166.

Blein, O., Corriveau, L., Montreuil, J.-F., Ehrig, K., Fabris, A., Reid, A. and Pal, D. 2022. Geochemical signatures of metasomatic ore systems hosting IOCG, IOA, albitite-hosted uranium and affiliated deposits: A tool for process studies and mineral exploration, *in* Mineral Systems with Iron Oxide Copper-Gold (IOCG) and Affiliated Deposits, Geological Association of Canada, Special Paper 52, p.263-298.

Card, K.D., Church, W.R., Franklin, J.M., Frarey, M.J., Robertson, J.A., West, G.F. and Young, G.M. 1972. The Southern Province; *in* Variations in Tectonic Styles in Canada, Geological Association of Canada, Special Paper 11, p.335-380.

Chen, H. and Zhao, L. 2022. Mineralization, alteration, and fluid compositions in selected Andean IOCG deposits; *in* Mineral Systems with Iron Oxide Copper-Gold (IOCG) and Affiliated Deposits, Geological Association of Canada, Special Paper 52, p.365-381.

Corfu, F. and Andrews, A.J. 1986. A U-Pb age for mineralized Nipissing diabase, Gowganda, Ontario; Canadian Journal of Earth Sciences. v.23, p.107-109.

Corriveau, L. 2007. Iron oxide-copper-gold deposits: A Canadian perspective; *in* Goodfellow, W.D., ed., Mineral Deposits of Canada: A Synthesis of Major Deposit-Types, District Metallogeny, the Evolution of Geological Provinces, and Exploration Methods, Geological Association of Canada, Mineral Deposits Division, Special Publication 5, p.307-308.

Corriveau, L. and Mumin, A.H. 2010. Exploring for iron oxide copper-gold deposits: The need for case studies, classifications and exploration vectors; *in* Corriveau, L. and Mumin, A.H., eds., Exploring for Iron Oxide Copper-Gold Deposits: Canada and Global Analogues, Geological Association of Canada, Short Course Notes, No.20, p.1-12.

Corriveau, L., Mumin, A.H. and Setterfield, T. 2010a. IOCG environments in Canada: Characteristics, geological vectors to ore and challenges; *in* Hydrothermal Iron Oxide Copper-Gold and Related Deposits: A Global Perspective, v.4: PGC Publishing, Adelaide, p.311-344.

Corriveau, L., Williams, P.J. and Mumin, H. 2010b. Alteration vectors to IOCG mineralization – From uncharted terranes to deposits; *in* Corriveau, L and Mumin, A.H., Eds, Exploring for Iron Oxide Copper-Gold Deposits: Canada and Global Analogues, Geological Association of Canada, Short Course Notes, No.20, p.89-110.

Corriveau, L., Montreuil, J.-F. and Potter, E.G. 2016. Alteration facies linkages among IOCG, IOA and affiliated deposits in the Great Bear magmatic zone, Canada; *in* A Special Issue Devoted to Proterozoic Iron Oxide-Apatite (± REE) and Iron Oxide-Copper-Gold and Affiliated Deposits of Southeast Missouri, USA, and the Great Bear Magmatic Zone, Northwest Territories, Canada, Economic Geology, v.111, no.8, p.2045-2072.

Corriveau, L., Potter, E.G., Montreuil, J.-F., Blein, O., Ehrig, K. and De Toni, A. 2018. Iron-oxide and alkali-calcic alteration ore systems and their polymetallic IOA, IOCG, skarn, albitite-hosted U±Au±Co, and affiliated deposits: A short course series. Part 2: Overview of deposit types, distribution, ages, settings, alteration facies, and ore deposit models, Geological Survey of Canada, Scientific Presentation 81, 154p. https://doi.org/10.4095/306560.

Corriveau, L., Montreuil, J.-F., Blein, O., Ehrig, K., Potter, E.G., Fabris, A. and Clark, J. 2022a. Mineral systems with IOCG and affiliated deposits: Part 2 – Geochemical footprints; *in* Mineral Systems with Iron Oxide Copper-Gold (IOCG) and Affiliated Deposits, Geological Association of Canada, Special Paper 52, p.59-204.

Corriveau, L., Montreuil, J.-F., de Toni, A.F., Potter, E.G. and Percival, J.B. 2022b. Mapping mineral systems with IOCG and affiliated deposits: A facies approach; *in* Mineral Systems with Iron Oxide Copper-Gold (IOCG) and Affiliated Deposits, Geological Association of Canada, Special Paper 52, p.69-111.

Corriveau, L., Montreuil, J.-F., Potter, E.G., Blein, O. and de Toni, A.F. 2022c. Mineral systems with IOCG and affiliated deposits: Part 3 – Metal pathways and ore deposit model; *in* Mineral Systems with Iron Oxide Copper-Gold (IOCG) and Affiliated Deposits, Geological Association of Canada, Special Paper 52, p.205-245.

Corriveau, L., Montreuil, J.-F., Potter, E.G., Ehrig, K., Mumin, A.H. and Williams, P.J. 2022d. Mineral systems with IOCG and affiliated deposits: Part 1 – Alteration facies; *in* Mineral Systems with Iron Oxide Copper-Gold (IOCG) and Affiliated Deposits, Geological Association of Canada, Special Paper 52, p.113-158.

Corriveau, L., Mumin, A.H. and Potter, E.G. 2022e. Mineral systems with iron oxide copper-gold (Ag-Bi-Co-U-REE) and affiliated deposits: Introduction and overview; *in* Mineral Systems with Iron Oxide Copper-Gold (IOCG) and Affiliated Deposits, Geological Association of Canada, Special Paper 52, p.1-26.

Davey, S., Bleeker, W., Kamo, S.L., Davis, D.W., Easton, R.M. and Sutcliffe, R.H. 2019. Ni-Cu-PGE potential of the Nipissing sills as part of the ca. 2.2 Ga Ungava large igneous province; *in* Targeted Geoscience Initiative: 2018 Report of Activities; Geological Survey of Canada, Open File 8549, p.403-419.

Davidson, A. and Ketchum, J.W.F. 1993. Grenville Front studies in the Sudbury region, Ontario; *in* Current Research, Part C; Geological Survey of Canada, Paper 93-1C, p.271-278.

Davidson, A., van Breemen, O. and Sullivan, R.W. 1992. Circa 1.75 Ga ages for plutonic rocks from the Southern Province and adjacent Grenville province: What is the expression of the Penokean Orogeny?; Radiogenic Age and Isotopic Studies: Report 6, Geological Survey of Canada, Paper 92-2, p.107-118. https://doi.org/10.4095/134170

Del Real, I., Reich, M., Simon, A.C., Deditius, A., Barra, F., Rodríguez-Mustafa, M.A., Thompson, J.F.H. and Roberts, M.P. 2021. Formation of giant iron oxide-copper-gold deposits by superimposed, episodic hydrothermal pulses; Nature, v.192, 9p.

Deutsch, A., Grieve, R.A.F., Avermann, M., Bischoff, L., Brockmeyer, P., Buhl, D., Lakomy, R., Muller-Mohr, V., Ostermann, M. and Stoffler, D. 1995. The Sudbury Structure (Ontario, Canada): A tectonically deformed multi-ring impact basin; Geologische Rundschau, v.84, p.697-709.

Dhnaram, C., Lisitsin, V., Gopalakrishnan, S., Tang, J., Killen, D. and von Gnielinski, F. 2021. Eastern Mount Isa Province IOCG data package; Geological Survey of Queensland, Technical Notes 2021/06.

Dressler, B.O. 1980. Wanapitei Lake area (southern part); Ontario Geological Survey, Preliminary Map P.2228; scale 1:15 840.

——— 1984. The effects of the Sudbury Event and the Intrusion of the Sudbury Igneous Complex on the Footwall Rocks of the Sudbury Structure; *in* The Geology and Ore Deposits of the Sudbury Structure, Ontario Geological Survey, Special Volume 1, p 97-136.

Easton, R.M. 2006. Complex folding and faulting history in Huronian Supergroup rocks located north of the Murray fault zone, Southern Province, Ontario; *in* 52nd Institute on Lake Superior Geology, Proceedings, v.52, pt.1, p.15-16.

Easton, R.M. and Murphy, E. 2002. Precambrian geology of Street Township, District of Sudbury; Ontario Geological Survey, Open File Report 6078, 149p.

Easton, R.M., Rainsford, D.R.B. and Préfontaine, S. 2020. Preliminary interpretation of the Sturgeon River area aeromagnetic survey, northeastern Ontario; *in* Summary of Field Work and Other Activities, 2020; Ontario Geological Survey, Open File Report 6370, p.6-1 to 6-15.

Ehrig, K., McPhie, J. and Kamenetsky, V. 2012. Geology and mineralogical zonation of the Olympic Dam iron oxide Cu-U-Au-Ag deposit, South Australia; *in* Geology and Genesis of Major Copper Deposits and Districts of the World: A Tribute to Richard H. Sillitoe, Society of Economic Geologists, Special Publication, v.16, p.237-267.

Engvik, A., Putnis, A., Fitz Gerald, J.D. and Austrheim, H. 2008. Albitization of granitic rocks: The mechanism of replacement of oligoclase by albite; The Canadian Mineralogist, v.46, p.401-1415.

Fabris, A., Katona, L., Gordon, G., Reed, G., Keeping, T., Gouthas, G. and Swain, G. 2018. Characterising and mapping alteration in the Punt Hill region: A data integration project; Government of South Australia, Department of the Premier and Cabinet, Report Book, 2018/00010, 604p.

Farrow, D. 2016. Soda metasomatism as a possible iron oxide-copper-gold (IOCG) deposit indicator in the Sudbury District; Ontario Geological Survey, Resident Geologist Program, Recommendations for Exploration 2016–2017, p.65-67.

Fueten, F. and Redmond, D.J. 1992. Structural studies in the Southern Province, south of Sudbury, Ontario; Geological Survey of Canada, Current Research 92-1C, p.179-187.

Gadd, M.G., Lawley, C.J., Corriveau, L., Houlé, M, Peter, J.M., Plouffe, A., Potter, E.G., Sappin, A.-A., Pilote, J.-L., Marquis, G. and Lebel, D. 2022. Public geoscience solution for diversifying Canada's critical mineral production; Geological Society, London, Special Publications, v.526, https://doi.org/10.1144/SP526-2021-190

Gates, B.I. 1991. Sudbury mineral occurrence study; Ontario Geological Survey, Open File Report 5771, 235p.

Hayward, N., Enkin, R.J., Corriveau, L., Montreuil, J-F. and Kerswill, J. 2013. The application of rapid potential field methods for the targeting of IOCG mineralization based on physical property data, Great Bear Magmatic Zone, Canada; Journal of Applied Geophysics, v.94, p.42-58.

Hayward, N., Corriveau, L., Craven, J.A., and Enkin, R.J. 2016. Geophysical signature of the NICO Au-Co-Bi-Cu deposit and its iron oxide-alkali alteration system, Northwest Territories, Canada; *in* A Special Issue Devoted to Proterozoic Iron Oxide-Apatite (± REE) and Iron Oxide-Copper-Gold and Affiliated Deposits of Southeast Missouri, USA, and the Great Bear Magmatic Zone, Northwest Territories, Canada, Economic Geology, v.111, no.8, p.2087-2110.

Hitzman, M.W., Oreskes, N. and Einaudi, M.T. 1992. Geological characteristics and tectonic setting of Proterozoic iron oxide (Cu-U-Au-REE) deposits; Precambrian Research, v.58, p.241-287.

Hofstra, A.H., Meighan, C.J., Song, X., Samson, I., Marsh, E.E., Lowers, H.A., Emsbo, P. and Hunt, A.G. 2016. Mineral thermometry and fluid inclusion studies of the Pea Ridge iron oxide–apatite–rare earth element deposit, Mesoproterozoic St. Francois Mountains terrane, Southeast Missouri, USA; *in* A Special Issue Devoted to Proterozoic Iron Oxide-Apatite (± REE) and Iron Oxide-Copper-Gold and Affiliated Deposits of Southeast Missouri, USA, and the Great Bear Magmatic Zone, Northwest Territories, Canada, Economic Geology, v.111, no.8, p.1985-2016.

Hofstra, A.H., Lisitsin, V., Corriveau, L., Paradis, S., Peter, J., Lauzière, K., Lawley, C., Gadd, M., Pilote, J.-L., Honsberger, I., Bastrakov, E., Champion, D., Czarnota, K., Doublier, M., Huston, D., Raymond, O., VanDerWielen, S., Emsbo, P., Granitto, M. and Kreiner, D. 2021. Deposit classification scheme for the critical minerals mapping initiative global geochemical database; USGS, Open-File Report 2021–1042, 60p., https://doi.org/10.3133/ofr20211049.

Hou, T., Charlier, B., Holtz, F., Veksler, I., Zhang, Z., Thomas, R. and Namur, O. 2018. Immiscible hydrous Fe–Ca–P melt and the origin of iron oxide–apatite ore deposits; Nature Communications, v.9, p.1415.

Ismail, R. 2015. Spatial-temporal evolution of skarn alteration in IOCG systems: Evidence from petrography, mineral trace element signatures and fluid inclusions studies at Hillside, Yorke Peninsula, South Australia; unpublished PhD thesis, The University of Adelaide, Adelaide, South Australia, Australia, 352p.

Jackson, S.L. 2001. On the structural geology of the Southern Province between Sault Ste. Marie and Espanola, Ontario; Ontario Geological Survey, Open File Report 5995, 55p.

James, R.S., Easton, R.M., Peck, D.C. and Hrominchuk, J.L. 2002. The East Bull Lake Intrusive Suite: Remnants of a ~2.48 Ga large igneous and Metallogenic Province in the Sudbury area of the Canadian Shield; Economic Geology, v.97, p.1577-1606.

Keyser, W., Ciobanu, C.L., Ehrig, K., Dmitrijeva, M., Wade, B.P., Courtney-Davies, L., Verdugo-Ihl, M. and Cook, N.J. 2022. Skarn-style alteration in Proterozoic metasedimentary protoliths hosting IOCG mineralization: The Island Dam prospect, South Australia; Mineralium Deposita, v.57, p.1227-1250.

Ketchum, K.Y., Heaman, L.M., Bennett, G. and Hughes, D.J. 2013. Age, petrogenesis and tectonic setting of the Thessalon volcanic rocks, Huronian Supergroup, Canada; Precambrian Research, v.233, p.144-172.

Klondike Bay Resources. 1999. Alwyn Porcupine Gold-Copper Project; Ontario Assessment File Database, Report 41I10NE2008, AFRI 2.19741, 85p.

Kontak, D.J., Archibald, D.A., Creaser, R.A. and Heaman, L.M. 2008. Dating hydrothermal alteration and IOCG mineralization along a terrane-bounding fault zone: The Copper Lake deposit, Nova Scotia; Atlantic Geology, v.44, p.146-166.

Krogh, T.E. 1994. Precise U-Pb ages for Grenvillian and pre-Grenvillian thrusting of Proterozoic and Archean metamorphic assemblages in the Grenville Front tectonic zone, Canada; Tectonics, v.13, p.963-982.

Krogh, T.E., Davis, D.W. and Corfu, F. 1984. Precise U-Pb zircon and baddeleyite ages for the Sudbury area; *in* The Geology and Ore Deposits of the Sudbury Structure; Ontario Geological Survey, Special Volume 1, p.431-446.

Krogh, T.E., Corfu, F., Davis, D.W., Dunning, G.R., Heaman, L.M., Kamo, S.L., Machado, N., Greenough, J.D. and Nakamura, E. 1987. Precise U-Pb isotope ages of diabase dikes and mafic to ultramafic rocks using trace amounts of baddeleyite and zircon; *in* Mafic Dike Swarms, Geological Association of Canada, Special Paper 34, p.147-152.

Le, T. 2021. Geological characteristics, genesis and ore controlling factors of the Tick Hill Au deposit, Dajarra District, NW Queensland, Australia; unpublished PhD thesis, James Cook University, Australia, 209p.

Lafrance, B. and Kamber, B.S. 2010. Geochemical and microstructural evidence for in situ formation of pseudotachylitic Sudbury breccia by shock-induced compression and cataclasis; Precambrian Research, v.180, p.237-250.

Lightfoot, P.C. and Naldrett, A.J. 1996. Petrology and geochemistry of the Nipissing Gabbro: Exploration strategies for nickel, copper, and platinum group elements in a large igneous province; Ontario Geological Survey, Study 58, 81p.

McCafferty, A.E., Phillips, J.D., Hofstra, A.H. and Day, W.C. 2019. Crustal architecture beneath the southern Midcontinent (USA) and controls on Mesoproterozoic iron-oxide mineralization from 3D geophysical models; Ore Geology Reviews, v.111, 102966. https://doi.org/10.1016/j.oregeorev.2019.102966

Metcalf, M. 2021. 2021 Exploration report for the Rathbun property, Macdonald Mines Exploration Ltd.; Ontario Assessment File Database, Report 20000519754, 93p.

Montreuil, J.-F., Corriveau, L. and Grunsky, E.C. 2013. Compositional data analysis of IOCG systems, Great Bear magmatic zone, Canada: To each alteration type its own geochemical signature; Geochemistry: Exploration, Environment, Analysis, v.13, p.229-247.

Montreuil, J.-F., Corriveau, L. and Potter, E. 2015. Formation of albitite-hosted uranium within IOCG systems: The Southern Breccia, Great Bear magmatic zone, Northwest Territories, Canada; Mineralium Deposita, v.50, p.293-325.

Montreuil, J.-F., Corriveau, L. and Davis, W. 2016a. Tectonomagmatic evolution of the southern Great Bear magmatic zone (Northwest Territories, Canada) – Implications on the genesis of iron oxide alkali-altered hydrothermal systems; *in* A Special Issue Devoted to Proterozoic Iron Oxide-Apatite (± REE) and Iron Oxide-Copper-Gold and Affiliated Deposits of Southeast Missouri, USA, and the Great Bear Magmatic Zone, Northwest Territories, Canada, Economic Geology, v.111, no.8, p.2111-2138.

Montreuil, J.-F., Corriveau, L., Potter, E.G. and De Toni, A.F. 2016b. On the relation between alteration facies and metal endowment of iron oxide–alkali-altered systems, southern Great Bear magmatic zone (Canada), *in* A Special Issue Devoted to Proterozoic Iron Oxide-Apatite (± REE) and Iron Oxide-Copper-Gold and Affiliated Deposits of Southeast Missouri, USA, and the Great Bear Magmatic Zone, Northwest Territories, Canada, Economic Geology, v.111, no.8, p.2139-2168.

Mukwakwami, J., Lafrance, B. Lesher, M.C. Tinkham, D.K., Rayner, N.M. and Ames, D.E. 2014. Deformation, metamorphism, and mobilization of Ni–Cu–PGE sulfide ores at Garson Mine, Sudbury; Mineralium Deposita, v.49, p.175-198. https://doi.org/10.1007/s00126-013-0479-y

Murphy, E.I. 1999. Geology, metamorphism, and geochemistry of Southern and Grenville Province rocks in the vicinity of the Grenville Front, Timmins Creek area, near Sudbury, Ontario; unpublished MSc thesis, Laurentian University, Sudbury, Ontario, 266p.

Naldrett, A.J. 1984. Mineralogy and composition of the Sudbury Ores; *in* The Geology and Ore Deposits of the Sudbury Structure, Ontario Geological Survey, Special Volume 1, p.309-325.

Natural Resources Canada. 2021. Canada's list of critical minerals: Available at https://www.nrcan.gc.ca/criticalminerals.

O'Callaghan, J.W., Osinski, G.R., Lightfoot, P.C., Linnen, R.L. and Weirich, J.R. 2016. Reconstructing the geochemical signature of Sudbury Breccia, Ontario, Canada: Implications for its formation and trace metal content; *in* A Special Issue Devoted to Proterozoic Iron Oxide-Apatite (± REE) and Iron Oxide-Copper-Gold and Affiliated Deposits of Southeast Missouri, USA, and the Great Bear Magmatic Zone, Northwest Territories, Canada, Economic Geology, v.111, no.8, p.1705-1729.

Oliver, N.H.S., Mark, G., Pollard, P.J., Rubenach, M.J., Bastrakov, E., Williams, P.J., Marshall, L.C., Baker, T. and Nemchin, A.A. 2004. The role of sodic alteration in the genesis of iron oxide-copper-gold deposits: Geochemistry and geochemical modelling of fluid-rock interaction in the Cloncurry district, Australia; Economic Geology, v.99, p.1145-1176.

Oliver, N.H.S., McLellan, J.G., Cleverley, J., Babo, J., Marshall, L.J. and Brown, M.C. 2017. Chaos and control: The interplay between discordant IOCG-related breccias and their bounding fault and shear arrays, Cloncurry District, northern Australia; Proceedings of the 14th Society for Geology Applied to Mineral Deposits (SGA) Biennial Meeting, 20–23 August 2017, Québec City, p.875-879.

Ontario Geological Survey 2011. 1:250 000 scale bedrock geology of Ontario; Ontario Geological Survey, Miscellaneous Release—Data 126–Revision 1.

——— 2023. Ontario Mineral Inventory; Ontario Geological Survey, Ontario Mineral Inventory (January 2023 update), online database.

Ootes, L., Snyder, D., Davis, W.J., Acosta-Góngora, P., Corriveau, L., Mumin, A.H., Montreuil, J.-F., Gleeson, S.A., Samson, I.A. and Jackson, V.A. 2017. A Paleoproterozoic Andean-type iron oxide copper-gold environment, the Great Bear magmatic zone, Northwest Canada; Ore Geology Reviews, v.81, p.123-139.

Ovalle, J.T., La Cruz, N.L., Reich, M., Barra F., Simon A.C., Konecke B.A., Rodriguez-Mustafa M.A., Deditius A.P., Childress T.M. and Morata D. 2018. Formation of massive iron deposits linked to explosive volcanic eruptions; Scientific Reports v.8, 14855. https://doi.org/10.1038/s41598-018-33206-3

Papapavlou, K., Darling, J.R., Lightfoot, P.C., Lasalle, S., Gibson, L., Storey, C.D. and Moser, D. 2018. Polyorogenic reworking of ore-controlling shear zones at the South Range of the Sudbury impact structure: A telltale story from in situ U–Pb titanite geochronology; Terra Nova, v.30, no.3, p.254-261, https://doi.org/10.1111/ter.12332

Parmenter, A.C., Lee, A.B. and Coniglio, M. 2002. "Sudbury Breccia" at Whitefish Falls, Ontario: Evidence for an impact origin; Canadian Journal of Earth Sciences, v.39, no.6, p.971-982. https://doi.org/10.1139/e02-006

Piercey, P., Schneider, D.A. and Holm, D.K. 2007. Geochronology of Proterozoic metamorphism in the deformed Southern Province, northern Lake Huron region, Canada; Precambrian Research, v.157, p.27-143.

Potter, E.G. 2009. Genesis of polymetallic mineralization and the metallogeny of the Paleoproterozoic Cobalt Embayment, Northern Ontario; unpublished PhD thesis, Carleton University, Ottawa, Ontario, 353p.

Porter, T.M. 2000. Hydrothermal iron oxide copper-gold and related deposits: A global perspective, volume 1; Porter Geoscience Consultancy Publishing, Adelaide, South Australia, Australia, 349p.

——— 2002. Hydrothermal iron oxide copper-gold and related deposits. A global perspective, volume 2; Porter Geoscience Consultancy Publishing, Adelaide, South Australia, Australia, 377p.

——— 2010a. Current understanding of iron oxide associated-alkali altered mineralised systems: part 1 – An overview; *in* Hydrothermal Iron Oxide Copper-Gold and Related Deposits: A Global Perspective, volume 3; Porter Geoscience Consultancy Publishing, Adelaide, South Australia, Australia, p.5-32.

——— 2010b. Current understanding of iron oxide associated-alkali altered mineralised systems: part II – A review; *in* Hydrothermal Iron Oxide Copper-Gold and Related Deposits: A Global Perspective, volume 3; Porter Geoscience Consultancy Publishing, Adelaide, South Australia, Australia, p.33-106.

Poulet, T., Karrech, A., Regenauer-Lieb, K., Fisher, L. and Schaubs, P. 2012. Thermal–hydraulic–mechanical–chemical coupling with damage mechanics using ESCRIPTRT and ABAQUS; Tectonophysics, v.526-529, p.124-132.

Putnis, A. 2009. Mineral replacement reactions; Reviews in Mineralogy and Geochemistry, v.70, p.87-124.

——— 2015. Transient porosity resulting from fluid–mineral interaction and its consequences; Reviews in Mineralogy and Geochemistry, v.80, p.1-23.

Raharimahefa, T., Lafrance, B. and Tinkham, D.K. 2014. New structural, metamorphic, and U–Pb geochronological constraints on the Blezardian Orogeny and Yavapai Orogeny in the Southern Province, Sudbury, Canada; Canadian Journal of Earth Sciences, v.51, no.8, p.750-774, https://doi.org/10.1139/cjes-2014-0025

Riller, U. 2005. Structural characteristics of the Sudbury impact structure, Canada: Impact-induced versus orogenic deformation – A review; Meteoritics and Planetary Science, v.40, p.1723-1740.

Robertson, J.A., Card, K.D. and Frarey, M.J. 1969. The Federal–Provincial Committee on Huronian Stratigraphy–Progress Report; Ontario Department of Mines, Miscellaneous Paper 31, 26p.

Rousell, D.H., Gibson, H.L. and Jonasson, I.R. 1997. The tectonic, magmatic and mineralization history of the Sudbury Structure; Exploration and Mining Geology, v.6, p.1-22.

Rousell, D.H., Fedorowich, J.S. and Dressler, B.O. 2003. Sudbury Breccia (Canada): A product of the 1850 Ma Sudbury Event and host to footwall Cu–Ni–PGE deposits; Earth Science Reviews, v.60, p.147-174.

Schandl, E.S. and Gorton, M.P. 1994. Albitization at 1700 +/- 2 Ma in the Sudbury – Wanapitei Lake area, Ontario: implication for deep-seated alkalic magmatism in the Southern province, Canadian Shield: Canadian Journal of Earth Sciences, v.31, p.597-607.

——— 2007. The Scadding gold mine, east of the Sudbury Igneous Complex, Ontario: An IOCG-type deposit?; The Canadian Mineralogist, v.45, p.1415-1441.

Schandl, E.S. and Gorton, M.P. 2007. The Scadding gold mine, East of the Sudbury Igneous Complex, Ontario: An IOCG-type deposit?; The Canadian Mineralogist, v.45, p.1415-1441.

Schulz, K.J. and Cannon, W.F. 2007. The Penokean Orogeny in the Lake Superior region; Precambrian Research, v.157, nos.1-4, p.4-25, https://doi.org/10.1016/j.precamres.2007.02.022

Shanks, W.S. and Schwerdtner, W.M. 1991. Structural analysis of the central and southwestern Sudbury Structure, Southern Province, Canadian Shield; Canadian Journal of Earth Sciences, v.28, no.3, p.411-430.

Skirrow, R.G. and Davidson, G. 2007. A special issue devoted to Proterozoic iron oxide Cu-Au-(U) and gold mineral systems of the Gawler craton: preface; Economic Geology, v.102, p.1373-1375.

Slack, J., Corriveau, L. and Hitzman, M. 2016. A special issue devoted to Proterozoic iron oxide-apatite (± REE) and iron oxide-copper-gold and affiliated deposits of Southeast Missouri, USA, and the Great Bear magmatic zone, Northwest Territories, Canada – Preface; Economic Geology, v.111, no.8, p.1803-1814.

Spray, J.G., Butler, H.R. and Thompson, L.M. 2004. Tectonic influences on the morphometry of the Sudbury impact structure: Implications for terrestrial cratering and modeling; Meteoritics and Planetary Science, v.39, no.2, p.287-301, https://doi.org/10.1111/j.1945-5100.2004.tb00341.x

Tornos, F., Velasco, F. and Hanchar, J.M. 2017. The magmatic to magmatic-hydrothermal evolution of the El Laco deposit (Chile) and its implications for the genesis of magnetite-apatite deposits; Economic Geology, v.112, p.1595-1628.

Tschirhart, P. and Morris, B. 2012. Grenville age deformation of the Sudbury impact structure: evidence from magnetic modelling of the Sudbury diabase dyke swarm; Terra Nova, v.24, no.3, p.213-220. https://doi.org/10.1111/j.1365-3121.2011.01056.x

Wade, C.E., Payne, J.L., Barovich, K.M. and Reid, A.J. 2019. Heterogeneity of the sub-continental lithospheric mantle and 'non-juvenile' mantle additions to a Proterozoic silicic large igneous province; Lithos, v.340-341, p.87-107.

Williams, P.J., Barton, M.D., Johnson, D.A., Fontboté, L., de Haller, A., Mark, G., Oliver, N.H.S. and Marschik, R. 2005. Iron-oxide copper-gold deposits: Geology, space-time distribution, and possible modes of origin; Economic Geology 100th Anniversary Volume, p.371-405.

Wood, J. 1973. Stratigraphy and depositional environment of the Upper Huronian rocks of the Rawhide Lake–Flack Lake area; Ontario; *in* Huronian Stratigraphy and Sedimentation, Geological Association of Canada, Special Paper 12, p.73-95.

Wray, N. and Yarie, Q. 2018. 2018 Exploration report for the Jovan-Powerline property, geological sampling and overburden stripping, Macdonald Mines Exploration Ltd.; Ontario Assessment File Database, Report 20000018958.

Yarie, Q. and Wray, N. 2019. National Instrument 43-101 Technical Report for the SPJ Project: Available at www.sedar.com , effective date October 18, 2019.

Metric Conversion Table

Conversion from SI to Imperial			Conversion from Imperial to SI		
SI Unit	*Multiplied by*	*Gives*	*Imperial Unit*	*Multiplied by*	*Gives*
		LENGTH			
1 mm	0.039 37	inches	1 inch	**25.4**	mm
1 cm	0.393 70	inches	1 inch	**2.54**	cm
1 m	3.280 84	feet	1 foot	**0.304 8**	m
1 m	0.049 709	chains	1 chain	20.116 8	m
1 km	0.621 371	miles (statute)	1 mile (statute)	**1.609 344**	km
		AREA			
1 cm^2	0.155 0	square inches	1 square inch	**6.451 6**	cm^2
1 m^2	10.763 9	square feet	1 square foot	**0.092 903 04**	m^2
1 km^2	0.386 10	square miles	1 square mile	2.589 988	km^2
1 ha	2.471 054	acres	1 acre	0.404 685 6	ha
		VOLUME			
1 cm^3	0.061 023	cubic inches	1 cubic inch	**16.387 064**	cm^3
1 m^3	35.314 7	cubic feet	1 cubic foot	0.028 316 85	m^3
1 m^3	1.307 951	cubic yards	1 cubic yard	0.764 554 86	m^3
		CAPACITY			
1 L	1.759 755	pints	1 pint	0.568 261	L
1 L	0.879 877	quarts	1 quart	1.136 522	L
1 L	0.219 969	gallons	1 gallon	**4.546 090**	L
		MASS			
1 g	0.035 273 962	ounces (avdp)	1 ounce (avdp)	28.349 523	g
1 g	0.032 150 747	ounces (troy)	1 ounce (troy)	**31.103 476 8**	g
1 kg	2.204 622 6	pounds (avdp)	1 pound (avdp)	**0.453 592 37**	kg
1 kg	0.001 102 3	tons (short)	1 ton(short)	**907.184 74**	kg
1 t	1.102 311 3	tons (short)	1 ton (short)	**0.907 184 74**	t
1 kg	0.000 984 21	tons (long)	1 ton (long)	**1016.046 908 8**	kg
1 t	0.984 206 5	tons (long)	1 ton (long)	**1.016 046 9**	t
		CONCENTRATION			
1 g/t	0.029 166 6	ounce (troy) / ton (short)	1 ounce (troy) / ton (short)	34.285 714 2	g/t
1 g/t	0.583 333 33	pennyweights / ton (short)	1 pennyweight / ton (short)	1.714 285 7	g/t

OTHER USEFUL CONVERSION FACTORS

	Multiplied by	
1 ounce (troy) per ton (short)	31.103 477	grams per ton (short)
1 gram per ton (short)	0.032 151	ounces (troy) per ton (short)
1 ounce (troy) per ton (short)	20.0	pennyweights per ton (short)
1 pennyweight per ton (short)	0.05	ounces (troy) per ton (short)

*Note: Conversion factors in **bold** type are exact. The conversion factors have been taken from or have been derived from factors given in the* Metric Practice Guide for the Canadian Mining and Metallurgical Industries*, published by the Mining Association of Canada in co-operation with the Coal Association of Canada.*

ISSN 0826-9580 (print)
ISBN 978-1-4868-7217-6 (print)

ISSN 1916-6117 (online)
ISBN 978-1-4868-7218-3 (PDF)